In vivo Characterization of a Pseudotyped Vesicular Stomatitis Virus for the Treatment of Hepatocellular Carcinoma

von Melanie Jäkel

Inaugural-Dissertation zur Erlangung der Doktorwürde
der Tierärztlichen Fakultät der Ludwig-Maximilians-Universität
München

In vivo Characterization of a Pseudotyped Vesicular Stomatitis Virus for the Treatment of Hepatocellular Carcinoma

von Melanie Jäkel

aus Potsdam

München, 2020

Aus dem Veterinärwissenschaftlichen Department
der Tierärztlichen Fakultät
der Ludwig-Maximilians-Universität München

Lehrstuhl für Virologie

Arbeit angefertigt unter der Leitung von
Univ.-Prof. Dr. Gerd Sutter

Angefertigt an der Klinik und Poliklinik für Innere Medizin II
Klinikum rechts der Isar der Technischen Universität München

Mentor: Dr. Jennifer Altomonte

Gedruckt mit der Genehmigung der Tierärztlichen Fakultät

der Ludwig-Maximilians Universität München

Dekan:	Univ.-Prof. Dr. Reinhard K. Straubinger, Ph.D.
Berichterstatter:	Univ.-Prof. Dr. Gerd Sutter
Korefferent/en:	Univ.-Prof. Dr. Johannes Hirschberger

Tag der Promotion: 8. Februar 2020

Table of Contents

1. Introduction

It has been more than 100 years since the potential use of oncolytic viruses in cancer treatment was proposed, [1] and we are still at the beginning to make use of this clever twist in nature that gives us the opportunity to use a pathogen to treat one of the most deadly diseases in the world. The huge time span between the initial hypothesis and finally the first approved viral cancer therapy reflects not only the challenges oncolytic viruses had to face, but also the promising prospects they offer that kept scientists motivated to continue their research.

In viro-immunotherapy, the strategy is to optimise the combined effects of the virus's inherent oncolytic properties and its ability to trigger an immune response at the tumor site, supporting the destruction of malignant cells and is at the same time a great approach to break the immune tolerance towards the tumor[2]. The challenge is to find a balance between the direct oncolytic effect of the virus and the induction of a strong immune response without clearing the virus before it can reach its maximum effect [3].

In this study, the new pseudotyped oncolytic virus (rVSV-NDV) based on a vesicular stomatitis virus (VSV) backbone, with the attachment proteins of Newcastle disease virus (NDV) in place of the endogenous glycoprotein, is tested for its safety and efficacy *in vivo*. Findings, achieved in this study are partly already published in Journal of Virology [4] in December 2018. Parameters of interest were toxicity in virus-treated rodents with special attention to neuropathogenicity, as this is a major problem in VSV-treated rodents and non-human primates[5], as well as pathogenicity in avian species, treatment-efficacy of the hybrid-virus *in vivo* and information about viral kinetics.

2. Literature Review

2.1. Hepatocellular Carcinoma

Liver cancer was the sixth common cancer worldwide in 2012 with rising incidence. It is listed as second common cancer-related cause of death [5]. The high mortality rate in hepatocellular carcinoma (HCC) is due to the facts that HCC is often diagnosed in late stages and additionally is relatively unresponsive to chemotherapy. Today the most effective and curative treatment for HCC is surgical resection or liver transplantation at early stages of the disease [7]. A major challenge in HCC therapy is that not even 40% of the patients are diagnosed at early stages, and later on, when the disease is more progressed, patients are often only eligible for palliative treatments [8]. Even successfully treated patients face 70% recurrence rates and only a 30-50% chance of a five-year survival [7].

The main catalysts for the development of HCC are, by a clear margin (60-70% of the reported HCC cases), Hepatitis C (HCV) and B virus (HCB) infections[9]. Further causalities that drive hepatic malignancy are alcoholic-liver disease, as well as non-alcoholic fatty liver disease and other autoimmune or hereditary liver disease such as hemochromatosis and Wilson's disease[10]. The leading viral factor driving liver cancer depends on the prevalence of HCV and HBV in different regions. In northern Europe, the United States and Japan, HCV is predominant, and in Africa and Asia, HBV is the main cause[6]. Although these two viruses both cause HCC, their pathogenicity differs clearly. HCV is known to cause liver malignancy by indirect pathways. Inflammation of the liver leads to cell death, proliferation and therefore induces a high turnover of newly produced cells. In addition, cirrhosis occurs regularly in inflamed livers and complicates the treatment because of the reduced accessibility of infected cells. These circumstances promote an accumulation of mutations and can eventually lead to HCC. In fact, HCC caused by HCV infection is almost exclusively seen in patients with cirrhosis. HBV infection induces HCC additionally via a direct pathway. The direct mechanism includes genomic integration and interference with growth signalling of the cell [10].

In 2012, 745.000 patients died from HCC. As the incidence of HCC is rising, even higher numbers can be expected in the future if no new treatment opportunities are developed.

Although in humans HCC ranks high under newly diagnosed cancers with even rising incidence, in dogs and cats reported cases of HCC are less common. Nevertheless, 0.6-1.3% of canine neoplasms are primary hepatic tumors[11]. HCC is the most common primary liver cancer in dogs and the second most common primary liver cancer in cats. The cause of the disease in animals is unknown, although a correlation between old age and HCC incidence can be observed. The best treatment opportunity provides liver resection in early stages[11]. To prevent often old-aged patients from invasive surgery the establishment of an alternative and mild treatment protocol would be beneficial for the patient's life quality.

2.2. Oncolytic Viruses

Oncolytic viruses (OVs) are viruses that can specifically replicate in and lyse cancer cells, taking advantage of their often impaired interferon response. These viruses could become the new weapon in the fight against HCC. Very different from chemotherapeutic approaches that kill unspecific cells with a high turnover rate and are a threat to both, cancer and the patient, OVs offer a different angle of cancer treatment, as they can mediate both direct cytopathic effects in cancer cells, as well as a break in immune tolerance towards malignant cells and induction of adaptive immune responses directed at tumor antigens. They therefore exploit the body's own resources to fight the disease using the new immunogenic trigger that the viral infection poses, combined with the direct oncolytic activities of the virus to lead to an immune response, not only directed against the virus but against tumor antigens as well. Since reverse genetics methods became standardized laboratory practice, it is possible to equip the virus with foreign genes, allowing the introduction of tumor antigens or proteins with specific antitumor functions into the targeted cells. This not only allows the use of viruses as vaccines, which provides the opportunity to vaccinate patients with a predisposition for special cancer types against typical epitopes and protect them from tumor challenge, but it also offers the possibility to cause infiltration of established tumors with immunologic components to attack the tumor cell. A prolonged survival of OV treated patients could also give hope for patients on the waiting list for liver transplantation. In recent years the number of patients dying while waiting for liver transplantation increased and only 69% survive their first year on the waiting list [12].

It becomes apparent that OVs represent a promising anti-cancer agent combining several advantages. The question arises: what does a virus need in order to be an oncolytic virus? Two important aspects, which determine the oncolytic activity of a virus, are the tropism and interferon (IFN) sensitivity. These characteristics provide the specificity of the virus for malignant cells. The first thing to consider is whether the virus is able to target tumor cells and which other cells the virus might infect. The tropism describes an interplay between the ability of a virus to enter a cell (receptor dependent tropism) and the cell being a suitable host for viral replication and progeny production (receptor independent tropism)[13]. As viruses often target receptors present on many cell types, it is important for a cell that is not the natural target of the viral infection to be able to mount an anti-viral defense to protect itself from virus-mediated cytotoxicity. The natural cellular response to viral infection is to produce and release IFN to hinder viral replication in the affected cell and increase major histocompatibility complex I (MHC I) molecules on neighbouring cells to stop viral spreading and rapidly eradicate the virus from the system[14]. Malignant cells are often impaired in their IFN responses[15] to avoid detection by immune cells and thus allow IFN sensitive viruses to replicate effectively whereas non-malignant cells clear the infection.

Before a virus can be considered as a candidate for cancer therapy, there are certain aspects of its natural replication cycle to consider. Some of the features provided by OVs offer great advantages over conventional drugs. An example would be the increasing viral titer due to viral replication at the treatment site, compared to traditional therapeutic agents, in which the concentrations usually decline after application. Nevertheless, some of the viral properties also need to be carefully considered, as they can provide an unforeseeable risk in

a host, e.g. tropism to not only cancer cells, but neurons as well (VSV) or genomic integration and latent infection (herpes simplex virus, adeno-associated viruses). The replication process will be explained in closer detail later on for the parental viruses of rVSV-NDV. For now, the focus lies on the benefits and risks associated with different OVs at specific steps of infection.

Viral entry and tropism are crucial for a successful infection. The attachment protein of a virus determines which cells can be infected and is the natural attribute that determines the host-specificity of a virus. Many of the OVs in clinical trials are animal viruses that had only restricted contact to humans, and thus, most patients do not face pre-existing immunity, allowing the virus to be more effective. To be considered oncolytic, the virus must of course enter and replicate in tumor cells, but it is also important to consider which other cells the virus is able to infect. A significant dose-limiting side effect of VSV is that it can result in neurotoxicity, because VSV is able to enter olfactory neurons and travel retrograde into the brain [16]. On the other hand VSVs broad tropism allows entry in nearly all known types of human tissue[17], and therefore, a broad variety of tumor cells is susceptible for infection. In general, viral attachment proteins are strongly immunogenic, and in many cases, vaccination against attachment proteins is enough to create a resilient immune response[18]. This poses a threat to the efficacy of oncolytic-viral treatment, as fast clearance of the virus is one of the main problems OV's have to overcome.

Once inside the cell, the virus uses the cell's replication machinery or a combination of this with its own enzymes to create its individual components and copies of genetic material. Some viruses replicate in the cytoplasm and some in the nucleus of the host cell. Cytoplasmic replication offers some advantages over replication in the nucleus in the sense that some viruses are capable of genomic integration. As an additional feature, viruses replicating in the cytoplasm suppress host translation by interference with nuclear pores leading to cell death.

Tumor cells that are successfully infected with an oncolytic virus tend to lead to immunogenic apoptosis. In contrast to cells undergoing a silent apoptosis, these can attract the attention of the immune system[19] and lead to immunologic responses against the viral antigens as well as newly derived tumor cell antigens.

2.3. Oncolytic Viruses in Clinical Trials

Many viruses possess oncolytic potential, among them DNA viruses such as herpes simplex virus, vaccinia virus and adenovirus as well as RNA viruses like vesicular stomatitis virus (VSV) and Newcastle disease virus (NDV), which will be the centre of this study. Of these oncolytic viruses, each has its own set of benefits that contributes in a unique way to tumor destruction but all of them have similar obstacles to overcome.

The adenovirus H101 is an approved oncolytic agent in china. It is deprived of the E1B gene, which inactivates the transcription factor p53 that stops cell proliferation when accumulated in a cell. A virus with this modification would be unable to replicate in a cell with normal p53 function, but not in a cancer cell lacking p53, which is a commonly seen genetic aberration in human cancer[20]. This leads to an undamped viral replication and finally cell burst from virus overload. Phase III trials in treatment of head and neck cancer

lead to 79% response rate for patients treated with H101 plus chemotherapy in comparison to a 40% response rate in chemotherapy only treated patients [21]. On the downside, this virus has a deletion in the E3 gene, which influences immune modulation e.g. by preventing the expression of MHC molecules or leading the transport of apoptosis receptors into lysosomes. As a result, H101 is eradicated from the patients system rather early and cannot be given intravenously, but only intratumorally. Also, the capacity as a vector for gene therapy is limited and makes the use of other viruses with the possibility to act as a platform for transfection superior.

Another OV is the vaccinia virus. Jennerex Inc. has marketed the Wyeth strain of vaccinia virus as the basis of oncolytic JX-594. This vector has already been applied in Phase II trials. It is attenuated through a disrupted thymidine kinase gene and carries insertions to express human granulocyte-macrophage colony-stimulating factor (GM-CSF) and β-galactosidase transgenes for an anti-tumor immune stimulation[22]. It is stable in delivery and shows enhanced potency combined with an efficient immune response compared to wild type vaccinia. More over the genome offers a large capacity for transgene encoding[23]. The tumor response to treatment with this oncolytic agent is highly dose dependant and is only available for systemic delivery in doses up from 10^9PFU. A disadvantage here is that 50 % of the patients have a baseline neutralizing antibody titer from vaccination against smallpox.

Imlygic® (talimogene laherparepvec, T-VEC) is the first "US Food and Drug Administration" approved oncolytic virus. This genetically modified herpes simplex virus type 1 is approved for therapy against melanoma and acts as antitumor vaccine agent in injectable, non-resectable tumors. T-VEC is genetically engineered to enhance safety by deletion of infected cell protein (ICP) 34.5 and ICP 47 (neuro virulence factors) to undermine the viruses immune evasion mechanisms and additionally contains a cassette encoding granulocyte-macrophage colony-stimulating factor (GM-CSF) to activate antigen presenting cells [24]. These modifications not only allow healthy cells and neurons to clear the virus and prevent latent infections, but also alter immune presence in tumor tissue, which supports the virus in tumor destruction and offers antigenic material from tumor tissue to be used as a matrix. 16,3% of patients developed a durable response after being treated with T-VEC in comparison to 2.1% of GM-CSF treated patients with durable response [25].

The focus of the work presented here is on a hybrid virus, constructed by merging components of two parental viruses, both of which have been shown to be oncolytic and have been applied in Phase I-III clinical trials.

Different strains of NDV have been used as treatment for neoplastic diseases in 33 patients with advanced cancer, non-responsive to standard treatment. Attenuated NDV-MTH-68/N administered via inhalation showed objective favorable responses (regression and stabilization) in 55% and a one-year survival in 66% of treated patients in comparison to 8% objective favorable response in the placebo-group and 6.5% one-year survival[26]. Also PV701 was extensively used in a Phase I and II clinical trial evaluating the maximum tolerated dose of this replication-competent OV for intravenous administration as a bolus ($2.4x10^{10}$PFU for the first dose and $1.2x10^{11}$PFU for subsequent doses). Also, a slow-infusion administration system over one

to three hours was established, which led to increased patient tolerability and higher tolerated dose escalation for the first administration. [27]

Although many attempts exist to alter VSV's characteristics as an oncolytic agent, from VSV-mp53 expressing murine p53 over VSV-TK that expresses tyrosine-kinase (TK) which can improve oncolysis in combination with the prodrug Ganciclovir, neurotoxicity remains a major challenge to the clinical translation of VSV.

A promising approach to exploit the diverse advantages of the rhabdovirus VSV is under constant development and evaluation by the group of von Laer. They attempt to circumvent neurotoxicity, the major concern about this otherwise powerful oncolytic agent, by using a pseudotyped recombinant VSV with the Glycoprotein of the lymphocytic choriomeningitis virus (LCMV-GP). This recombinant (VSV-GP) has been tested in several *in vitro* and *in vivo* studies concerning neurotoxicity, systemic safety, off-target toxicity[28], oncolytic activity in several cancer types (glioma[28], ovarian cancer[29], malignant melanoma[30] and prostate cancer[31], it's abilities to circumvent humoral immunity[32] as well as it's modulation abilities in tumor microenvironment[33]. Those studies have proven VSV-GP to be a potent candidate to boost oncolytic viruses into clinical translation and to elevate awareness of this treatment opportunity.

VSV-GP turned out to be a safe oncolytic agent in terms of neurotoxicity. As the glycoprotein inherent to wildtype VSV is exchanged as mentioned above neurotropism is no longer mediated. Systemic application of the viral vector (10^9 PFU in immunodeficient CD-1 mice) led to a minor loss in body weight that the mice regained in only a few days after administration[28]. Off-target toxicity has examined by measurement of serum ALT, -creatinine and measurement of viral RNA by RT-PCR in blood, brain, heart, kidney, liver, lung and spleen. For the VSV-GP vector no off-target toxicity has been observed[28]. The oncolytic effect of the new vector was altogether promising but varied dependent on the tissue type. An additional feature that this recombinant virus provides is the ability to successfully circumvent humoral immunity what allows for a repetitive administration scheme[32]. Specifications will be given in the Discussion.

Summarizing this overview, it can be concluded that there are different approaches to make use of oncolytic viruses as anti-cancer agents. So far all concerns about the tested viruses come down to a narrow set of obtacles. Namely, limited effectivity of the virus either due to pre-existing immunity, reduced susceptibility of the tumor cells to viral infection or a fast clearance of the oncolytic agent by the patient's immune response and safety concerns due to toxic side effects or a reduced sensitivity of the virus to Interferon and therefore the host's ability to restrict the infection.

2.4. Immune Reactions to Viral Infections and Immune Evasion in Cancer

A critical point in OV therapy is the clearance of the viral vector by the immune system. It is both, desired immediately in not-targeted cells and in the targeted tumor cells, but only at a specific point in time. The optimal point in time for immune interference of virus infected tumor cells would be when the virus has gained access to a majority of tumor cells. At this point the immune response could effectively support the virus in killing tumor cells and clear the virus from the system. Thus, a fast viral replication cycle, rapid viral

spread inside the tumor tissue and a delayed but strong immune response against viral and tumoral antigens are desirable for a successful treatment.

When the OV is injected for treatment, it gets in contact with a variety of tissue types. In a selective process, a combination of viral tropism and innate immunity defines which cells can be infected. The virus attaches to specific host cells according to its own tropism and gets removed from some of these cells by the body's "first line of defense"[34], the IFN response. The presence of pathogens inside the body is recognized by pattern recognition receptors (PRR) to be found mainly on cells of the innate immune system such as dendritic cells (DC), macrophages and natural killer cells (NK cells), but as well on T and B Lymphocytes and non-immune cells, such as epithelial cells or fibroblasts [35]. Among others, Toll-like receptors (TLR) 3, 7 and 8 and retinoic acid inducible gene 1 (RIG-1) belong to the class of PRR. These receptors recognise highly conserved viral structures, known as pathogen-associated molecular patterns (PAMPS) [36], and induce a Type I IFN response [37]. An infected cell with an intact IFN signalling pathway will react to viral infection with transcription of IFN-stimulated-genes (ISG) and translation of ISG-encoded proteins, leading to an antiviral state in the infected cell and neighbouring cells [38]. This antiviral state is characterised by direct interference and reduction of viral replication through ISG-encoded proteins and an upregulation of MHC-I molecules on neighbouring cells. Early after infection, the circulating virus is inactivated by DCs, macrophages and NK cells that recognize PAMPS and engulf the virus via phagocytosis. However, once inside a host cell, the virus becomes invisible to cells of the innate immune system. MHC-I molecules, which display antigens from the inside on the cell surface to T cell receptors (TCR), become the identification mark for virus infected cells. Some viruses try to avoid recognition by downregulation of the production of MHC molecules. Those cells displaying down-regulated MHC molecules are destroyed by NK cells. Activated T cells and NK cells release cytotoxic factors that induce apoptosis in infected cells [14]. CD8 is a co-receptor for MHC-I molecules on T cells and some NK cells. It activates T cells, when bound to viral antigen on MHC-I molecules, and the T cell matures into a $CD8^+$ cytotoxic T cell. These kill the infected cell by granzyme-mediated induction of apoptosis or the extrinsic apoptotic pathway. Viral antigens that have been internalised by an antigen-presenting cell (APC) are displayed in MHC-II molecules on the surface. These antigens can be recognised by $CD4^+$ T helper cells, which activate other cells of the adaptive immunity. T cell receptors are additionally associated with the CD3 complex, that is necessary for signal transduction and amplification [39]. Another component of adoptive immunity is the B-lymphocyte compartment. When a naïve, membrane-bound B lymphocyte gets activated by a pathogen and a helper T cell, it starts to differentiate into either a memory cell or an effector cell, which then produces soluble antibodies with the same receptor as the naïve B lymphocyte[40]. Effector cells mature into plasma cells and continuously secret antibodies, that inactivate a pathogen either by neutralization through binding to vitally important sites by agglutination, thereby creating clumps that are attractive for phagocytosis or marking pathogens for the complement system [41].

Although tumor cells emerge endogenously and therefore do not carry exogenous antigens [42], there are innate and adaptive immune responses against cancer cells. This requires a discrimination between self-antigens and

altered-self-antigens [43]. Similar mechanisms as in pathogen eradication should also clear malignant cells from the system, but tumor cells, as well as many viruses, establish strategies for immune evasion. A process known as "immunoediting" describes immune evasion by random mutations during the high turnover in cancer cell proliferation. Mutations can, by chance be related to tumor antigens creating a heterogeneity that exhausts immune capacities and leads to clinical cancer. Other strategies include production or attraction of regulatory T cells as $CD4^+CD25^+$ that possess immune suppressive functions, productions of immune suppressive cytokines, such as TGF-β, TNF-α, CSF-1 and interleukins, and also downregulation of MHC-I molecules or expression of programed cell death 1 ligand 1 (PD-L1) [44]. However, some of these modifications also allow an effective invasion of the tumor cells by the oncolytic virus.

Tumor cells often show altered IFN pathways to impede lymphocyte function and thus be protected from immune recognition and to support tumor progression [15]. One mediator for the impaired IFN function is the downregulation of RIG-I that can be found in HCC cells. This is moreover connected with a poor prognosis for the patient [45]. Other studies suggest that an activated Ras/Raf 1/MEK/ERK pathway, which usually regulates gene expression and cell proliferation, leads to a defect in the IFNα-mediated response in about 30% of all cancers, many of them with limited therapeutic options[46]. Since IFN interferes with viral replication, these features allow an effective invasion of the tumor by the OV, leaving the surrounding tissue uninfected.

2.5. Problems and Beneficial Effects of Immune Interference

The previous sections outlined what powerful weapons OV's can be in the fight against cancer and the immune reaction to viral infection as well as tumoral immune evasion. As a matter of fact, the immune response can be both, an enemy and ally for cancer treatment with oncolytic viruses. The viro-immunotherapy approach attempts to overcome the obstacles to reinforce OV therapy with all the advantages of immunological interference.

To begin with, the immune response in healthy cells is what makes the virus tumor-specific in the first place, but a very important factor in viro-immunotherapy is the limitation of viral efficacy because of the fast clearance by the immune system. This confronts the application of viro-therapy with a number of challenges that need to be addressed. For some viruses, e.g. vaccinia virus or measles virus, this might be a bigger threat than for others because of pre-existing immunity in human patients from vaccination programs. However, the use of animal viruses, that usually do not face pre-existing immunity in the general human population, still encounter the challenge of sufficient delivery to the tumor target. Although systemical application of viral vectors would be favourable to treat metastatic lesions, they tend to be cleared from the bloodstream before an effective amount of virus can accumulate in the tumor bed. Another problem that arises from a strong immune response is the limited efficacy of multiple-dosing-strategies due to the creation of virus-specific neutralizing antibodies[47]. There are attempts not only to evade immune cells to reach the tumor, but to use them as a transport vehicle. This allows the virus to stay hidden in an immune cell that can even be directed against tumor antigens and be transported safely to its target. When the OV reaches the tumor and

successfully invades the cell, it is capable of directly killing the cell. In so doing, it induces an immunogenic cell death, in contrast to the silent cell death a normal apoptotic cell undergoes, and tumor-associated antigens (TAA) derived from cell fragments are released. In this manner or by loading the virus with genetic information of TAA the virus is able to break immune tolerance and induce an anti-cancer immunity[48]. Additionally, the production of chemokines during viral infection can create an inflamed status in the tumor bed and attract immune cells for an anti-tumor response. Once an immune response is established, it is possible to treat the primary lesion, and potentially, metastatic lesions, and the production of memory cells could provide protective immunity against tumor rechallenges. As cancer cells are basically "self-cells", a major concern for the treatment targeting a TAA is the induction of autoimmunity [49]. It can be concluded, that it is an appealing idea to trigger the body's own defense mechanisms to heal cancer, but it is necessary to find the right balance between the destructive and supportive power of immune interference.

2.6. Parental Viruses

2.6.1. Newcastle Disease Virus

As a single-stranded RNA virus with negative polarity NDV is taxonomically classified in the order of *Mononegavirales*. Within this order it belongs to the family of Paramyxoviridae and as such it contains the genome structure typical for this virus family [50]. The genus Avulavirus indicates the natural host of NDV, which is a wide variety of bird species. Its shape is spherical to pleomorphic and it has a size of 150-300nm [51](Figure 1).

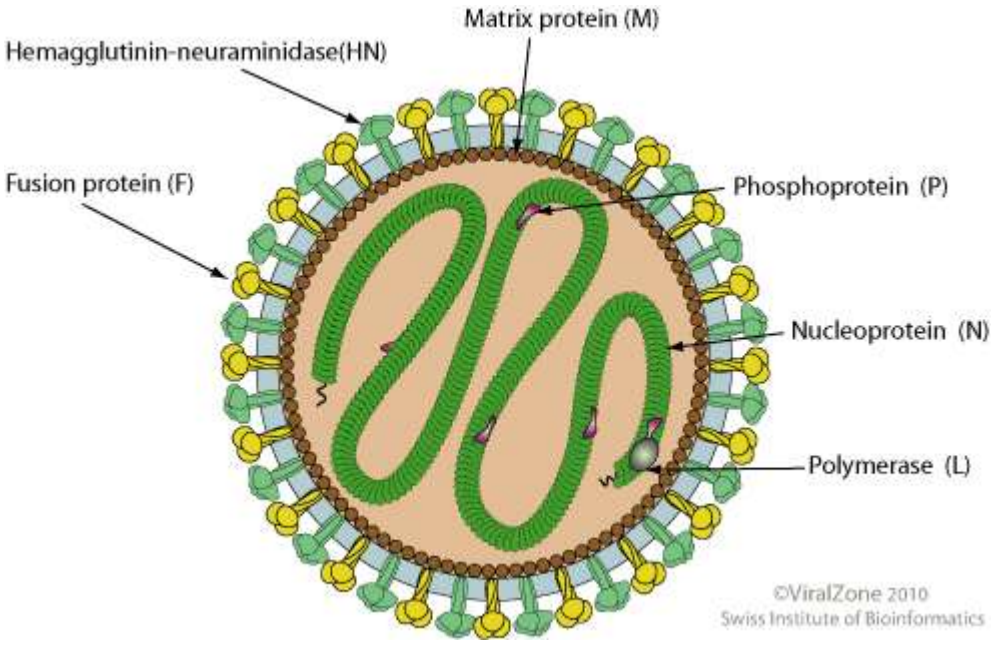

Figure 1: Virion of Newcastle Disease Virus

Spherical shaped virion consisting of viral envelope with integrated membrane proteins surrounding the nucleocapsid. The viral RNA, surrounded in a complex of nucleoprotein, phosphoprotein and large protein, comprise the nucleocapsid together with the M protein.

Source: Le Mercier, P.; Hulo, C.; Masson, P. (2010), [Avulavirus-Virion]. ViralZone-ExPASy, Retrieved 17.01.2018, from https://viralzone.expasy.org/84?outline=all_by_species

2.6.1.1. Epidemiology and Newcastle Disease

The first reported outbreaks of this disease go back to Scotland in 1898, when high losses of poultry were observed while waterfowl appeared to be unaffected [52]. Nowadays Newcastle disease is known to be endemic in many countries. While distribution via wild animals plays a minor role in spread of the virus, the main problem is trade with latently infected poultry, eggs or frozen products from poultry[53]. Once the virus is established in a herd, the main infection route is close contact to infected individuals or their feces[36].An airborne infection by dust is also possible over short distances[54]. It appears as a disease with variable pathogenicity. In fact NDV strains can be categorized in one of the three pathotypes: lentogenic with no case of disease, mesogenic with intermediate pathogenicity and velogenic with severe pathogenicity [55]. More than 250 avian species are susceptible to NDV [56], but outbreaks of Newcastle disease gain most attention in infected poultry in which it can lead to severe symptoms and cause serious damage to the poultry industry. Virus shedding occurs via all secretions from infected birds and can additionally be passed on to chicken embryos by ovarian transfection. Depending on the pathogenicity of the virus strain, the symptoms range from unapparent disease to reduced egg production, fever, gastrointestinal symptoms and respiratory symptoms to neurological symptoms and peri-acute death. In humans, there is a certain zoological potential with conjunctivitis and mild flu-like symptoms, but it is only reported in persons exposed to high virus concentrations, such as farm workers or veterinarians in close contact with infected material or individuals [57].

2.6.1.2. Genome and Viral Replication Cycle

NDV's genome consists of six genes (Figure 2) comprised of 15186 nucleotides in a highly preserved order. Like all paramyxoviridae, these genes encode the nucleocapsid protein (N), phosphoprotein (P), matrix protein (M), fusion protein (F), haemagglutinin-neuraminidase (HN) and large polymerase protein (L).

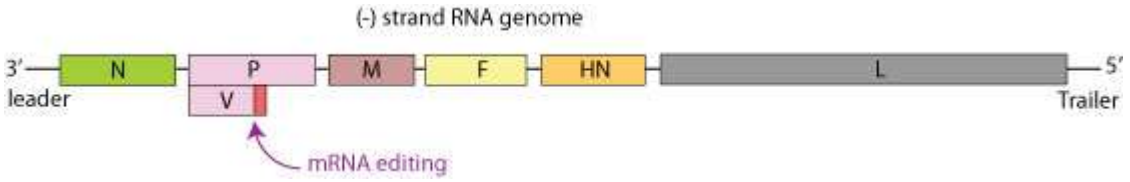

Figure 2: Genome of Newcastle Disease Virus

Negative sensed, single-stranded RNA genome of Newcastle Disease Virus. The six Genes N, P, M , F, HN and L in the highly preserved order. An mRNA editing step renders the possibility of expressing a V protein from the P gene.

Source: Le Mercier, P.; Hulo, C.; Masson, P. (2010), [Avulavirus-Genome]. ViralZone-ExPASy, Retrieved 17.01.2018, from https://viralzone.expasy.org/84?outline=all_by_species

These genes are interrupted by non-transcripted intergenic nucleotide sequences (junction sequences) whose purpose seems to be the creation of a transcription gradient. Each junction sequence has three sections, the gene-end section, intergenic section and gene-start section [55]. With each junction sequence that the transcription machinery has to overcome, it is more likely to fall off the RNA-strand, and therefore proteins

on the 3'-end are much more often transcribed than proteins on the 5'-end. The production of continuous end-to-end antigenomic matrices is dependent on the amount of transcribed N protein, which prevents interrupted transcription at the gene-end section of junction sequences. These continuous matrices can finally be used as matrices for new virus genomes. A distinctive feature of the NDV genome is an RNA-editing step that integrates "non-templated G-residues" [55] into the P gene, which leads to the expression of an additional V protein. The V protein acts as Type I IFN antagonist via STAT1 degradation in infected cells and is crucial in highly virulent NDV strains [58]. This antagonism is species-specific for avian cells lines and is an important determinant for the avian tropism of NDV. In human cell lines, NDV shows a strong IFN response [55].

The viral attachment to a targeted cell is accomplished by the HN protein. HN possesses two binding sites for sialoglycoconjugates displayed on the host cells surface. Site I mediates receptor binding and sialidase activity, while site II acts as a binding-site only [59]. Once HN binds sialic acids, the F protein can attach to the membrane and generate fusion of the viral envelope with the host cell membrane. The F protein exists as an inactive precursor (F0). After cleavage by host cellular proteases, the F protein splits into two active disulfide-linked polypeptides (F1, F2)[55]. The hydrophobic N-terminus of the F1-subunit connects to the host cell membrane. The conformational change triggered by the F1- and HN binding mediates membrane fusion [50]. In fact, the cleavage site of F is known to be responsible for the pathotype of NDV. Whereas lentogenic NDV strains have monobasic cleavage sites cleaved by proteases mostly found in the respiratory and digestive tract, velogenic strains have multibasic cleavage sites cleaved by ubiquitous proteases, which allows systemic infection [55]. When the first steps, viral attachment and membrane fusion, are completed, viral RNA can enter the host cell cytoplasm where replication of the genome takes place. Here an RNA-dependent RNA-polymerase (RdRp) complex, consisting of P protein and L protein, transcribes N protein-bound RNA into mRNA [60]. The N protein coats RNA to prevent nuclease digestion. It shows two major domains. N_{Core}, a N-terminal region and N_{Tail}, a C-terminal region. N_{Core} binds RNA while N_{Tail} mediates the connection between the N-RNA complex and the P protein [61]. The P protein on the one hand leads to connection of the N-protein-bound RNA and the RdRp complex and thus to transcription of the viral genome into mRNA. On the other hand, a complex of P protein and unassembled N monomers seems to lead to a switch from transcription to synthesis of progeny RNA [60]. As already described above, junction sequences between structural genes create a transcription gradient in which proteins encoded in genes near the 3'-end are more often transcribed than proteins encoded near the 5'-end. This causes a high number of transcribed N monomers, needed for the switch to synthesis of continuous (-) RNA. This is necessary to form the genomes of the following generation of viruses. After protein translation by host cell ribosomes, assembly and budding of newly synthesized virus follows. For this purpose HN, F and N are transported to the host cell membrane where they accumulate. Interactions between P protein, N-RNA template and L protein form the nucleocapsid, and further interactions between the N and M protein incorporate the nucleocapsid into new virus particles [60].

2.6.1.3. Virus-Induced Apoptosis and Oncolytic Activity

As a potent oncolytic vector, NDV can reliably kill tumor cells. Several studies revealed that NDV- infected cells undergo apoptosis showing typical signs such as "syncytium-formation, rounding and increased granularity" [62]. A variety of direct and indirect mechanisms might be involved in this process, partly depending on the infected cell line and virus strain. The intrinsic and extrinsic apoptotic pathways seem to play a dominant role, but also ER stress pathways, receptor tyrosine kinase pathways and indirect mechanisms such as chemokine and cytokine release and thus, activation of the innate and adaptive immune response [55].

A study by Elankumaran et al. showed that induction of apoptotic cell death induced by NDV is independent of intact IFN signalling pathways. Moreover they conducted several experiments to gain insight into the importance of different apoptotic pathways in NDV-infected cells. Different NDV-infected cell lines showed different levels of TNF- α, but even the highest titers observed did not necessarily mediate apoptosis. A time course study of TRAIL showed that TRAIL mediated apoptosis is a late event and begins 14 h post infection (p.i.). TNF- α and TRAIL are members of the death receptor family. Together with the Fas-associating protein and proximity of caspase-8, they mediate the extrinsic apoptotic pathway. Caspase-8 was shown to be activated rather late at 48 h p.i. in some tumor cell lines, and there was no caspase-8 activation in colorectal cancer cell lines (CaCo2, HT29). Therefore, caspase-8 seems to be activated, but not the initiator of apoptosis. Investigation of the intrinsic apoptotic pathway by localization of cytochrome c after a drop in mitochondrial membrane potential in NDV-infected cells showed a two-fold increase of cytochrome c in the cytosol. Additionally, there was no activation of inhibitors of apoptosis, but rather, a caspase-9 activation with significant levels 6 h p.i. It can be summarized that NDV infection leads to a destabilization of mitochondrial membrane potential and activation of caspases-9 and -3 and thus to an activation of the intrinsic apoptotic pathway. Subsequently, caspase-8 and the extrinsic pathway are also activated [62]. Furthermore, sequencing of NDV's genome indicated the existence of pro-apoptotic Bcl-2 homology-3 (BH3) domain-like regions in the M, F and L protein [55], which can be activated by caspase-3 and induce the intrinsic apoptotic pathway.

Indirect induced tumor cell killing is accomplished by activation of innate and adaptive immune responses. Infection of murine macrophages with NDV showed enhanced production of macrophage enzymes and TNF-α [55]. Monocytes were able to induce apoptosis in tumor cells by activation of TRAIL after infection[63], and NK cells stimulated with NDV showed enhanced cytotoxicity against tumor cells[55]. In fact, NDV-HN is known to have powerful immunogenic effects, making HN a valuable component for antitumor vaccines [64].

2.6.1.4. Genetically Engineered NDV as Anti-Cancer Agent

Since the early 1990's, when recombinant DNA technology became a laboratory standard and genetical engineering of viruses a reasonable perspective, research in this field started its second upturn [1]. The number of newly designed OVs that address specific problems from virus delivery to decreased toxicity to altered efficacy, increases from year to year.

Concerning NDV, various modifications have been engineered to enhance to its properties as an oncolytic agent. Some attempts deal with the enhancement of NDV virulence. The more virulent the strain, the more effective its intratumoral spread, replication and apoptosis. Thus, higher virulence correlates with improved oncolytic properties of NDV, making velogenic and mesogenic strains lytic in human cancer, whereas lentogenic strains are often classified as non-lytic in human cancer[55]. As explained above the cleavage site in the F-protein (monobasic in lentogenic strains and polybasic in velogenic strains) determines the virus's pathogenicity. Building on this, lentogenic NDV Hitchner B1 strain was engineered with a polybasic cleavage site in the F-protein (F3aa), and an additional point mutation at base pair 289 in the F protein from leucine to alanine (L289A) was introduced to enhance fusogenicity. The result is rNDV/F3aa (L289A), which results in enhanced oncolytic effects *in vitro* and *in vivo*[65]. *In vitro*, a significantly higher syncytial index in HCC and normal cell lines could be observed in cells treated with rNDV/F3aa (L289A) compared to rNDV/F3aa (Figure 3). *In vivo* treatment led to only mild and transient body weight loss and alteration of liver enzymes, which returned to normal by day three after injection. Moreover an increase in tumoral necrotic areas was observed, as well as a prolonged survival in HCC-bearing rats. Two animals in the rNDV/F3aa (L289A)-group even showed complete tumor regression [65]. Another step in the same direction is a study by Park et al., where the anti-tumor activity of IFN-sensitive NDV Hitchner B1, modified to express a mammalian IFN-antagonist, the NS1 protein from Influenza A, was investigated[66]. Their hypothesis, a repressed immune response would support viral replication and intratumoral spread, could be confirmed in human and mouse melanoma cell-lines. A comparison showed that NDV(F3aa)-NS1 is as effective as its parental virus NDV(F3aa). At low MOIs it appears to be more effective than NDV(F3aa). *In vivo* studies on melanoma-

bearing mice treated with NDV(F3aa)-NS1 confirmed a decelerated tumor growth compared to NDV(F3aa) and PBS [67].

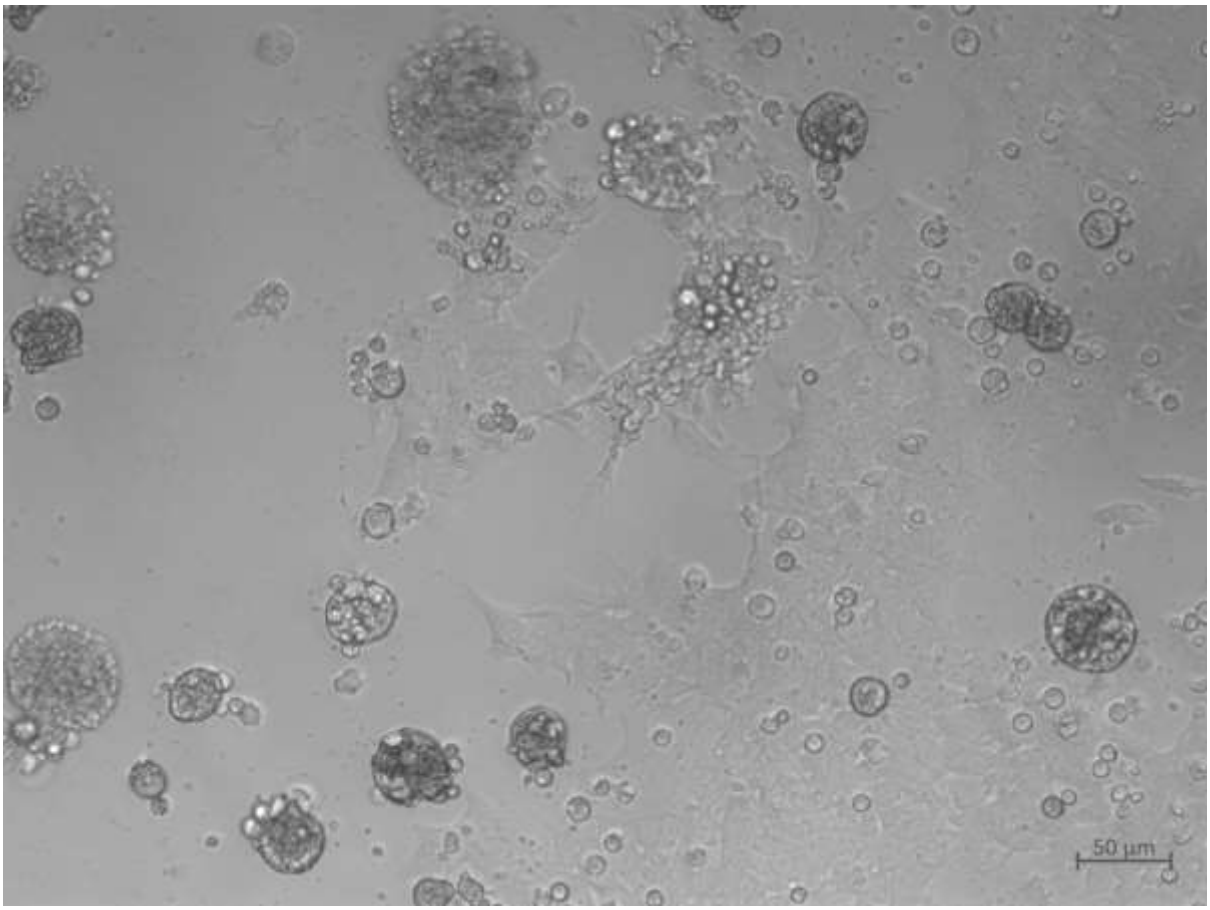

Figure 3: AGE1.CR pIX cells forming syncytia from NDV/F3aa (L289A) infection

Photo microscopy of AGE1.CR.pIX cells infected with NDV at an MOI of 0.001 and 48h after infection. Images were captured under 100x magnification.

The idea of NDV expressing apoptin, a proapoptotic protein from chicken infectious anemia virus provides another strategy to improve the oncolytic effect, but is potentially problematic. Experiments with this recombinant NDV strain demonstrated that high MOI's are necessary to improve induction of apoptosis compared to the parental virus. Also this treatment results in an early cell death of the host cell, which impedes multi-cycle replication and further spread of the virus into the tumor tissue [68].

Another exciting approach is to arm the viral vector with immune agents such as cytokines or complete antibodies. An *in vitro* study with NDV expressing human IL-2 showed stimulation of T-cells in a tumor-neutralization assay. Moreover, an increased expression of activation marker CD69 and increased production of IFN-γ was noted. *In vivo* experiments in mice with subcutaneously implanted colon carcinoma indicated a clear advantage of rNDV/F3aa-IL-2 over rNDV/F3aa, with a drastic reduction in tumor size and partial and long-lasting remission. Mice that underwent complete tumor regression were furthermore protected from ongoing tumor challenge [69]. Pühler and colleagues demonstrated that it is possible to integrate two transgenes into the genome of mesogenic NDV-MTH68, leading to expression of a complete monoclonal antibody

(rNDV-MTH146). The transgenes have been inserted between NDV-F and NDV-HN and encode the heavy and light chain of immunoglobulin G (IgG) directed against the extradomain-B of fibronectin (ED-B fibronectin), a tumor specific antigen. *In vitro* experiments demonstrated that rNDV-MTH146 does not impede viral replication or tumor selectivity. Indeed only tumor cells were able to produce functional antibodies after infection and also cell lysis has only been observed in tumor cells [70].

A very promising approach is to employ an OV carrying tumor antigen in a vaccination scheme to mediate an immune response against the tumor. NDV vectors expressing tumor-associated antigens (TAA) have been used in this regard. The same group that worked with NDV expressing human IL-2, designed rNDV/F3aa-minigal, an NDV encoding for a β-gal-specific $CD8^+$ T cell epitope. Experiments conducted *in vivo* confirmed the importance of specific T-cell responses as a means to attack the tumor. They treated tumor-bearing nude mice, with a known deficiency of T cells, and immunocompetent BALB/c mice with PBS, rNDV/F3aa-IL-2 or rNDV/F3aa-minigal. Their results showed no survivors in the T cell-deprived mice but a clear survival benefit in both virus treated immunocompetent groups. A combination therapy of both recombinant viruses however showed tumor regression in 90% of the treated mice compared to 50% in r NDV/F3aa-minigal injected mice[71].

Considering the endless number of possibilities recombinant oncolytic viruses provide for cancer therapy it is a promising path for future research in this field. It is clear now that NDV is a potent oncolytic viral vector with no severe toxicity concerns in mammalian species, but there is a risk of treated patients shedding a low amount of virus, thereby creating an environmental risk [72]. Previous studies indicated that mesogenic and velogenic strains are more effective as anti-cancer agents. However, this poses a substantial risk of an outbreak of disease among bird populations, and could jeopardize the poultry industry. In fact, this problem put virulent NDV strains on the list of "USDA select agents and toxins" severely limiting the further development of NDV for clinical application.

2.6.2. Vesicular Stomatitis Virus

VSV like NDV, is a non-segmented, negative-sense RNA virus, and as such, in the order of *Mononegavirales*. It is classified in the family of Rhabdoviridae and genus Vesiculovirus. It comprises a broad host range, including vertebrates, as well as insects and plants. The two major serotypes, VSV-Indiana (VSV-IN) and VSV-New Jersey (VSV-NJ), infect horse, cattle, swine, mosquitos and sandflies. VSV has the distinct bullet-shaped profile, characteristic for the virus family[73], and a size of 70x200nm[74]. The nucleocapsid consists of the viral RNA that lays surrounded tightly by up to 1200 molecules of N protein and fewer L and P proteins in a helical complex coated in a layer of M protein (Figure 4). The viral envelope is made of a phospholipid bilayer from the host cell, which is left on the virus after budding, and trimers of Glycoprotein (G protein) build spikes on the outside of the lipid membrane [75].

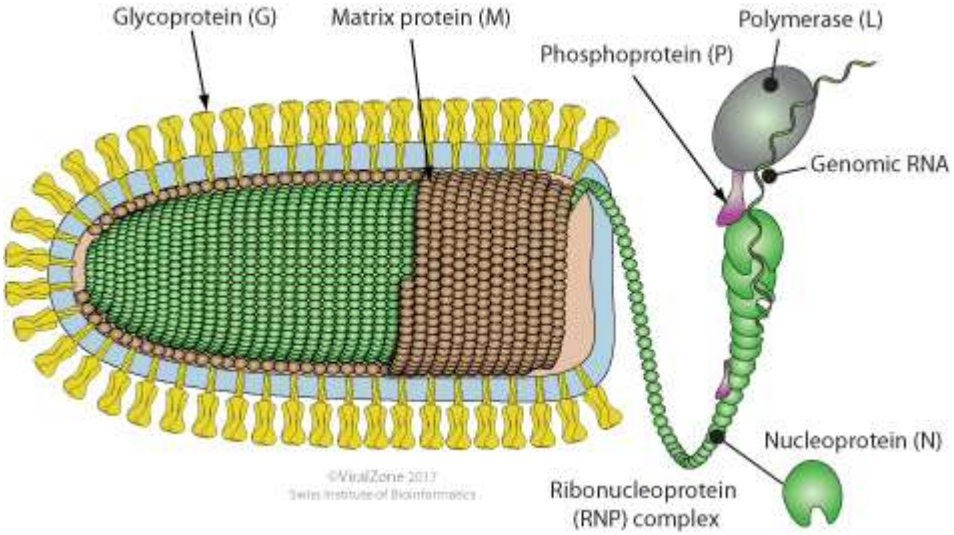

Figure 4: Virion of Vesicular Stomatitis Virus

Bullet-shaped virion of VSV. The envelope equipped with trimers of G protein surrounds the nucleocapsid. Viral RNA and the nucleoprotein are combined as ribonucleoprotein core. Accompanied by L, P and M protein they build the nucleocapsid.

Source: Le Mercier, P.; Hulo, C.; Masson, P. (2010), [Avulavirus-Genome]. ViralZone-ExPASy, Retrieved 17.01.2018, from https://viralzone.expasy.org/84?outline=all_by_species

2.6.2.1. Epidemiology of Vesicular Stomatitis

VSV was first reported as a disease in 1916 in the US. In retrospect, it might also have occurred in 1862 during the US Civil War in army horses. VSV-IN and VSV-NJ are enzootic in North-, Central and South America, and outbreaks have been reported occasionally until 1995 [73]. In cattle, horses and swine VSV causes vesicular stomatitis, a disease accompanied by fever and vesicles on the oral mucus membrane, feet and teats. Transmission of VSV is accomplished by infection via arthropods, or direct contact to infected material, such as water, food or milking machines [76]. Other than a decrease in productivity of infected animals, the disease results in low mortality rates. The main problem with VSV infections is its clinical similarity to Foot and Mouth Disease, which is on the OIE list of notifiable diseases (OIE listed diseases, 2018). VSV-IN and VSV-NJ possess a mild zoonotic potential. Infections can lead to flu-like symptoms in humans. Another vesiculovirus, Piry virus, causes mild symptoms with headaches, myalgia and arthralgia over three to four days and is endemic in Brazil. Also common in Africa and Asia, is Chandipura virus. In India, there is a high prevalence of animals in different species infected with Chandipura virus. It is also known to be zoonotic and the symptoms are similar to Piry virus infection, besides one reported case of encephalitis caused by Chandipura virus in an eleven-year-old indian girl [77].

2.6.2.2. Genome and Viral Replication

As NDV and VSV are both in the order of *Mononegavirales* there are striking similarities in their genome structure and replication. VSVs genome has five genes composed of 11000-12000 nucleotides encoding five proteins, the N protein, P protein, M protein, G protein and L protein (Figure 5). Throughout the *Mononegavirales*, all viruses are transcribed by sequentially interrupted mRNA synthesis, leading to a transcription gradient[78] as described for NDVs "Genome and Viral Replication Cycle".

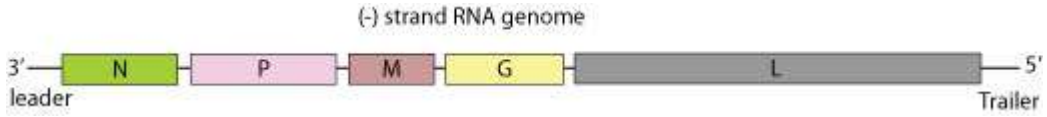

Figure 5: Genome of Vesicular Stomatitis Virus

The negative sensed, single-stranded RNA encodes 5 genes: the Nucleoprotein (N), phosphoprotein (P), matrix protein (M), glyco protein (G) and large protein (L).

Source: Le Mercier, P.; Hulo, C.; Masson, P. (2010), [Avulavirus-Genome]. ViralZone-ExPASy, Retrieved 17.01.2018, from https://viralzone.expasy.org/84?outline=all_by_species

One advantage that makes VSV a favoured OV is its ability to enter a broad range of cells, giving VSV a pantropic infectivity. Viral attachment and entry are performed by the G protein. Finkelsthein et al. conducted an experiment in which soluble low density lipoprotein receptor (LDLR) completely inhibited entry of VSV into the host cell by binding to the virus or a cellular VSV receptor, when given before VSV challenge or at the same time. The results indicated that the LDL receptor is the major entry receptor for VSV on the host cell surface. The ubiquitous expression of the LDLR family on various cells also explains the broad tropism of VSV [79]. Although VSV is an extensively investigated virus, there are still parts of the entry process, which are not yet clarified. It is known that the trimeric associated G proteins on the virus surface mediate viral attachment, as they bind to LDL receptors. This leads to endocytic internalization of VSV via the clathrin-mediated endocytic route [80]. The acidic milieu inside the endosome triggers a conformational change of the G protein at a pH in the range between 6.2 and 5.0. Each monomer in the VSV-G trimer has a tertiary structure that allows the division into four domains (I-IV). Of these, domain IV is the fusion domain, which contains fusion peptides on two internal loop regions. With increasing acidity of the endosomal milieu, the G protein becomes more hydrophobic, and the fusion loops penetrate the endosomal membrane leading to fusion with the viral envelope [75]. After viral fusion is completed, the nucleocapsid can enter the cytoplasm of the host cell, where VSV replicates. Transcription is accomplished by the RNA-dependent RNA polymerase (RdRp) complex consisting of P and L protein. N protein-coated RNA serves as a template for this complex. Transcription begins with synthesis of a plus-strand leader-RNA whose purpose is still unknown [81]. As already described in section "Newcastle Disease Virus", mRNA of the five genes is synthesized following a transcription gradient caused by intergenic sequences that interrupt the process of translation. The number of copies of each proteins in each nucleocapsid illustrates that different proportions of proteins are required for the construction of a new virion. In a completed nucleocapsid are 1250 copies of N, 470 copies of P and only 50 copies of L, as it is transcribed the least. The RdRp complex also functions as a capping enzyme for mRNA and caps during mRNA synthesis and polyadenylates when reaching the termination-sequence $AUACU_7$ at the end of a gene. In this way, the five genes are transcribed, capped and polyadenylated before release from the transcription complex. The switch from transcription of mRNAs to transcription of a full-length genome with positive polarity, which can be used as a template for progeny RNA, is again dependent on the presence of N protein. M protein may also play a role in the regulation of mRNA synthesis [82]. At early points in time during replication, newly synthesized nucleocapsids are distributed in clusters in the perinuclear region. Transport of the viral components to the cell membrane, where budding takes place, is accomplished via active transport by actin filaments as well as microtubules [83]. The G protein, is transported first into the

endoplasmic reticulum for glycolysation and then transported to the cell membrane [82]. Near plasma membranes, selected nucleocapsids and free cytosolic, as well as membrane bound M protein form a nucleocapsid-M protein complex [73]. M protein acts hereby as an adaptor between G protein present on the host cell membrane and nucleocapsids on the inside and, therefore, mediates budding of new virions from an infected cell into neighboring cells [82]. Progeny viruses are internalized into neighboring cells via endosomes, which they enter again after acidification of the endosome [84]. Compared to other viruses, VSV has a very short replication cycle and first assembly of progeny occurs at approximately 2-3h post infection [5].

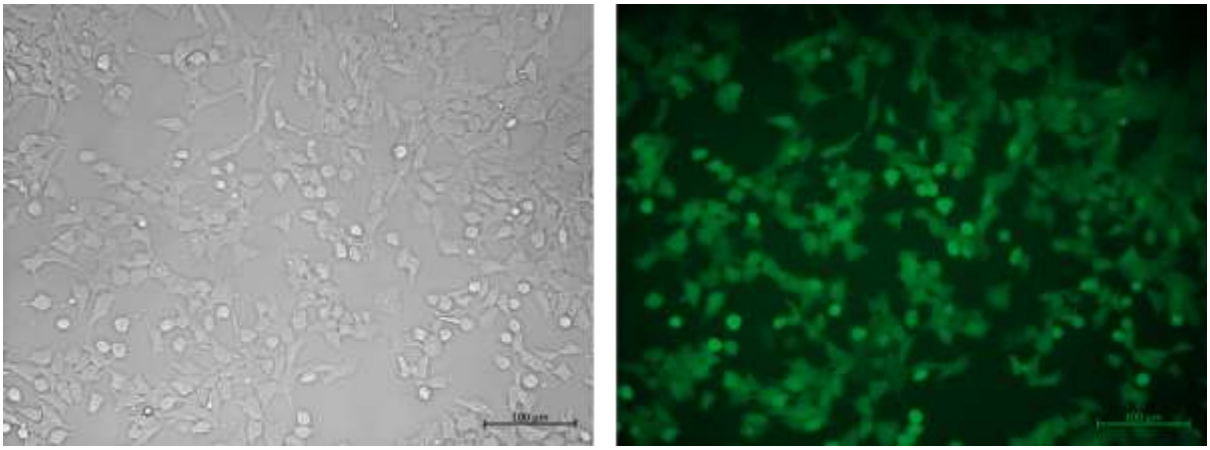

Figure 6: AGE1.CR pIX cells showing CPE and GFP expression after infection with VSV-GFP

Photo microscopic picture of AGE1.CR.pIX cells expressing GFP at 18h after infection with rVSV-GFP at on MOI of 0.01. The picture was captured under 100x magnification.

2.6.2.3. VSV Induced Oncolytic Activity and Neurotoxicity

VSV is known to be a potent oncolytic agent, and an important aspect of the cell lysing activity is the M protein [85]. Its natural purpose is to impede cellular gene expression and thus prevent antiviral activity, such as IFN production. It inhibits export of mRNA from the nucleus by interference with two important proteins of the mRNA export machinery, Rae1 and Nup98. These proteins also play an important role in spindle assembly during mitosis. Rae1 is a Ran-regulated factor for spindle assembly. It is crucial in formation of organized microtubules in the nucleus to form the spindle apparatus. Nup98 can enhance binding between Rae1 and importin β [86], which is a regulator of Ran-dependent spindle assembly factors [87]. M protein interacts with a Rae1-Nup98 complex, which impedes formation of a functioning spindle in mitotically active cells, leading to cell death during metaphase. As tumor cells have high mitotic indices, they preferentially undergo cell death when infected with VSV, as compared to normal cells[85]. This feature keeps infected cells from alerting the immune system and is, together with the fast replication cycle, responsible for the high production yields of VSV in infected cells. Another mechanism involved in VSV-induced cell death is the induction of the intrinsic pathway of apoptosis by caspase-9 activation [88].

That an intact IFN response in healthy cells is an effective instrument against viral infection is impressively shown in the central nervous system (CNS), where VSV infection leads to neurological symptoms and death at comparatively low virus titers. Neurons are highly developed cells with high metabolic rates and at the same time a very low capacity for regeneration. Virus induced cell death has much more impact in this isolated environment and is tolerated less than in regenerative tissues. Another component that increases the effect on infected cells of the CNS is the blood brain barrier. Once a virus overcomes this security mechanism that allows entry only to selected components of the blood stream (gases, glucose, substances with high lipid solubility [89]), they are effectively shielded from immune functions of the peripheral immune system as well. Detection of viral infections is all the more difficult as there is no expression of MHC-I molecules in the brain and also MHC-II molecules can only be found on microglia and astrocytes, dependent on TNFα and IFN-γ, which are not present at early stages of viral infection in the CNS [90]. If present, inflammatory cytokines from infected glial cells can induce encephalitis [16].These conditions emphasize why VSV can lead to severe neurotoxicity accompanied with paralysis and excitability in immunocompetent Buffalo rats at doses higher than $1x10^7$ PFU administered via the hepatic artery [91].

2.6.2.4. Geneticallly Engineered VSV

Again, there are several recombinant versions of the wild type virus designed to either enhance oncolytic abilities, diminish safety concerns or add completely new features to the viruses repertoire.

Many of these strategies aim to improve the profile for safety and oncoselectivity. There have been studies with VSV expressing mutant versions of the M protein to prevent healthy cells from being defenseless against viral infection. As the M protein effectively inhibits cellular transcription and RNA transport from the nucleus into the cytoplasm, it is potentially cytotoxic even in a healthy cell. The idea is that recombinants with a mutant M protein can still replicate productively in tumor cells, which are defective in the IFN pathway, and at the same time can be cleared by normal cells. Studies with rVSV*M_QG_{133}, which is VSV with a mutant M protein and fusion-defective G protein showed enhanced IFN production *in vitro* compared to rVSV-GFP and continuing propagation of infected Vero cells [92]. Experiments conducted *in vivo* in immunocompetent, tumor-bearing mice showed that treatment with rVSV-M(mut)-mp53, a VSV with mutated M protein and murine tumor suppressor, p53, even led to elevated titers of antitumor $CD8^+$ T cells, which makes this recombinant an attractive candidate for viro-immune therapy [93].

Another approach is alteration of the VSV G protein. In rVSV-CT1 and rVSV-CT9-M51, the G protein has deletions in the cytoplasmic tail reducing it from 29 amino acids to 1 and 9 amino acids, respectively. rVSV-CT9-M51 has additionally a deletion of the amino acid at position 51 in the M protein (methionin). Both recombinant viruses are attenuated compared to rVSV-GFP and show a much better safety profile. Intracebral injection of the viruses into immune competent 16-day-old mice showed significantly prolonged survival in the rVSV-CT9-M51 group. Both attenuated viruses also led to reduced neuroinvasion compared to rVSV-GFP after intranasal inoculation, with survivors showing no neurological symptoms. rVSV-CT9-M51 also retained its oncolytic abilities in multiple human and rodent tumor cell lines *in vitro* [94].

Furthermore, there are recombinant VSV vectors in which the entire G protein is replaced by glycoproteins derived from other viruses for retargeting viral attachment. Muik et al. created a VSV recombinant, which expresses the glycoprotein of lymphocytic choriomeningitis virus (rVSV-LCMV-GP). This recombinant, when injected systemically in immunocompetent mice, has shown no neurotoxicity even at high doses (10^9 PFU). rVSV-LCMV-GP remained oncolytic as shown *in vivo* in immunodeficient mice, where both viruses, rVSV-LCMV-GP and rVSV-GFP, led to effective tumor regression. Although while a majority of rVSV-GFP mice died from neurotoxicity, even when the virus was administered intratumorally at low doses ($2x10^5$ PFU), rVSV-LCMV-GP-treated mice survived without signs of illness. An additional advantage provided by the glycoprotein exchange in this case, is a reduced response from the humoral immunity against the virus, which allows multidose regimens for tumor treatment [95].

The attempt to integrate thymidine kinase (rVSV-TK) into VSVs genome and treatment in combination with the prodrug ganciclovir also had significant effects on subcutaneous tumor growth when administered intratumorally in melanoma or mammary tumors. Following the treatment, also an uptake of antitumor cytotoxic T cell activity was also shown, which adds an immunotherapeutic feature to the treatment [96].

Other recombinants exploit the viro-immune therapy approach. There are VSV vectors expressing INF-β to support antiviral defense in non-malignant cells [97, 98] and VSV expressing interleukins 4, 12 and 23 as immunomodulatory therapies [96, 99, 100]. These treatments aim at an enhanced antitumor immune response. An alternate approach is to suppress immune responses in order to give the virus time for replication and intratumoral spreading before being cleared by the immune system. This is accomplished by rVSV-gG_{EHV-1} which expresses the glycoprotein of equine herpes virus (EHV-1). It acts as a viral chemokine binding protein (vCKBP) and was shown to enhance intratumoral viral replication, tumor necrosis and prolonged survival of immunocompetent rats bearing HCC[101].

Here again recombinant viral vectors provide an infinite number of possibilities for cancer treatment. What remains to be proven, is an efficient and long-lasting effect *in vivo* of recombinants without neurotoxic component, ideally when given intravenously to reach inoperable tumors as well as metastases.

3. The Pseudotyped Vesicular Stomatitis Virus: rVSV-NDV

3.1. Construction of rVSV-NDV

rVSV-NDV is a combination of the viruses VSV and NDV. As its parental viruses, VSV-NDV is a single stranded RNA virus with negative polarization. The genome consists of six genes encoding six proteins. Four of them, the N, P, M and L protein are derived from the VSV genome. Proteins F and HN from the NDV genome replace the attachment protein G (Figure 7).

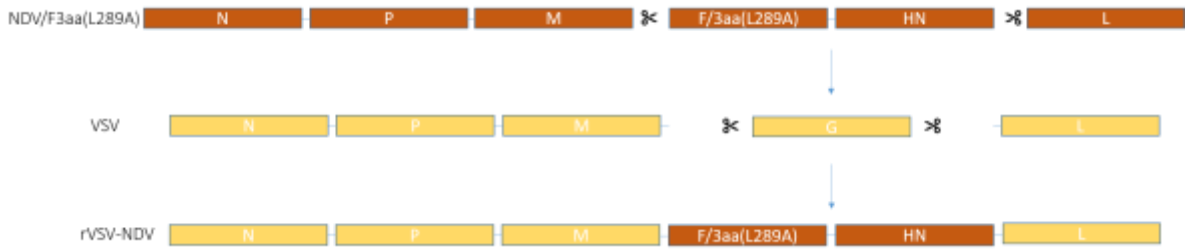

Figure 7: Genome of VSV-NDV

Illustrated is the construction of recombinant VSV-NDV vector from its parental virus genomes, NDV (red) and VSV (yellow). The envelope proteins, F and HN, from NDV are integrated into the genome of VSV. The negative sense, single-stranded RNA of VSV-NDV encodes 6 genes: the nucleoprotein (N), phosphoprotein (P), matrix protein (M), large protein (L) from VSV and the fusion protein (F) and hemagglutinin-neuraminidase (HN) protein from Newcastle disease virus.

For this modification we postulate several advantages. The deletion of the VSV-G protein and replacement by NDV-F3aa(L289A) and –HN addresses the problem of neurotoxicity associated with wild type VSV (wtVSV). In contrast to VSV-G, that allows entry and replication in a large number of tissues in nearly all species including neurons of rodents and non-human primates [102], the safety profile of NDV as an oncolytic agent in clinical trials is very promising. With flu-like symptoms, tumor-site-specific adverse events and acute dosing reactions, human patients in phase I clinical trials reacted comparatively well to NDV treatment. Further experiments conducted to prove this hypothesis are shown in section "Preliminary Data".

Moreover, rVSV-NDV is not expected to lead to any toxicity in birds. The NDV strain used to create rVSV-NDV is NDV/F3aa(L289A), a mesogenic NDV strain. It is shown that the NDV-HN, - F and -P protein can individually or collectively take part in the pathogenicity of NDV. A study conducted with the lentogenic NDV strain LaSota, the velogenic NDV strain Beaudette C and several recombinants of those (e.g. LaSota expressing a virulent F cleavage site rLaSoVF, Beaudette C experessing a low virulent HN protein rBCLaSoHN or La Sota expressing a virulent HN protein rLaSo BCHN) investigated the influence of the named proteins in NDVs virulence. Among other things, the results showed that both a virulent F-cleavage site and HN from a virulent strain are required to achieve high virulence and severe diseases [103]. Additionally the recombinant rVSV-NDV does not include the NDV-P protein, therefore no expression of the V protein is possible either. As the V protein acts as a species-specific IFN-antagonist in avian species, the absence of the V protein significantly diminishes viral replication *in vitro* and *in vivo* in embryonated chicken eggs[58]. According to these findings the integration of F and HN from a mesogenic strain into the genome of VSV

and deletion of the P protein could maybe even impede the virulence in birds compared to the NDV/F3aa(L289A) strain.

One last advantage of rVSV-NDV over VSV is its ability to fuse infected cells into multi nucleated giant cells (syncytia) and spread effectively inside the tumor tissue (Figure 8). Additionally, by syncytia formation, the virus avoids humoral immune responses as the virus spreads predominantly inside the tumor mass [84] and potentially leads to an extended time span between infection of tumor cells and clearance by the immune system. While the virus evades an immune response inside these giant cells, it is at the same time a more immunogenic cell death than silent apoptosis, leading to an antitumor immune response through activation of dendritic cells and tumor-specific T cells[104]. Experiments have also been conducted with rVSV-NDV/F (L289A) [84], a construct that contains the endogenous VSV glycoprotein in addition to a mutated NDV-F protein, which is fusogenic even in the absence of the hemagglutinin-neuraminidase. These results showed intratumoral syncytia formation in rats bearing orthotopic HCC, treated with rVSV-NDV/F-(L289A) as soon as on day one after treatment. Also survival of rVSV-NDV/F-(L289A)-treated rats was significantly prolonged.

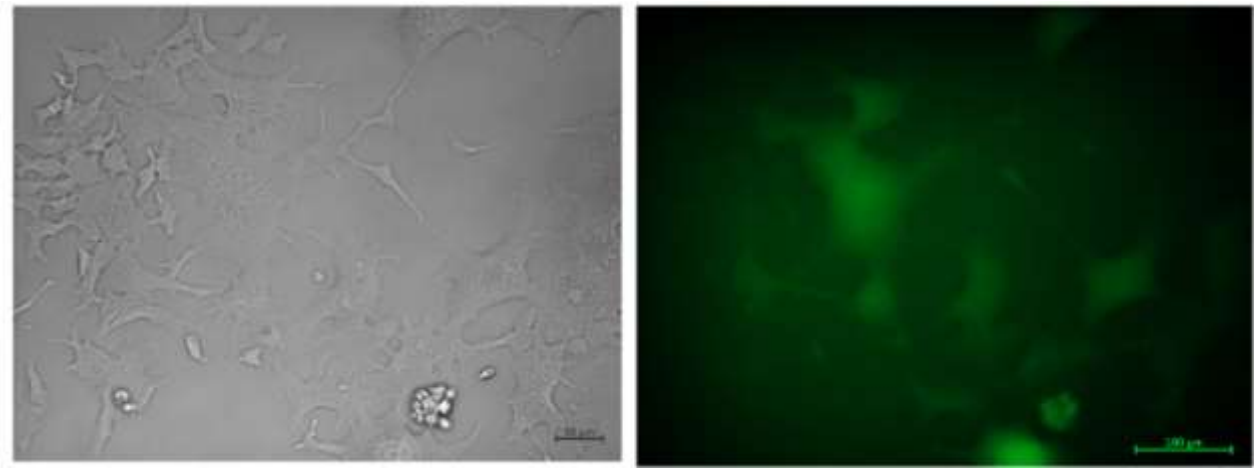

Figure 8: AGE1. CR pIX cells forming syncytia and expressing GFP after infection with VSV-NDV-GFP

Photo microscopic picture of AGE1.CR.pIX cells 18h after infection with VSV-NDV at MOI 0.01. The picture was captured at 100x magnification.

3.2. Preliminary Data

VSV-NDV has already been characterized *in vitro*. Crucial features that rVSV-NDV should provide in order to be a safe OV are a strong replication in tumor cell lines and a reliable inhibition by healthy, IFN producing cells. It was first investigated for its replication and syncytia induction abilities in human HCC cell lines. The results show that rVSV-NDV replicated to similar titers as the parental viruses at 72 hours after infection although under microscopic surveillance (Figure 10) infection of rVSV-NDV treated cells appeared more rapid than the growth curve (Figure 9) indicates. These results are consistent with the data derived from a lactate dehydrogenase (LDH) cytotoxicity assay. Here again, complete cytotoxicity was reached after 72 hours.

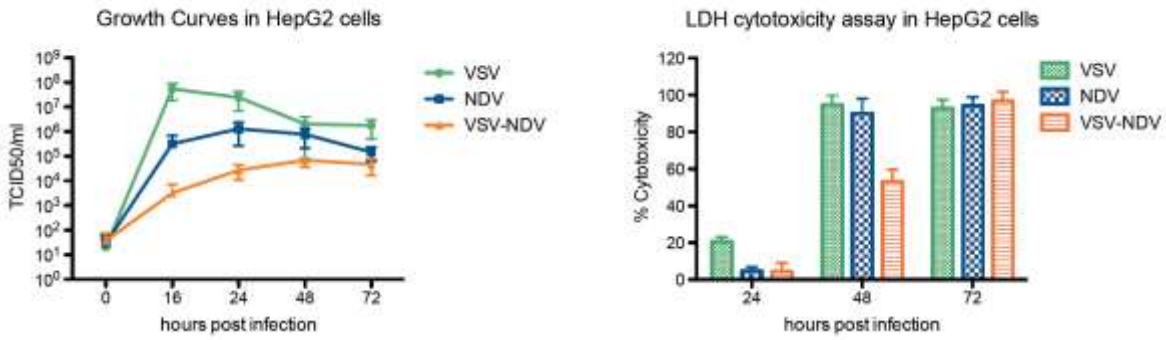

Figure 9: Growth curve and cytotoxicity assay in an HCC cell line (HepG2)

Growth curve and LDH assay were conducted on human HCC cell lines HepG2. Cells were infected at an MOI of 0.01 of rVSV, rNDV or rVSV-NDV. One hour after infection cells were washed and medium was replaced by fresh medium. At various time points after infection aliquots of the supernatant were taken and used for LDH cytotoxicity assay. Cells were harvested and used for TCID50 assay. Experiments were performed in triplicates and are presented as mean +/- standard deviation.

To confirm that rVSV-NDV can still induce syncytia formation in HCC cell lines, Huh7 cells were infected with rVSV-NDV and compared to rNDV and rVSV infected cells at different points in time after infection. A non-infected PBS group was used as control. Here, syncytia formation was first detectable in the rVSV-NDV treated group at 16 hours after infection, whereas NDV-treated cells showed first signs of syncytia at 24 hours after infection. VSV-infected cells showed typical CPE already earlier than 16 hours after infection, but as expected, no syncytia formation.

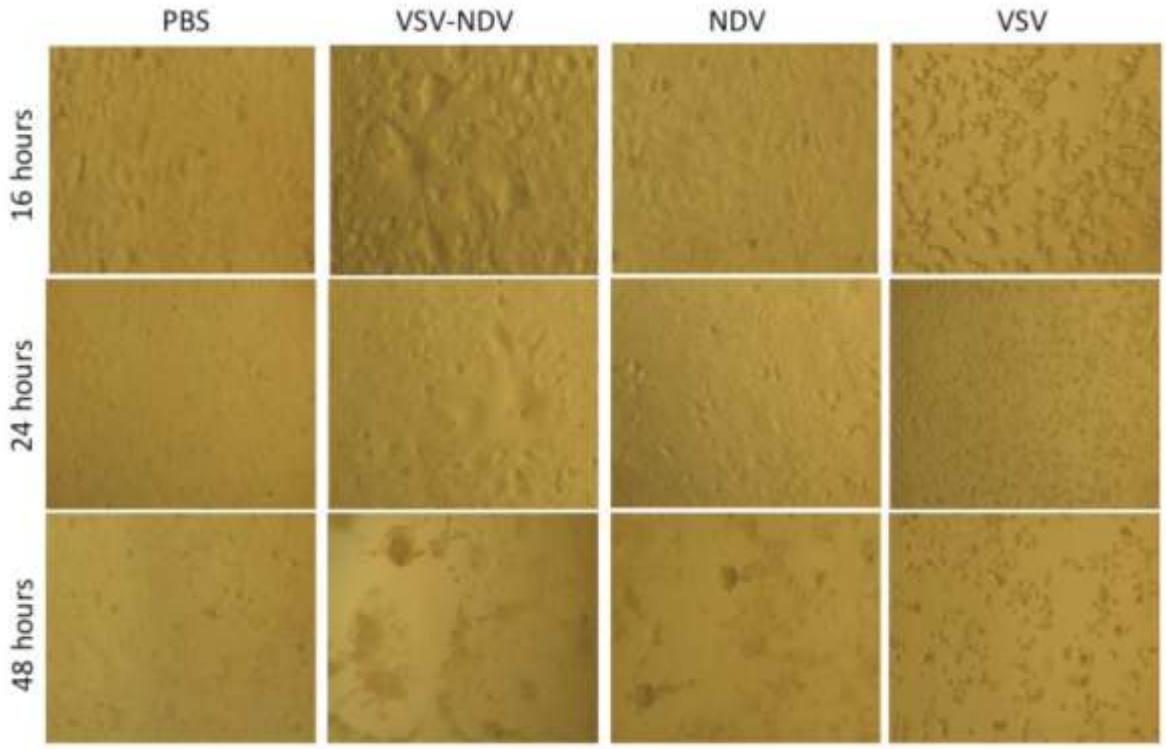

Figure 10: Photo microscopic comparison of HCC cells infected with rVSV-NDV, NDV and VSV

Human HCC cells, Huh7, were infected at an MOI of 0.01 with rVSV-NDV, NDV and VSV and observed over 48 hours. Here we see a comparison between the different virus-infected groups at representative points in time. Images were captured under 200x magnification.

As a selective oncolytic agent, rVSV-NDV is not expected to replicate in non-malignant tissues. To investigate the replication behaviour of rVSV-NDV in the tumor surrounding tissue, primary human hepatocytes were infected with rVSV-NDV and compared to its parental viruses rVSV and rNDV. The results confirm that rVSV-NDV is clearly less replicative in primary human hepatocytes in contrast to both VSV and NDV especially at later points in time around 24 hours after infection (Figure 11, left). Similar results were obtained with an LDH assay. Here no evidence of cytotoxicity in rVSV-NDV treated cells was found (Figure 11, right).

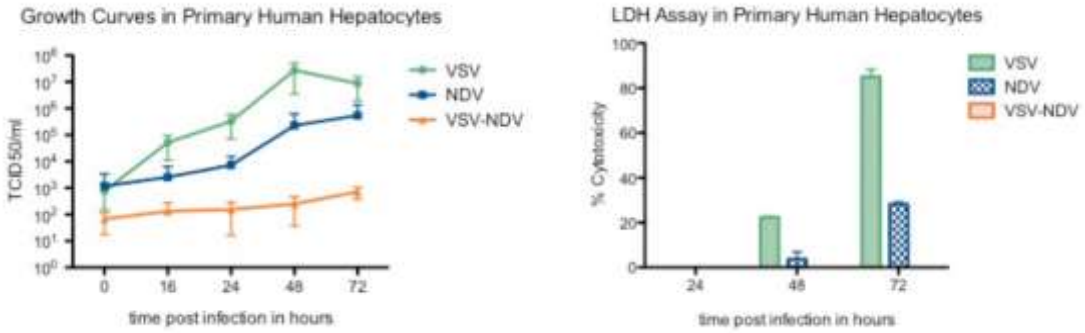

Figure 11: TCID50 and LDH assay of primary human hepatocytes infected with rVSV-NDV, rVSV and rNDV

Primary human hepatocytes were infected with rVSV-NDV, rVSV and rNDV at an MOI of 0.01. Cell lysates were used to perform $TCID_{50}$ at different points in time after infection. Aliquots of the supernatant were collected at different points in time and used for LDH assay. Experiments were performed in triplicate, and means +/- standard deviation are shown.

An important requirement of rVSV-NDV as a tumor-specific oncolytic agent is a good responsiveness to type I IFN. To make sure that healthy cells are protected from the virus by their natural defense mechanisms and only tumor cells are successfully infected, rVSV-NDV was tested in an IFN dose response assay and compared to its parental viruses. As rNDV appeared to be almost unresponsive, both rVSV and rVSV-NDV show an effective decrease in viral titers under IFN treatment (Figure 12).

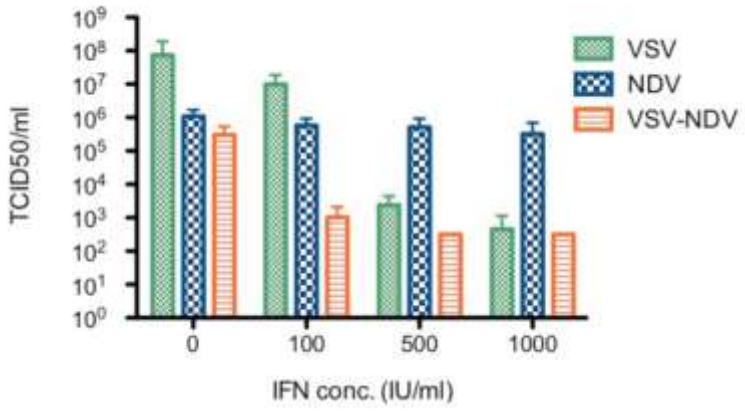

Figure 12: IFN dose response of rVSV-NDV compared to rVSV and rNDV

For this assay, an IFN sensitive cell line A549 was infected with rVSV-NDV, rVSV and rNDV at an MOI of 0.01. 48 hours after infection cells were lysed and used for viral titer measurement by $TCID_{50}$. This experiment was performed in triplicates and mean values +/- standard deviation are shown.

To confirm that cells of the nervous system are not susceptible for rVSV-NDV, and therefore no neuropathological side effects are expected, replication in primary, embryonic rat neurons was measured by $TCID_{50}$ and once again compared to rVSV and rNDV. Here, the titer of VSV increases by almost six logs within 16 hours after infection, while the titer of rVSV-NDV is five logs lower at the same point in time (Figure 13, left). Similar results were obtained in an MTS assay. Whereas the viability of rVSV-treated cells is already diminished by 50% at 24 hours after infection, rVSV-NDV and rNDV show comparable results with nearly 100% viable cells (Figure 13, right).

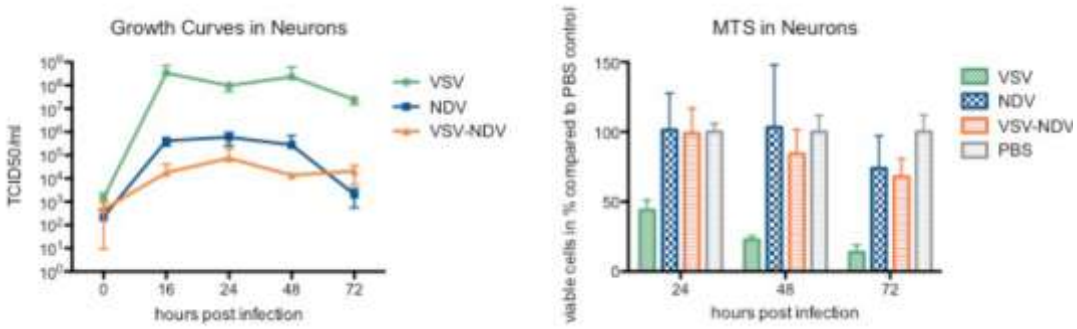

Figure 13: TCID50 and MTS assay in primary rat neurons infected with rVSV-NDV, VSV and NDV

Primary rat neurons were infected with rVSV-NDV, rVSV and rNDV at an MOI of 0.01 to perform $TCID_{50}$ and a standard MTS assay at various time-points post-infection. Cell lysates were used to measure viral titers with $TCID_{50}$. Cell monolayers were used for the MTS assay. Experiments were performed in triplicate, and means +/- standard deviation are shown.

4. Aim of the Project

In this study the newly created recombinant virus, rVSV-NDV was investigated for its efficacy and safety *in vivo*. To evaluate these parameters, experiments were conducted in immune-deficient NOD-SCID mice, as well as in immune-competent AST mice and Buffalo rats. Characteristics of interest were safety, viral shedding, the potential to induce an antitumor immune response, development of neutralizing antibodies, cross-reactions to neutralizing antibodies for parental viruses and survival benefit of treated animals.

Experiments on viral toxicity were performed in NOD-SCID mice. This animal model allows investigation regarding viral toxicity using only low virus titers. Furthermore, an immunodeficient animal model provides a more powerful test on neuropathogenicity as neurotoxicity is a major concern for VSV derived viruses.

Viral shedding and survival experiments were performed in immune-competent animal models. Since an important part of cancer treatment with oncolytic viruses is maintained through enhanced anti-tumor immune responses, the necessity of an immune-competent model is obvious. To test the benefit of the treatment on the therapeutic outcome, two animal models with a different focus on translation were chosen. One of them was a mouse model with the benefit of a highly translational, inducible HCC. The second was a rat model with implanted HCC and allows for a semi-selective and more translational virus delivery route. As the mouse model results in multifocal HCC nodules, intratumoral injection of virus is not really feasible, and systemic application via tail vein is more appropriate. In the rat model the size of the animals allows for injection into the hepatic artery, which supplies about 85-100% of the tumoral blood flow [105]. This injection route mimics the application of transarterial chemoembolization (TACE) in patients and gives the opportunity to inject the virus in close proximity to the actual tumor site and reduces inactivation of the virus by unspecific immune responses. The state of the art method for OV application in cancerous diseases is intratumoral injection. As the OV is injected directly into the tumor, this method offers the advantage of minimal immune responses against the virus before it has the opportunity to enter the cells. In order to mirror the possibilities of clinical treatment completely, we also performed intratumoral injection in Buffalo rats with implanted HCC, because currently only unifocal tumors can be treated using this application route.

In the controlled environment of the implanted tumor model in rats, experiments on viral kinetics were performed. These experiments included evaluation of neutralizing antibody induction, analysis of an antitumor immune response by tumor cell-PBMC co-culture and flow cytometric analysis of T cells and tumor cells, as well as measurement of viral titers in tumor, liver and brain of treated rats at different points in time after treatment.

5. Material and Methods

5.1. Cell Lines and Culture

All cell lines used were adhesive cell lines. AGE1.CR.pIX cells (obtained from ProBioGen AG, Berlin) were used for virus production and measurement of viral titers. Cells were maintained in Dulbecco's Modified Eagle Medium (DMEM) and nutrient mixture F12 supplemented with 5% fetal calf serum, 1% penicillin-streptomycin and 1% L-glutamine. The rat Morris Hepatoma 7777 cell line (McA-RH7777) was used for implantation of HCC in the liver of syngeneic Buffalo rats. Cells were maintained in high-glucose ATCC®-DMEM supplemented with 10% fetal calf serum and 1% Penicillin-Streptomycin. When T cells were involved in experimental use, they were kept in Rosewell Park Memorial Institute (RPMI) medium supplemented with Penicillin-Streptomycin, 1% non-essential amino acids and 1% sodium pyruvate (100mM). All cell lines were incubated at 37°C and with 90% humidity and 5% CO_2.

Table 1: Reagents Used for Cell Culture

Reagents	**Company**
DPBS	PAN Biotech
FBS Superior	Merck
L-Glutamine	PAN Biotech
Penicillin-Streptomycin	PAN Biotech
Trypsin/EDTA	PAN Biotech
DMEM-F12	biowest
DMEM High Glucose	ATCC
RPMI 1640	biowest
Antibiotics/Antimycotics	Gibco®

Table 2: Consumables Used for Cell Culture

Consumable	**Company**
75cm² Cell Culture Flask	Sigma-Aldrich
96-well Plate	Sigma-Aldrich
150cm² Cell Culture Dish	Sigma-Aldrich
Eppendorf Tubes /Safe Lock Tubes	Eppendorf
Reax top, tube shaker	Heidolph
100-1000µl pipet	Eppendorf Research plus
20-200µl pipet	Eppendorf Research
2-20µl pipet	Eppendorf Research

0.5-10µl pipet	Eppendorf Research
Tip One RPT, Pipet tip 10µl RNase, DNase, DNA and Pyrogen free	StarLab
RPT Filter tips, 20µl	StarLab
Universal Fit Pipet Tips, 200µl	Corning
Filter tips, 1000µl	Clear Line
Ultra pipet controler	Corning Stripettor™ Ultra
serological pipet, 5ml	Greiner bio-one
serological pipet, 10ml	Greiner bio-one
serological pipet, 25ml	Greiner bio-one
serological pipet, 50ml	Greiner bio-one
serological pipet, 2ml	Falcon
Combitips advanced®, 5ml	Eppendorf
Multipipet M4	Eppendorf
Microscope: OPTECH® Optical Technology	neoLab
Thermomixer compact	Eppendorf
Centrifuge 5424	Eppendorf
Centrifuge 5702 R	Eppendorf
HERAsafe, Scientific Biological Safety Cabinet	ThermoFisher Scientific
HERAcell Heraeus, CO_2 Incubator	ThermoFisher Scientific
Centrifuge Tubes 15ml/50ml	Sigma-Aldrich

5.2. Preparation of McA-RH7777 for Tumor Implantation

Cells were kept in culture as described above and last plated at least two days prior to preparation for implantation. On the day of implantation, cells were treated as follows: medium was aspirated and any dead cells washed off the culture dish with PBS. Cells were then trypsinized for 10 minutes in the incubator. All cells were pooled in 50ml centrifuge tubes in the appropriate cell culture medium. Cells were centrifuged at 500g for 5 minutes and the supernatant discarded. Cells were washed in PBS to dispose of possible residues of trypsin and counted. The washed cells were centrifuged again, the supernatant discarded and the cells resuspended in their culture medium without supplements in a volume calculated to achieve a dilution of $4x10^6$ cells per 20µl.

5.3. rVSV-NDV Production

AGE1.CR.pIX cells were expanded on 20 cell culture dishes (150mm diameter) following normal maintenance protocol. At about 80% confluence, medium was changed to DMEM-F12 with 1% penicillin-streptomycin and 1% L-glutamine. rVSV-NDV was added at an MOI of 0.001 and incubated for

approximately 48h. The optimal point in time of virus harvest is reached when the cells form large patches of syncytia, but before they completely detach from the dish. This time point is determined microscopically. To harvest the virus, the supernatant from culture dishes was collected in centrifuge tubes, and centrifuged at 300rcf for 10 minuntes to seperate cell debris, and the supernatant then transferred to ultracentrifuge tubes. 0.001% Triton X was added to the cell layer in the dishes and incubated for 30min at 37°C. After incubation, cells were scraped off the dishes and collected in centrifuge tubes. The harvested cells were pooled with cells seperated from supernatant and vortexed for 1min, sonicated for 3min and centrifuged at 300rcf for 10min. After centrifugation the cell pellet was washed in 3ml PBS and centrifuged again. Supernatant from both steps was combined and transferred to ultracentrifuge tubes. Both types of supernatant in ultracentrifuge tubes (supernatant from culture dish and supernatant from washing the cell pellet) are centrifuged at 643rcf using a Beckman 70Ti rotor for one hour at 4°C. After ultracentrifugation, a small pellet appeared in each tube. Pellets from all the tubes were combined in 3ml PBS. Ultracentrifuge tubes were prepared with a sucrose gradient (7ml 60% sucrose on the bottom, 6ml 30% sucrose in middle layer, 3ml 10% sucrose on top). The combined pellets from ultracentrifugation were run over the sucrose gradient in an additional ultracentrifugation step at 643rcf for one hour at 4°C. Finally, the virus appears as a white band approximately at the transition of the bottom and middle layer of the sucrose gradient. Aliquots of the virus were frozen and stored at -80°C.

5.4. Viral Titers

Measurement of viral titers was accomplished by 50% Tissue culture infective dose ($TCID_{50}$). $2x10^6$ AGE1.CR.pIX cells were plated on 96-well plates. A ten-fold serial dilution of virus containing material was pipetted in quadruplicates on the 96-well plate and incubated on the cells. Medium used for $TCID_{50}$ was cell culture medium without fetal calf serum. Cells were observed for signs of CPE typical for the virus used and viral titers were calculated using the Reed-Muench method.

5.5. Preparation of Tissue and Samples for $TCID_{50}$

Tissue samples were weighed and homogenized using a glass dounce homogenizer after resuspension in 10µl PBS per mg sample. Homogenized samples were then centrifuged at 100rcf for 5 minutes, and the supernatant was used for $TCID_{50}$. Feces samples were additionally supplemented with 1% antibiotic-antimycotic solution containing 10000 units/ml Penicillin, 10000µg/ml streptomycin and 25µg/ml amphotericin B. Urine samples were applied directly in $TCID_{50}$ assays. Saliva was taken by wiping off mouse saliva from the oral mucosa with a moistened, cotton-tipped applicator. After taking the sample, liquid from the applicator was pressed into a 1.5ml Eppendorf-tube® equipped with 300µl PBS. After centrifugation at 1rcf at 5 minutes to clear the supernatant from fiber of the cotton-tipped applicator, the supernatant was as well applied directly in $TCID_{50}$ assays.

5.6. McA-RH7777-T cell co-culture experiment

To determine if virus-treated rats have stimulated antitumor T cell responses, a co-culture of the implanted tumor cells with T cells from rat blood, isolated from treated rats was performed. McA-RH7777 cells were

plated at a density of $1x10^5$ cells per well in 12-well plates the day before the co-culture. Virus- and PBS-treated rats were sacrificed and their blood was collected in EDTA-tubes. The fresh blood was then diluted 1:2 in T cell medium and centrifuged over Biocoll separating solution, creating a Ficoll gradient. From this gradient, an aliquot of the plasma layer was aspirated and saved at -80°C for later use in neutralizing antibody assays. T cells were aspirated and pipetted into 2ml Eppendorf-tubes®. The pellet was washed twice in ice-cold PBS and centrifuged for 5 minutes at 700rcf. After the second centrifugation step, the pellet was resuspended in 1ml T cell medium. Cells were counted and used for Morris-T cell-co-culture and flow cytometric analysis.

After counting, the T cells were co-cultured together with the plated Morris cells in 12-well plates at effector-target ratios of 1:2.5, 1:5 and 1:10 in duplicates. T cell medium was used for co-culture.

After 48h, Morris cells were trypsinized and counted in a Neubauer chamber.

5.7. Neutralizing Antibody Assay

To compare the respective abilities of the virus to induce neutralizing antibody responses in their hosts, plasma samples from rats at different time-points post treatment were subjected to neutralizing antibody assays. Plasma samples were heat inactivated at 50°C and diluted 1:50 in DMEM-F12 supplemented with 1% Penicillin-Streptomycin and 1% L-glutamine. A 96-well plate was prepared with 100µl of the same medium in rows two to twelve. 200µl of the 1:50 plasma dilution was applied in quadruplicates to the first row. A 2-fold serial dilution was then performed by transferring 100µl from the first row into the second and pipetting up and down. This procedure was repeated in each row to create a dilution series. The last 100µl in the last row were discarded. Additionally, 100µl of a 500 PFU/ml dilution of the virus against which the neutralizing antibodies should be directed was added to each well of the 96-well plate. This mixture was incubated for 90 minutes and then pipetted onto the prepared AGE1.CR.pIX cells in a 96-well plate. The plates were evaluated microscopically after 48h. The neutralizing titer is determined as the highest plasma dilution in which at least 50% of the wells are free from CPE.

5.8. Flow Cytometry

Dissociated tumor tissue and PBMCs from OV-treated rats were examined for Tcell markers (CD3, CD4, CD8 and CD25) by flow cytometry using antibodies conjugated to fluorochromes (Table 3). T-cells were prepared as described under section "McA-RH7777-T cell co-culture experiment". The tumor tissue was minced and pressed through a cell strainer, and cells were resuspended in T cell medium and centrifuged 25min at 100rcf. The pellet was washed twice in ice-cold PBS, and cells were counted. $1x10^6$ cells of each sample (tumor and T cells) to prepare for flow cytometric analysis. For determination of cell viability, cells were washed in 1ml PBS and centrifuged for 10min at 300g. Cells were resuspended in 100µl PBS, and 1µl Viobility 405/520 Fixable Dye was added per sample to distinguish between living and dead cells by flow cytometry. The cells were then mixed well and incubated 15 minutes at room temperature for the dye to permeate the membrane of dead cells and bind intracellular proteins, which then fluoresce up to 50-fold brighter than living cells. Then 0.5µl CD25 monoclonal antibody (clone OX39) conjugated with Per-CP

eFluor 710 as a fluorochrome were added to each sample and incubated in the dark for 10 minutes. To eliminate unspecifically bound antibodies, samples were washed in FACS buffer, centrifuged at 0,4rcf for 5minutes and then resuspended in 30µl FACS buffer. Following, 3µl of monoclonal CD4, CD8 and CD3 antibody (conjugated to allophycocyanin [APC], phycoerythrin-cyanine dye [PE-Vio770] and phycoerythrin [PE], respectively) were added per sample. The samples were again mixed and incubated for 10 minutes at 4 °C in the dark. Unspecifically bound antibodies were washed off in FACS buffer, centrifuged at 0,4rcf for 5 minutes and the samples were resuspended in 200µl of 4% PFA to inactivate the virus. All samples were incubated 10 minutes on ice, washed in FACS buffer, centrifuged at 0,4rcf for 5min and resuspended in 200µl FACS buffer. All samples were analysed on a Gallios Flow Cytometer by Beckman Coulter.

Table 3: Reagents Used for Sample Preparation for Flow Cytometric Analysis

Reagent	**Supplier**	**Fluorochrome**	**Excitation Laser**	**Emission maximum**
Viobility 405/520 Fixable Dye	Miltenyi Biotec			
Anti-CD25 rat (OX39)	ThermoFisher	Per-CP eFluor710	488nm	710nm
Anti-CD4 rat APC	Miltenyi Biotec	Allophycocyanin	670nm	680nm
Anti-CD8 rat PE-Vio770	Miltenyi Biotec	Phycoerythrin-cyanine	488nm	780nm
Anti-CD3 rat PE	Miltenyi Biotec	Phycoerythrin	488nm	630nm

5.9. Virulence in Embryonated SPF Chicken Eggs

The pathogenic potential of VSV-NDV in birds was investigated by conduction of experiments to study the mean death time in 10-day old, embryonated and specific pathogen free chicken eggs. 40 Eggs were delivered from Charles River at a temperature of 36°C. The eggs were inoculated on the same day with either 10 PFU, 100 PFU, 1000 PFU or 10000PFU of VSV-NDV or NDV-GFP as a control. Eggs were candled using a torch light and the embryo averted side was marked. To inoculate the virus, the eggshell was first punctured at the top with a 27G-needle to release pressure for the virus injection. Afterwards, the virus was injected in a 100µl volume using a 1ml syringe and a 30G-needle on the marked side of the egg into the allantoic cavity. Punction sites were closed with candle wax and the eggs observed by candling twice daily for 90 hours and again after 7 days to determine the mean death time and minimum lethal dose.

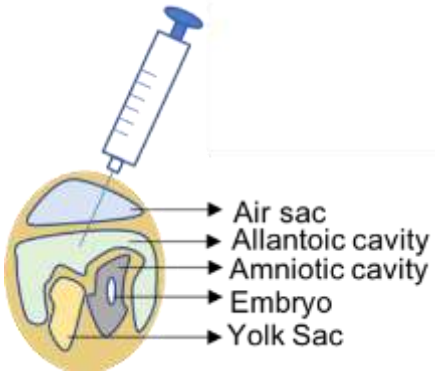

Figure 14: Procedure of egg inoculation

100µl of either rNDV-GFP or rVSV-NDV diluted according to the experimental groups was injected into the allantoic sack of embryonated, specific pathogen free chicken eggs using a 30G-needle.

5.10. Animal Models and Experimental Designs

All animals were kept in small groups under specific pathogen free conditions in IVC cages with controlled air and temperature conditions and humidity. Food and water were provided ad libitum. All experiments were conducted in agreement with §8 Animal Welfare Act ("Tierschutzgesetz") and approved by the government of Upper Bavaria ("Regierung von Oberbayern") under reference numbers 55.2-1-54-2532-43-13 and 55.2-1-54-2532-16-15.

For the viral safety studies, seven-week old NOD-SCID (non-obese diabetic severe combined immunodeficiency) mice were used to induce viral toxicity at lower virus titers. These mice provide a broad immune deficiency through impaired B and T cell function on the background of deficient Natural Killer cell function.

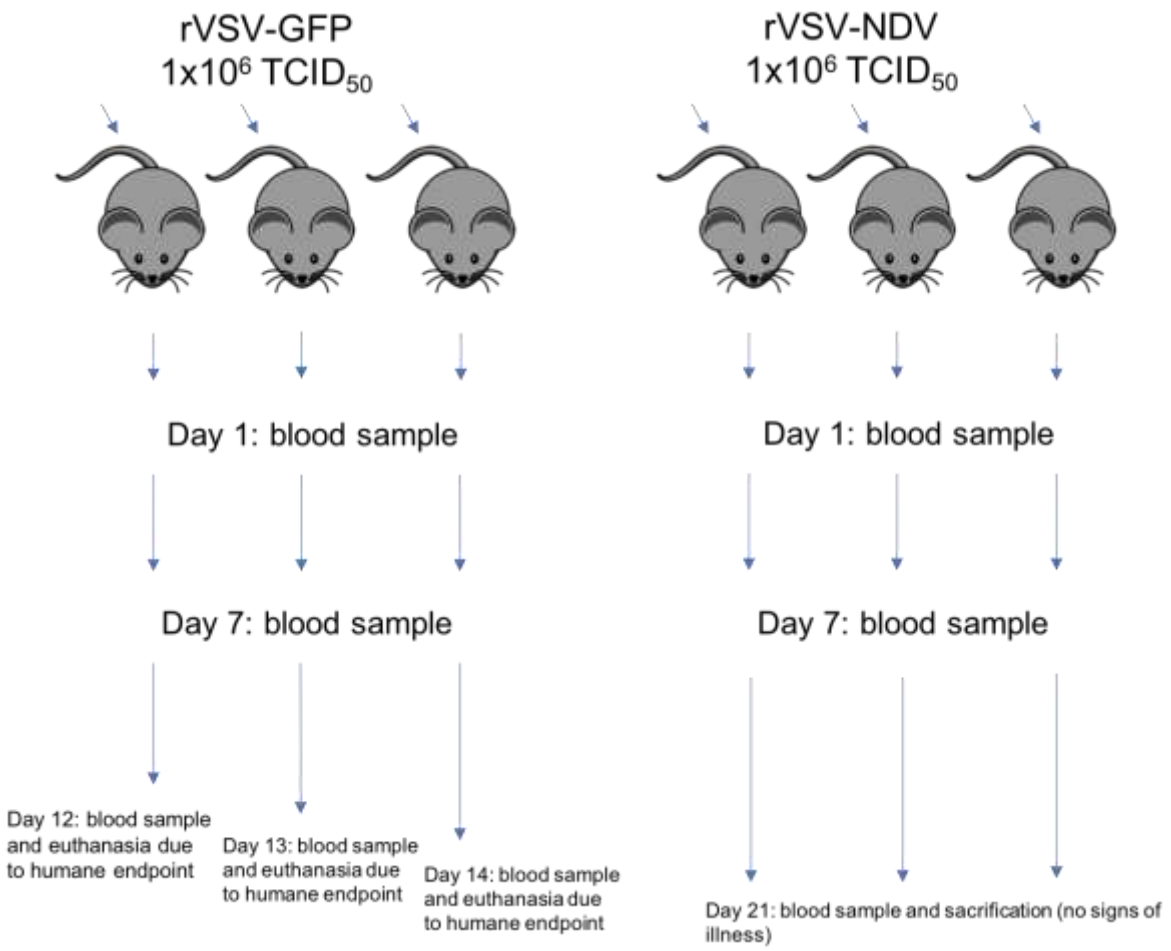

Figure 15: Setup of the viral safety study

7-week-old NOD-SCID mice were injected with $1x10^6$ $TCID_{50}$ of either rVSV-GFP or rVSV-NDV and observed until they reached endpoint criteria, determined by daily control of body weight and general condition. Blood samples were taken on days 1, 7 and the day of sacrification and used to measure BUN, CREA and GPT.

Survival experiments were performed in immune competent animal models. A mouse survival study was conducted in seven to ten week old AST-LTAg (albumin-floxstop-Tag, large T-Antigen) mice. This animal model allows inducible growth of spontaneously developed HCC, which mirrors the clinical conditions much better than an implanted tumor-model. The genome of these mice contains a Cre/loxP system on a C57BL/6J (often referred to as Black-/6) background. A lox/P-flanked stop cassette and the Simianvirus 40 (SV40) large tumor-antigen (LTag), a well-known oncogene in rodents, are integrated into the genome directly following the liver specific albumin promoter. These mice, when injected with an adenovirus expressing the Cre-recombinase develop spontaneous HCC. The Cre-recombinase results in cleavage of the lox/P site and cuts out the stop cassette [106]. This leads to expression of the L-Tag in a liver specific context and thus to development of HCC within 7-10 weeks after tail vein injection of $2.5x10^8$ PFU of rAd-Cre.

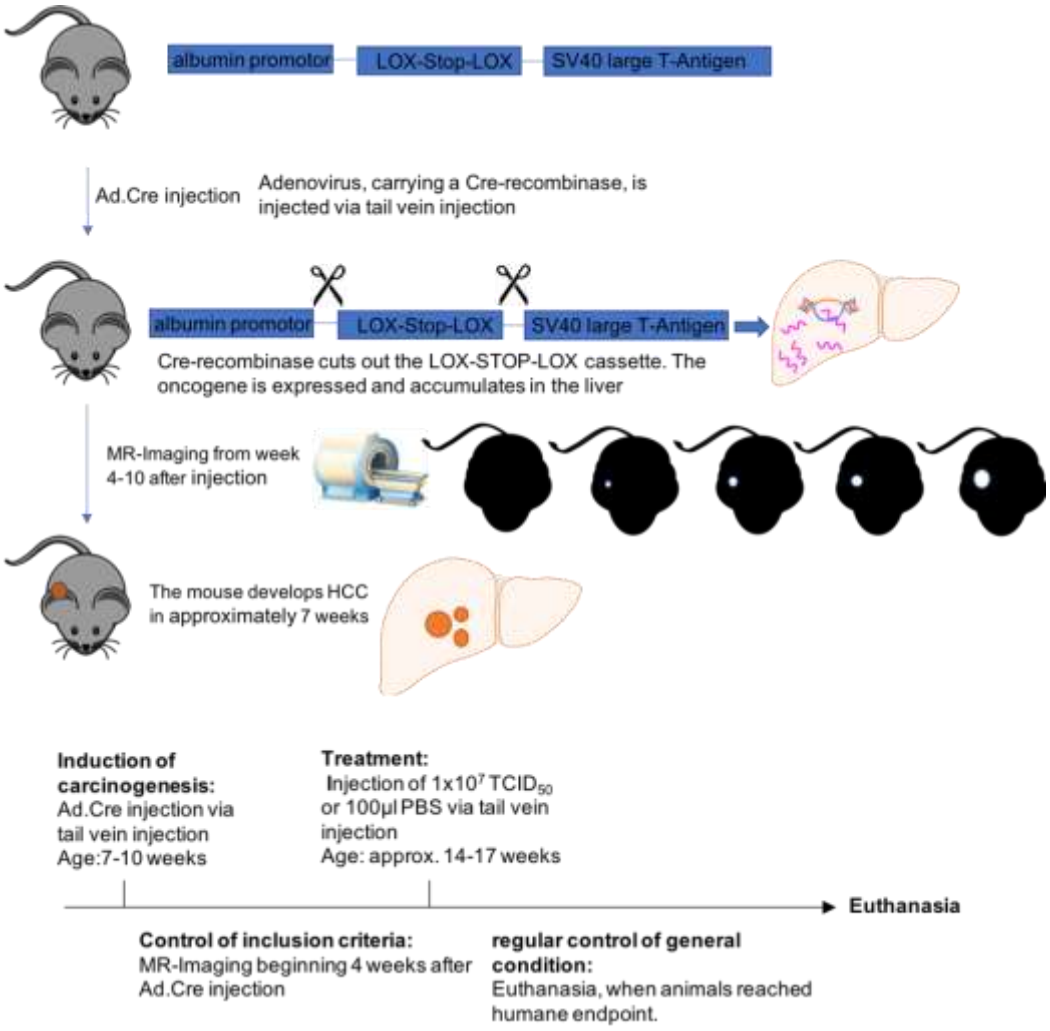

Figure 16: Setup of the HCC tumor model in AST-mice

The cre/loxP system induces expression of the oncogene in a liver specific context in AST-mice after injection of the Cre-recombinase via injection of an adenovirus carrying the recombinase. Tumors develop over time in a 4-9 week period. Starting in week 4 tumors were detected using MR Imaging. Mice that reached inclusion criteria were treated for survival studies according to their experimental group and euthanized when they reached endpoint criteria.

Additional survival experiments and studies on viral kinetics and distribution were conducted in seven to twelve week-old Buffalo rats. The rats were bred and delivered from Charles River (Calco). Buffalo rats are the syngeneic rat strain from which Morris Hepatoma 7777 cell line was derived, and therefore are the only immune-competent model in which these cells will grow.

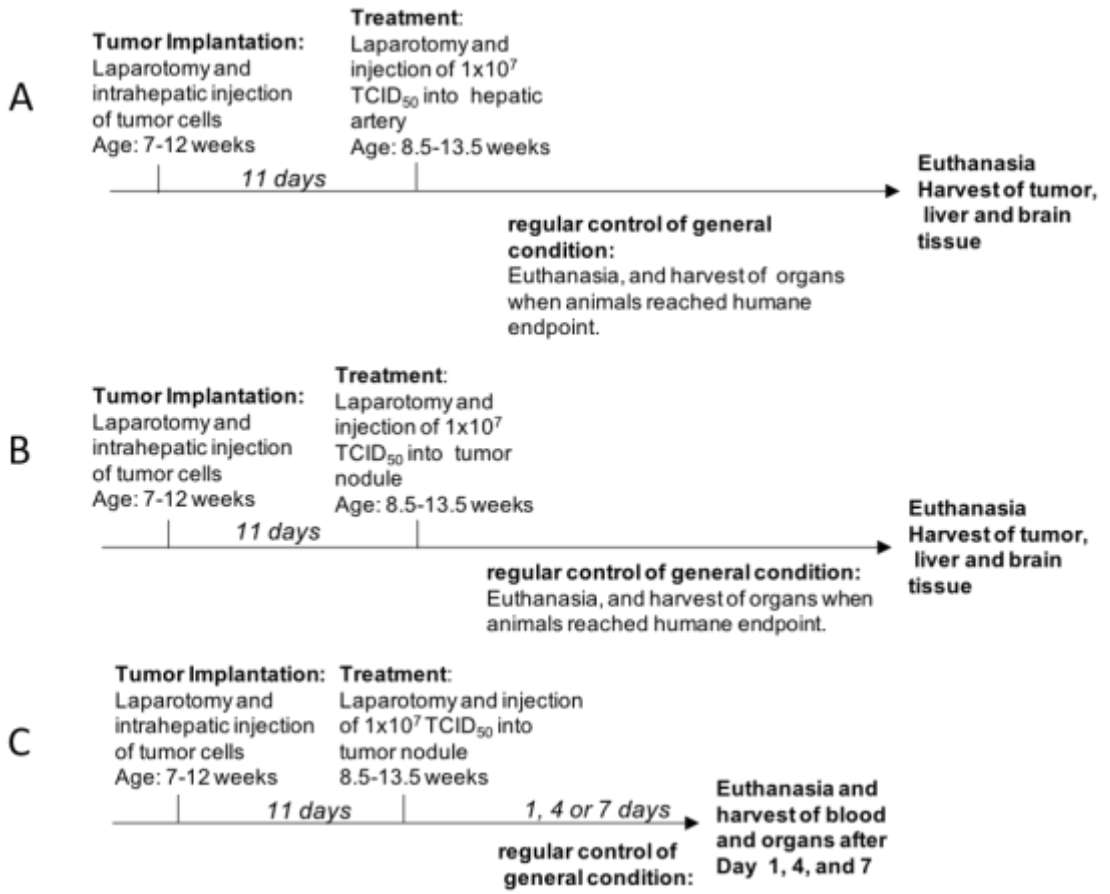

Figure 17: Time line of rat survival (A, B) and kinetics (C) experiments

Tumors were implanted in 7-12 week old Buffalo rats. 11 days after tumors were implanted a second laparotomy was performed and virus or PBS was injected according to the treatment group. **A** Virus or PBS was injected via the hepatic artery. The rats were monitored regularly and body weight and general condition were determined to evaluate if animals reached endpoint criteria in the survival study. **B** Virus or PBS was injected intratumorally. The rats were monitored regularly and body weight and general condition were determined to evaluate if animals reached endpoint criteria in the survival study. **C** Virus or PBS was injected intratumorally. The rats were sacrificed after 1, 4 or 7 days and blood and tissue was harvested for viral kinetics studies.

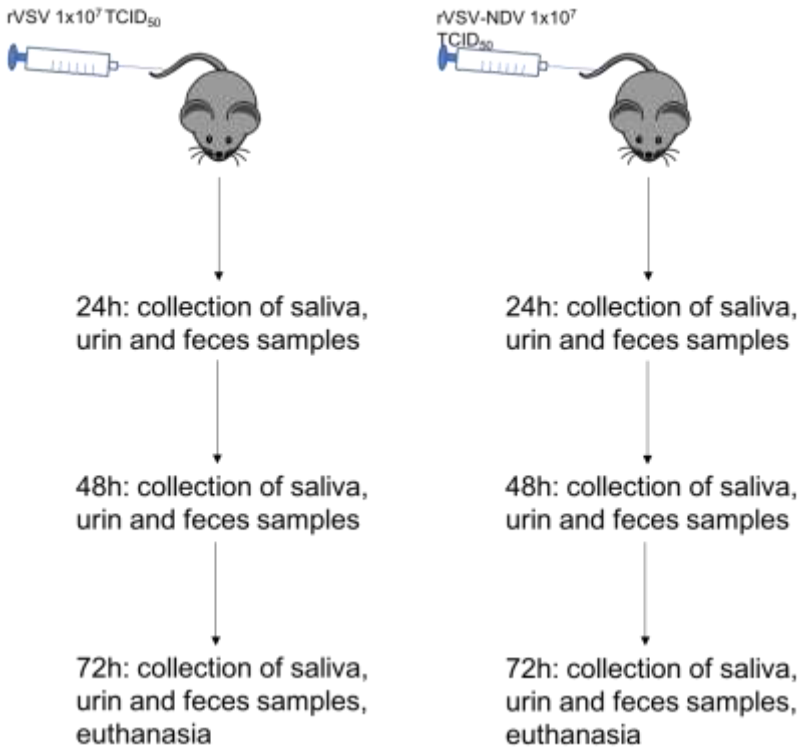

Figure 18: Setup of the experiment on viral shedding

AST-mice were injected with $1x10^7$ $TCID_{50}$ of either rVSV-NDV or rVSV-GFP via tail vein injection. Samples of saliva, urine and feces were collected within the first three days after injection and $TCID_{50}$ was performed to determine viral titers in secretions of injected mice.

5.11. Administration of Viral Vectors in the Mouse Model

Mice in the appropriate age range were fixated for a short time span in a tail-first restrainer. An infrared heat lamp was directed to the tail of the mouse in a distance of 30cm to dilate the veins. The tail was wiped with 80% ethanol. When the lateral tail veins were clearly visible, a 1ml syringe containing the appropriate virus at the appropriate dose in a volume of 100µl volume was used to inject the virus, in the absence of air bubbles into the vein, using a 30 Gauge needle. For survival studies, a dose of $1x10^7$ $TCID_{50}$/ mouse was applied. After the application, eventual-bleeding was stopped by the application of gentle pressure with a cellulose swab on the puncture site. Before the injection, the viruses were kept on ice at all times.

5.12. Magnetic Resonance Imaging

For magnetic resonance imaging (MR imaging, MRI) all mice were anaesthetized using Isoflurane as inhalation anaesthesia. Induction was reached with 4% Isoflurane in 100% oxygen. Anaesthesia was maintained with 2.5% Isoflurane in 100% oxygen (airflow: 1l/min). Anaesthetized mice were placed in a dStream wrist coil and imaged with "Ingenia 3.0T MR-System" by Philips. The sequence used was fat saturated T_2-weighted RARE (rapid acquisition with relaxation enhancement) imaging (3403.35/100.517 [repetition time msec/echo time msec]). Ointment was applied to the eyes of all mice during anaesthesia, and to maintain body temperature, the tail was placed on a glove filled with physiologically warm water during imaging.

5.13. Preparation for Surgery, Pain Medication and Euthanasia

After at least one week of quarantine, seven to twelve-week old Buffalo rats were assigned for experimental use. All rats were injected subcutaneously with 0.05mg/kg Buprenorphin 20min prior to surgery. The rats were then introduced into inhalation anaesthesia via a flooded chamber with 4% Isoflurane in 100% oxygen (airflow: 2l/min). For maintenance, the rats were placed in an inhalation mask and provided with 2% Isoflurane in 100% oxygen (airflow: 2l/min). To prepare the rats for surgery, they were placed on a heat mat, Bepanthen® eye-cream was applied on all rats under anaesthesia. The operation site was shaved and disinfected with 80% ethanol and Braunol® was applied as an antiseptic.

After surgery, all rats received subcutaneous injection of 4ml 0,9% saline solution, Metamizol 50mg/kg orally and subcutaneous injection of 0.05mg/kg Buprenorphin every 8 hours. The period of analgesia was dependent on the performed surgery. For tumor implantation and intratumoral injection, Buprenorphin was applied over a period of 36 hours after surgery. After hepatic artery injection, Buprenorphin was applied for 72 hours, as this surgery is much more invasive. The rats were weighed and scored frequently after surgery. Animals in survival studies were euthanized by injection of 200-400mg/kg Narcoren® under inhalation anaesthesia when humane endpoints were reached.

5.13.1.Tumor Implantation

The rats were prepared for surgery as described above. Laparotomy was performed by an approximately 3cm long incision of skin and muscle layer from the xiphoid process down. The skin and muscles were hold in place by a wound retractor. A gauze swab moistened with physiological saline solution was placed at the lower incision site and the left lateral hepatic lobe was lifted out gently on the swab using moistened cotton-tipped applicators. Using a dissection microscope, $4x10^6$ cells in a 20µl volume were injected through a 30 Gauge needle, attached to a Hamilton syringe into the liver lobe. The needle was inserted until the tip was visible directly under the liver capsule, then the cells were injected creating a visible bubble under the liver surface. A long injection canal was created in order to reduce tumor cell leakage and to prevent destruction of the tumor cells during the subsequent cauterization to close the injection site. After reassuring that no bleedings could be observed, the liver lobe was placed back into the abdomen. The muscle and skin layer were sutured separately with 4-0 PROLENE® suture material. Tumors grew for eleven days until either hepatic artery injection (survival) or intratumorale injection (viral kinetics) of therapy was performed.

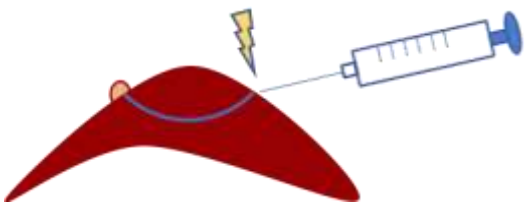

Figure 19: Procedure of intrahepatic tumor implantation

20µl of the Morris Hepatoma cell line McA-RH7777 were injected into the liver directly under the capsule, creating a long and curved needle track to circumvent cells from leaking out of the injection site. Additionally the needle track was closed by cauterizing the tissue at the entrance of the needle track.

5.13.2.Hepatic Artery Injection

At day eleven after tumor implantation, a second laparotomy was performed to inject the virus into the hepatic artery. Skin and muscle were incised approximately 5cm from the xiphoid down in caudal direction. The incision was kept wide open using a wound retractor. Gauze-swabs were moistened with physiological saline solution and placed on both ends, in a cranial and caudal direction, of the incision. With moistened, cotton-tipped applicators, the intestines were placed on the lower gauze-swab and covered. The gauze swab was kept moist at all times. Under magnification by a dissection microscope, the left lateral lobe, the anterior caudate lobe and the posterior caudate lobe were extricated from the liver capsule, a filamentous membrane surrounding each lobe, using delicate forceps. After extraction from the capsule, the lobes were wrapped in the upper gauze-swab to keep them moist and in place, out of the surgery area. With these preparations, the junction of the common hepatic artery and gastroduodenal artery to the proper hepatic artery became visible and was dissected from surrounding fat and ligaments. The gastroduodenal artery was then closed as far caudal as possible with a ligature using a 7-0 PROLENE®. The common hepatic artery was clamped using an artery clamp for at most 5min. In these 5min the virus was injected into the gastroduodenal artery, cranial of the ligature to create a flow into the proper hepatic artery and the thus the tumor providing vessels.

The virus was prepared in 1ml syringes with a concentration and volume of $1x10^7$ in 1ml PBS. Viruses were kept on ice at all times before injection.

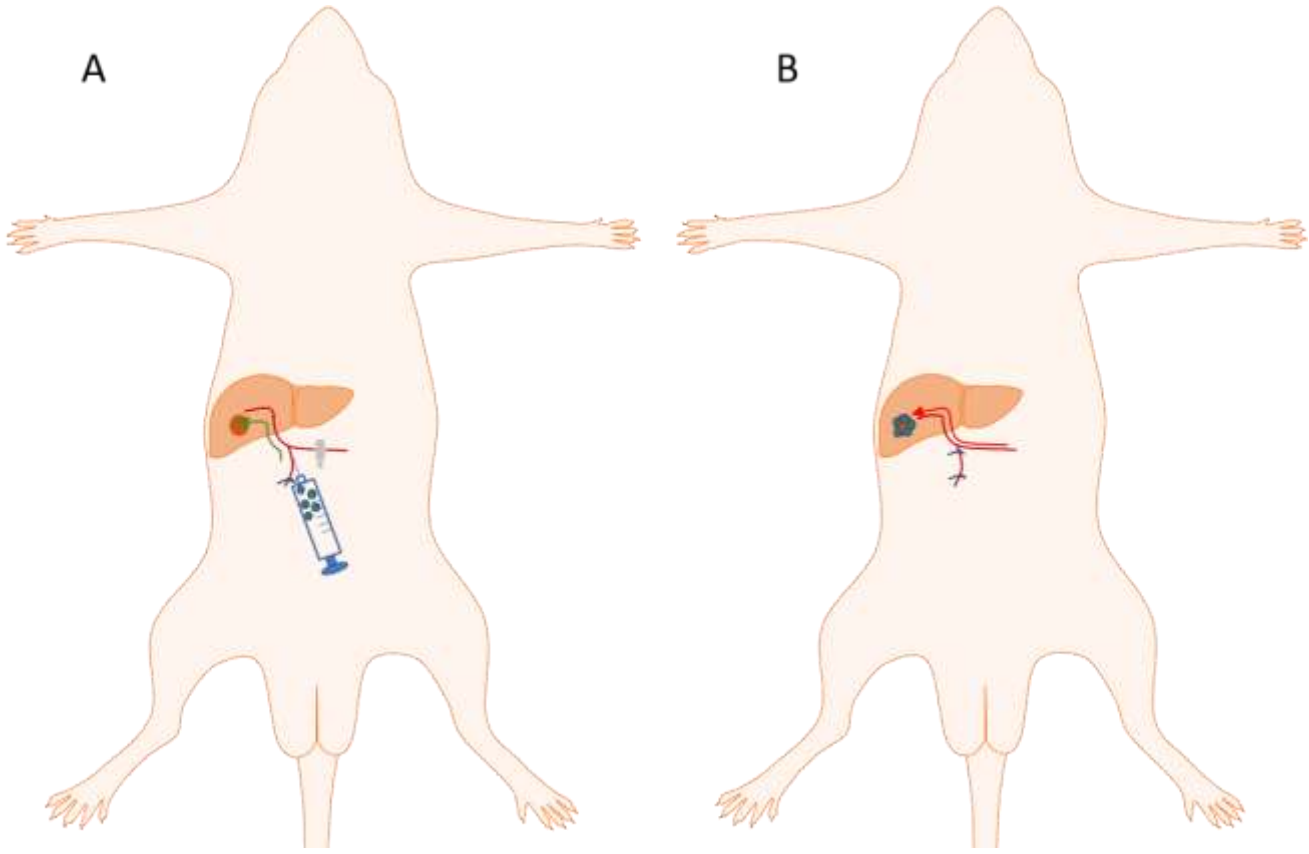

Figure 20: Surgery procedure of the hepatic artery injection

The rats received a second laparotomy 11 days after the tumor implantation. The liver lobes were decapsulated and flipped aside to achieve access to the blood vessels underneath. Using a microscope the branching of gastroduodenal

artery, common hepatic artery and proper hepatic artery was dissected. **A** A clamp positioned on the common hepatic artery and a ligature on the gastroduodenal artery prevents back flow of the injected virus. The flow of injected virus into the tumor is marked by a green arrow. **B** A second ligature inclosing the injection site on the gastroduodenal artery prevents bleeding after the clamp on the common hepatic artery is removed and the blood flow to the liver via the proper hepatic artery is restored. The blood flow after a successful surgery is indicated by a red arrow.

After the virus was carefully injected through a 30 Gauge needle, bleeding is prevented by a second ligature cranial to the puncture site and directly before the junction of the gastroduodenal artery and the common hepatic artery with a 7-0 PROLENE®. When the second ligature was safely in place the blood flow was re-established by removing the artery clamp from the common hepatic artery. When the absence of bleeding is confirmed, the liver was placed back in physiological order into the abdomen. The intestines were placed back with special attention to the correct orientation of the caecum. The muscle and skin layer were closed in separate layers with continuous suture using a 4-0 PROLENE®.

5.13.3.Intra-tumoral Injection

On day eleven after tumor implantation, a second laparotomy was performed to inject the virus directly into the tumor nodule. Rats were prepared for surgery as described, and again the skin and muscle layer were opened with an incision 3cm down from the xiphoid. The liver was lifted out on a moistened gauze swab using moistened cotton tipped applicators to expose the tumor nodule on the liver surface.

The virus was prepared in 1ml syringes in a concentration and volume of $1x10^7$ $TCID_{50}$ in 200µl in PBS. Viruses were kept on ice at all times before injection.

The virus dilution was injected into the tumor through a 30G needle directly into the centre of the nodule. After injection, the liver was placed back into the abdomen and the muscle and skin layers were closed with a continuous suture using a 4-0 PROLENE®.

Table 4: Surgery Instruments

Surgical instruments	**Surgery**
FST: Surgical scissors, sharp/blunt, straight, 17cm	Tumor implantation, Hepatic Artery injection, Intratumorale injection
FST: Alm Retractor, curved, 7cm	Tumor implantation, Hepatic Artery injection, Intratumorale injection
Feather: Disposable Scalpel No. 22	Tumor implantation, Hepatic Artery injection, Intratumorale injection
Ethicon: PROLENE 4-0	Tumor implantation, Hepatic Artery injection, Intratumorale injection
Sigma-Aldrich: Hamilton® Syringe 50µl	Tumor implantation
FST: Bovio Cauterizer Kit	Tumor implantation
FST: Vannas Spring Scissors, 2mm blades	Hepatic Artery injection
FST: Delicate Forceps 0.4mm, Tip Angled	Hepatic Artery injection
FST: Castroviejo Needle Holder, 9cm	Hepatic Artery injection

Ethicon: PROLENE 7-0	Hepatic Artery injection
FST: Schwartz Micro Serrefine, 26mm	Hepatic Artery injection
FST: Micro-Serrefine Clip Applying Forceps	Hepatic Artery injection

6. Results

6.1. Safety of the viral vector

Viral safety was investigated by tail vein injection of $1x10^6$ $TCID_{50}$ of either rVSV or rVSV-NDV, with three NOD-SCID mice randomly assigned per group. The mice were weighed daily and blood samples were taken on day 1, day 7 and the day of sacrifice. All VSV treated mice showed illness with neurological symptoms e.g. wandering in circles or paralysis, which led to sacrifice, at day 12, 13 and 14 after injection. rVSV-NDV treated mice survived three weeks without showing any illness and were sacrificed 21 days after injection (Figure 21). Weight measurements indicated a significant(*) weight loss of VSV treated mice accompanying the neurological symptoms compared to rVSV-NDV treated mice on their day of euthanization (Figure 25). The blood samples were centrifuged and serum was harvested and diluted 1:10 for photometric measurement of blood urea nitrogen (BUN), creatinine (CREA), and Glutamtate-Pyruvate-Transalaminase (GPT). BUN and CREA stayed within physiological range for this mouse strain (Figure 22). GPT values were strayed within a wide range, both lower and higher than physiological reference indicates (Figure 22). Blood samples were as well tested on viral titers by $TCID_{50}$. There were average titers of $1.8x10^3$ $TCID_{50}$/ml VSV in blood on day 1 and 7 after treatment and one mouse had a titer of 5.62 $TCID_{50}$/ml on the day of sacrifice. No titer of VSV-NDV was measurable at these points in time (Figure 24). On day of sacrification, liver and brain were harvested and examined on viral titers by $TCID_{50}$. There are average titers of $5.62x10^2$ $TCID_{50}$/ml VSV-GFP in the brain of VSV-GFP treated mice. Both treatment groups showed titers of $3.3x10^1$ $TCID_{50}$/mg for VSV-GFP and $2.2x10^1$ $TCID_{50}$/mg for VSV-NDV in liver tissue (Figure 23).

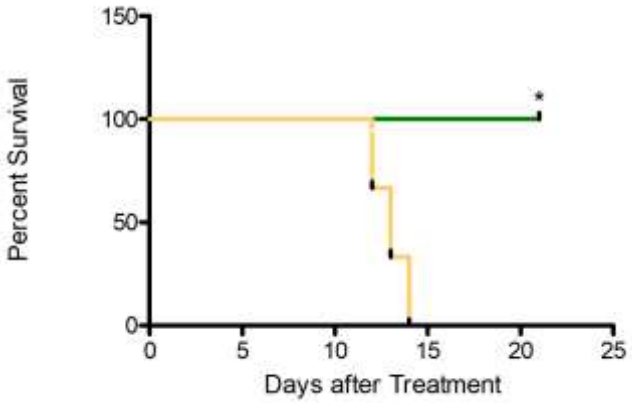

Figure 21: Survival of virus-treated NOD-SCID mice after systemic injection of $1x10^6$ $TCID_{50}$

rVSV-NDV and rVSV were injected at doses of $1x10^6$ $TCID_{50}$ via tail vein into NOD-SCID mice. Mice were monitored daily and euthanized at humane endpoints when signs of severe toxicity were observed. VSV-injected mice were euthanized on days 12, 13 and 14 after treatment, due to extreme weight loss and/or neurological symptoms, such as wandering in circles and paralysis. VSV-NDV-treated mice did not show any signs of toxicity over the course of the experiment, and were sacrificed on day 21 after injection for analysis of tissue.

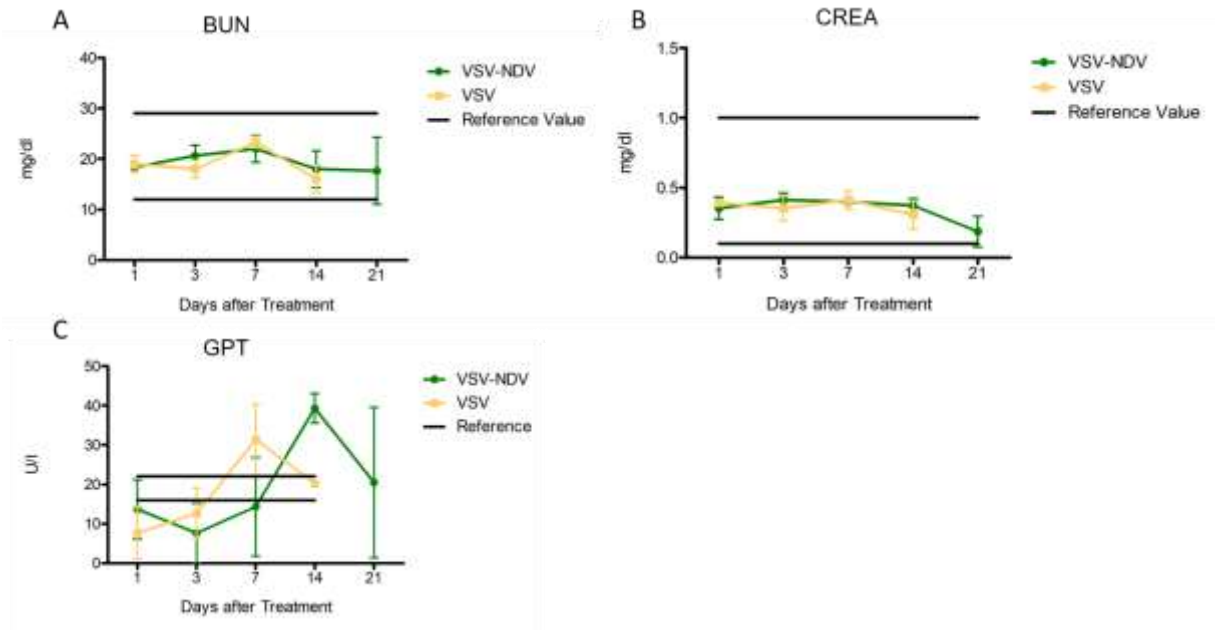

Figure 22: Blood Urea Nitrogen, Creatinine and Glutamate-Pyruvate Transalaminase of virus treated NOD-SCID mice after systemic injection of $1x10^6$ $TCID_{50}$

On day of sacrifice blood samples were taken and Serum was diluted 1:10 and measured via photometry by the blood chemistry lab of "Klinikum rechts der Isar".Plasma was used to determine **A** blood urea nitrogen (BUN), **B** creatinine (CREA) and **C** Glutamate-Pyruvate-Transalaminase (GPT)..All measured values for BUN and CREA are within reference range, indicating normal kidney function, regardless of virus therapy.

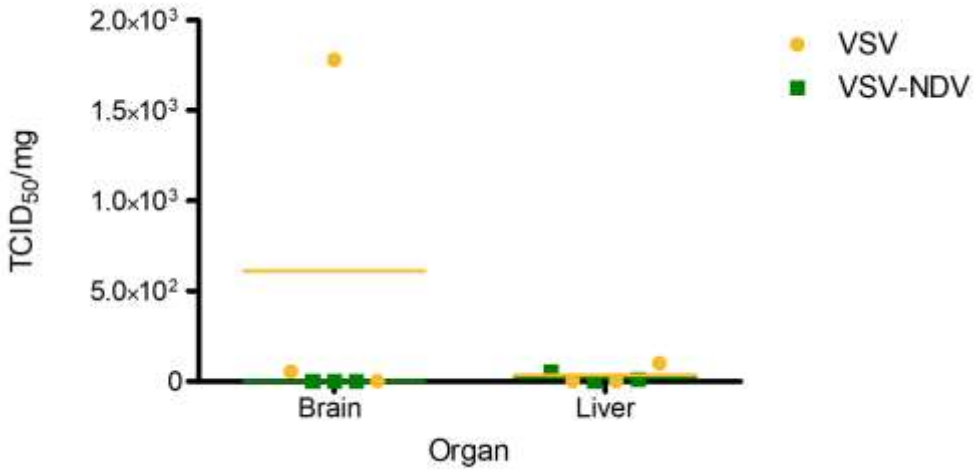

Figure 23: Viral titer in organs of virus treated NOD-SCID mice on day of euthanasia

After sacrification brain and liver were harvested and analysed by $TCID_{50}$. VSV-treated mice showed titers of around $5.62x10^2$ $TCID_{50}$/mg in the brain, whereas VSV-NDV treated mice had no measurable viral titer. In both treatment groups, low viral titers could be detected in the liver.

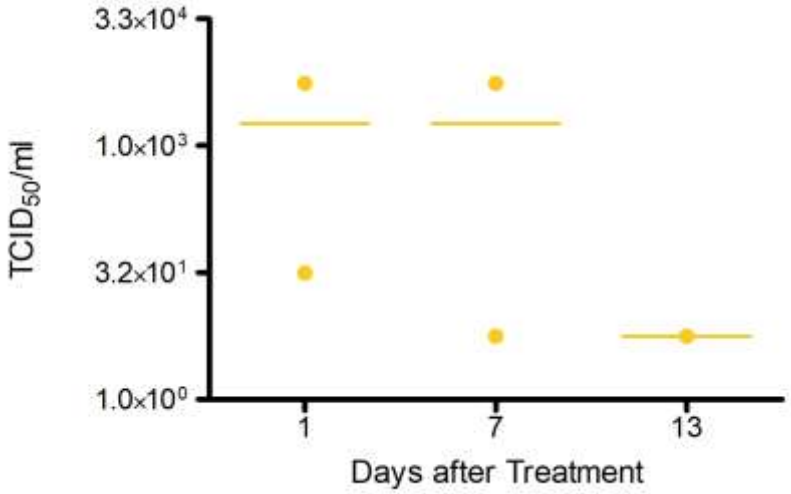

Figure 24: Viral titer from serum of virus-treated NOD-SCID mice after systemic injection of $1x10^6$ $TCID_{50}$

Blood samples were taken on day 1 and 7 and on day of sacrifice. Viral titers in serum were measured by $TCID_{50}$. There was no measurable titer of rVSV-NDV in serum samples, whereas VSV-treated mice showed average titers of $1.8x10^3$ $TCID_{50}$/ml on day one and seven and one of the mice a low titer of 5.62 $TCID_{50}$/ml on day of 13 after injection, which is not depicted in the figure.

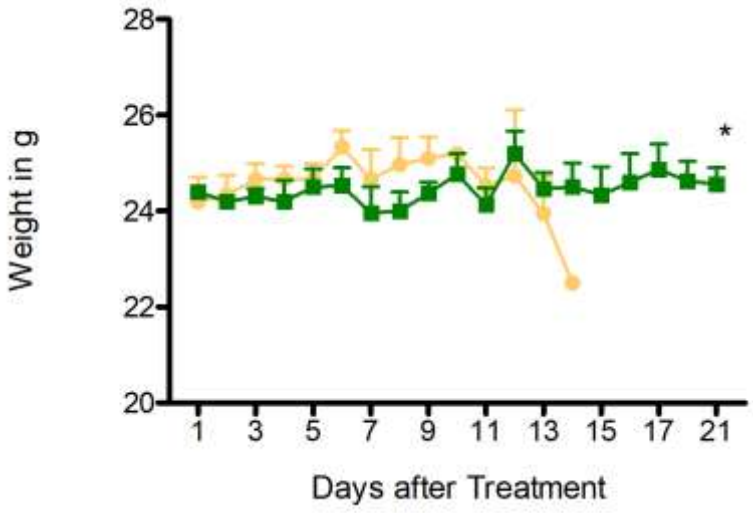

Figure 25: Weight of virus-treated NOD-SCID mice after systemic injection of $1x10^6$ $TCID_{50}$ of rVSV or rVSV-NDV

Over the course of the toxicity study, mice were weighed daily. Weights were stable until day eleven, at which time weights dropped in the VSV treated group. rVSV-NDV treated mice showed stable body weight throughout the course of the experiment.

6.2. Virus Shedding

Samples of feces, urine and saliva were collected in the first three days after viral treatment. Saliva was taken by wiping off mouse saliva from the oral mucosa with a moistened, cotton-tipped applicator. After taking the sample, liquid from the applicator was pressed into a 1.5ml Eppendorf-tube® equipped with 300µl PBS. Urine of fixated mice was collected from spontaneous emiction into a 1.5ml Eppendorf-tube®.

Samples were prepared as described in "Material and Methods" and $TCID_{50}$ was performed, to determine whether infectious virus could be recovered from the shed material. Evaluation of $TCID_{50}$ showed no viral titer at any point in time neither in VSV-GFP nor in VSV-NDV treated mice.

6.3. Virulence in Embryonated Chicken Eggs

To investigate the pathogenic potential of VSV-NDV in birds, a virulence test was performed. 10-day old embryonated chicken eggs with SOPF quality were inoculated with either rNDV-GFP or rVSV-NDV in one of the four dose levels. Mean death time was investigated by candling the eggs twice daily over the course of 90 hours and again seven days after inoculation. The minimum lethal dose is the virus dose that kills all embryos in its group and the mean death time is the mean time in which all embryos in a group die. No minimum lethal dose was detectable for VSV-NDV. None of the tested doses of VSV-NDV killed all the embryos in a group, so there was no minimum lethal dose or mean death time detectable. NDV showed a minimum lethal dose of 100PFU and a mean death time of 84 hours (Table 5), corresponding to a mesogenic strain, which is consistent to previous findings in the research group.

Table 5: Mean Death Time and Minimum Lethal Dose of NDV-GFP and VSV-NDV in Embryonated Chicken Eggs

	NDV-GFP			**VSV-NDV**		
Virus Dose	**Mean Death Time**		**Minimum Lethal Dose**	**Mean Death Time**		**Minimum Lethal Dose**
10 PFU	n=5	-		n=5	-	not applicable
100PFU	n=4	84 hours	100PFU	n=4	-	not applicable
1000 PFU	n=5	75.6 hours		n=5	-	not applicable
10.000 PFU	n=4	65 hours		n=5	-	not applicable

6.4. Survival Experiment

A survival experiment was conducted in AST mice and Buffalo rats. In Buffalo rats two models of OV treatment, intraarterial injection and intratumoral injection, were compared. Tumor growth in AST mice was induced by systemic Ad.Cre injection, leading to a spontaneous growth of multifocal tumors. To underline the translational aspect of the AST mouse model, data supporting this aspect will be given in the following section.

AST-LTAg mice developed HCC spontaneously after injection of Cre-recombinase adenovirus. To determine a start point for viral treatment of HCC-bearing mice, in context of the survival study, they were imaged using magnetic resonance tomography from four weeks after injection onwards. Treatment was started once a mouse reached either an intrahepatic tumor size of 0.5cm or at least three tumors with an additive diameter of 0.5cm. Most mice were ready for treatment between weeks seven and eight after injection of Cre-recombinase adenovirus (Figure 26), but in general the detection of tumors within criteria for treatment start was spread between four and twelve weeks . From this observation, a classification into fast

growing tumors with a tumor growth within eight weeks and slow growing tumors with a tumor growth from nine weeks onwards seemed useful. After Ad.Cre injection, 100% of male mice developed tumors fast within the first eight weeks. The Female population is divided almost in half between slow and fast growing tumors, which means significantly (***) less fast growing tumors than observed in the male population. (Figure 26). More over, fast growing tumors tended to be divided into multiple origins of tumor growth with smaller sizes. Slow growing tumors were often derived from two origins with bigger diameters (Figure 26). A one-tailed Mann Whitney test on statistical significance showed that female mice grow tumors significantly later than male mice (average start of tumor growth 61.33 days after treatment to 47.72 days after treatment, respectively).

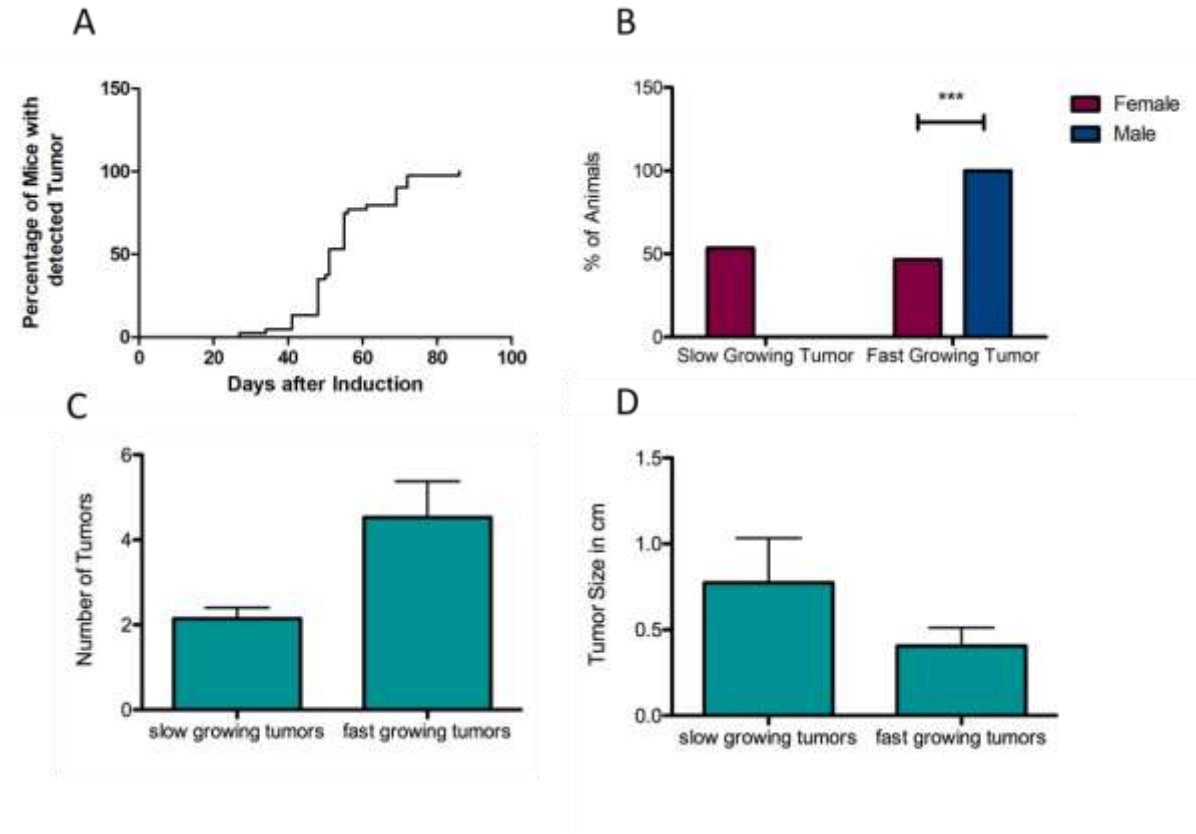

Figure 26: Specifications on tumor development in the AST mouse model

For a survival study in HCC-bearing mice with OV treatment, spontaneous tumor growth in AST mice was produced by injection of Ad.Cre. **A** The figure shows the distribution of tumor development over time in AST-LTAg mice. Depicted is the day of first tumor detection after Ad.Cre injection in 30 Mice (100%) using MR imaging. Tumors were identified as such with a minimum diameter of 0.2cm. **B** The figure shows the division of slow (within nine weeks) and fast growing (from nine weeks onwards) tumors in male and female mice. In total, 16 males and 14 females were injected with Cre-recombinase adenovirus. 100% of male mice developed fast growing tumors, whereas 53% of female mice developed slow growing tumors and 46% fast growing tumors. **C** When the start point for viral treatment was set by MR imaging, the number of tumors was counted. Depicted is the relation of tumor quantity to slow and fast growing tumors (n=7 and n=19, respectively). On average, two tumors were detected when tumors were slow growing, while five were detected when fast growing tumors reached inclusion criteria for treatment start. Means+/- standard deviation are shown. **D** When the start point for viral treatment was set by MR imaging, sizes of tumors were measured. Depicted is the relation of tumor size to slow and fast growing tumors (n=7 and n=19, respectively). The average size of a slow growing tumor at treatment start was 0,77cm. For fast growing tumors the average size was 0,4cm. Means+/- standard deviation are shown.

The rats were implanted intrahepatic with a single tumor node. When tumors reached inclusion criteria for treatment start, a viral vector or PBS as control was injected, systemically in the mouse model and via hepatic

artery injection or intratumoral injection in the rat model. The survival experiment in twelve AST-LTAg mice with the inducible HCC tumor model showed prolonged survival of the five rVSV-NDV treated mice compared to the four VSV-GFP and significantly(**) prolonged survival compared to the five PBS treated mice (Figure 27). Whereas most of the rVSV-GFP and PBS treated mice were euthanized between days 14 and 21, the rVSV-NDV treated mice were euthanized on day 33 and 35. Survival experiments in Buffalo rats with a single implanted HCC node and treatment via injection of the oncolytic viral vector or PBS into the proper hepatic artery resulted in euthanization ranging between day 10 and 46, evenly distributed between all groups (Figure 28). Whereas the day of euthanization for PBS-treated rats in the interquartile range varied in a wide span between days 18 and 38, these points in time lay in a more defined area between days 20 to 30 for virus-treated rats in the interquartile range (Figure 28). Survival experiments in Buffalo rats treated via the intratumoral application route resulted in significantly(*) prolonged survival of rVSV-NDV treated rats compared to the PBS control.

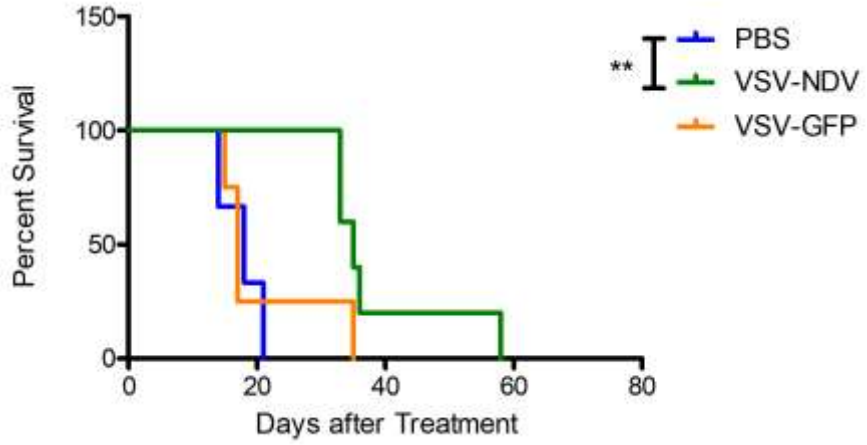

Figure 27: Survival of male, HCC-bearing AST-LTAg mice after injection of $1x10^7$ $TCID_{50}$

Male, HCC-bearing AST-LTAg mice were injected twice in a seven-day span with 10^7TCID_{50} of either rVSV-GFP or rVSV-NDV via tail vein injection for treatment. As a control mice were injected with an equal volume of PBS. Criteria for treatment start included a minimum tumor size of 0.5cm (single node or additive, with one node at least 0.2cm) and a maximum of 10 tumor nodes. Following the treatment mice were monitored regularly and euthanized when they reached human endpoints.

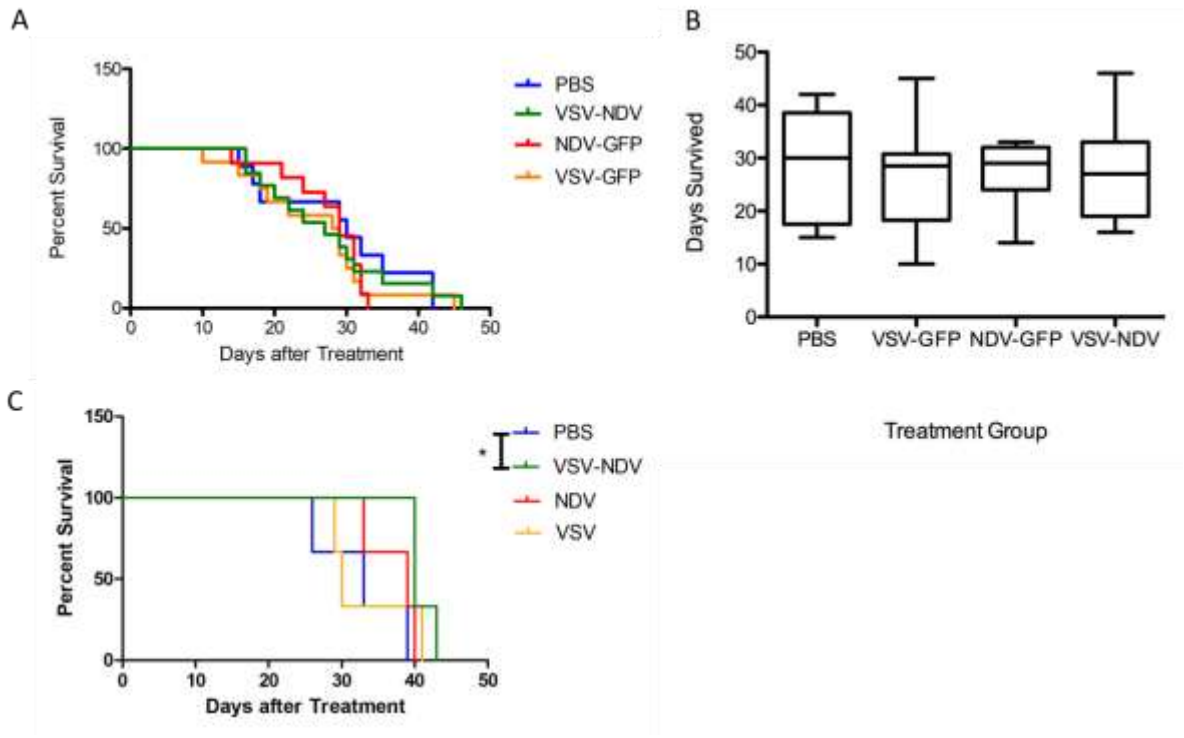

Figure 28: Survival of male, HCC-bearing Buffalo rats after hepatic artery injection of $1x10^7$ $TCID_{50}$

Male Buffalo rats were surgically implanted with intrahepatic HCC in a single node. Eleven days after implantation, tumors reached a size of approximately 0.5cm. At this point in time, in a second surgery, the virus or control buffer was injected for treatment **A** via the proper hepatic artery or **C** via intratumoral injection. The rats were monitored closely after treatment and euthanized when humane endpoints were reached. **A** OV-treatment of rats did not result in prolonged survival compared to the PBS control. **B** Depicted is the number of survived days of HCC-bearing Buffalo rats after intraarterial treatment. **C** OV-treatment of rats resulted in significantly(*) prolonged survival compared to the PBS control.

6.5. Viral Kinetics Experiment

For experiments on viral kinetics, Buffalo rats were implanted with a single, intrahepatic HCC node in the same manner as for the survival experiments. Treatment in this experiment set-up, was performed by intra-tumoral injection of the viral vector or PBS eleven days after tumor implantation. The rats were euthanized on either day one or seven after treatment and samples of blood, liver, tumor and brain were taken to perform experiments on viral kinetics. The different treatment groups were investigated with respect to viral titer in tumor, liver, and brain, the development of neutralizing antibodies, and the development of tumor-specific T cells by co-culture of the cell line used for tumor implantation and PBMCs derived from blood from the treated rats. It is important to note that these data are only preliminary, as the treatment group size was only one or two rats on day one, and on day seven, the control group consisted only of a single PBS-treated rat. Therefore, no conclusions can be drawn from these experiments.

Viral titers in organs were seen on day one in tumor tissue only for the rVSV-GFP and rVSV-NDV treated group with an average titer of $1.58x10^5$ $TCID_{50}$/mg and $1,09x10^2$ $TCID_{50}$/mg, respectively (Figure 29). Although the differences between the values varied a lot, viral titers were detectable in all rVSV-GFP and rVSV-NDV treated rats. On day seven, viral infection shifted in the VSV-GFP treated group to brain and

liver tissue with an average titer of $4.45x10^4$ $TCID_{50}$/mg and $7.9x10^1$ $TCID_{50}$/mg, respectively (Figure 29). In tumor tissue a viral titer of $1.58x10^1$ $TCID_{50}$/mg was measured for the VSV-GFP treated group. On day seven, no viral titer of NDV-GFP or VSV-NDV was measurable in any of the collected tissues.

Neutralizing antibodies were detected in the NDV-GFP treated rat as early as on day one after treatment with a neutralizing titer of 1:100 and on day seven after treatment the titer decreased to 1:50. Neutralizing titers for rVSV-GFP were detected on day seven after treatment with an average neutralizing titer of 1:25. At the measured time points no titer of neutralizing antibodies was found in rVSV-NDV treated rats (Figure 30).

Results of the Morris cell-PBMC co-culture showed that PBMCs isolated on day one after treatment resulted in a wide range of viable target cells and there is no correlation between percentage of viable cells and treatment group or effector-target ratio (Figure 31). On day seven, the Morris-PBMC co-culture resulted in consistent numbers of viable cells in the PBS treated group for each effector-target ratio. For the rVSV-NDV treated group, the percentage of viable cells increased with decreasing effector-target ratios. For rVSV-GFP, there is no change in the number of viable cells, regardless of the effector-target ratio (Figure 31). It is not possible to make a comparison between target cell viability after co-culture with PBMCs derived from virus-treated rats and PBS-treated rats, since there was only a single rat in the PBS-treatment group.

Flow cytometric analysis of CD3+, CD4+, CD8+ and CD25+ T cells on day one after treatment showed a trend indicating an increase of all subpopulations in rVSV-NDV treated rats compared to VSV-GFP or PBS (Figure 32). On day seven after treatment, there is no significant increase in activated T cell subpopulations of rVSV-NDV treated rats compared to rVSV-GFP or PBS. rNDV-GFP treated rats showed a trend toward increased activation of CD4+ T cells compared to the other groups (Figure 33). Analysis of tumor infiltrating T cells indicate an increase in CD8+T cells of all virus treated groups compared to PBS (Figure 33). However, it must be noted that these are only preliminary data and some treatment groups contain only one or two treated rats. Therefore, no definitive conclusion can be drawn.

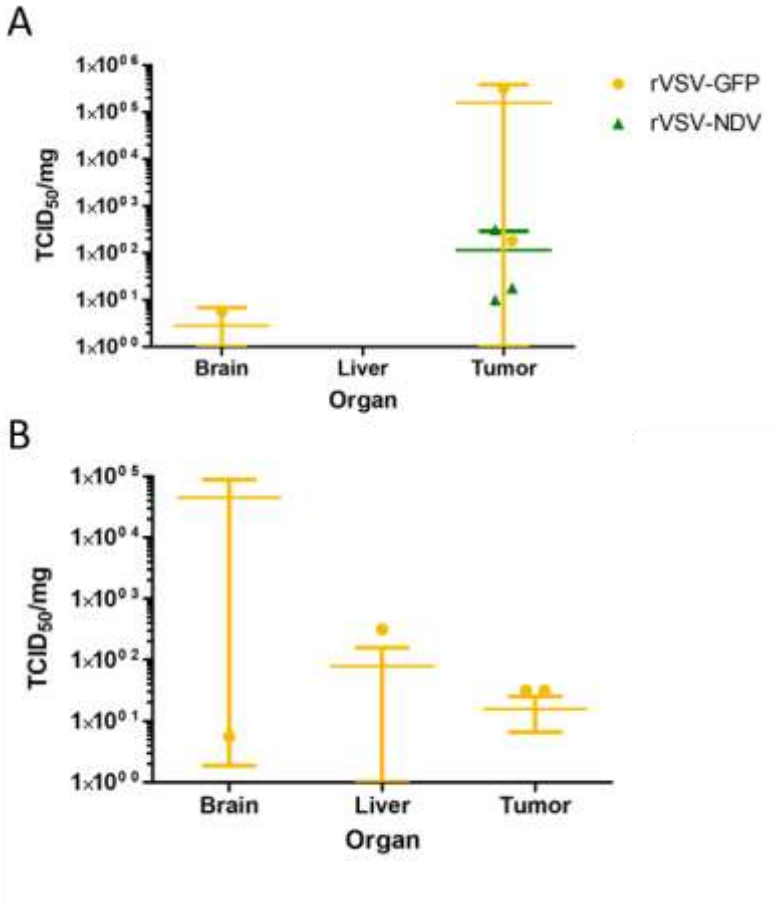

Figure 29: Viral titer in organs of virus-treated, HCC-bearing Buffalo rats

Buffalo rats were implanted with a single, intrahepatic HCC node and treated eleven days after implantation via intra-tumoral injection of either rVSV-GFP, rNDV-GFP (not shown), rVSV-NDV or PBS as control. On **A** day 1 or **B** day 7 after treatment the rats were euthanized and samples of liver tissue, tumor and brain were collected. Depicted is the viral titer in $TCID_{50}$/mg of tissue on day one after treatment. Means + standard deviation are shown.

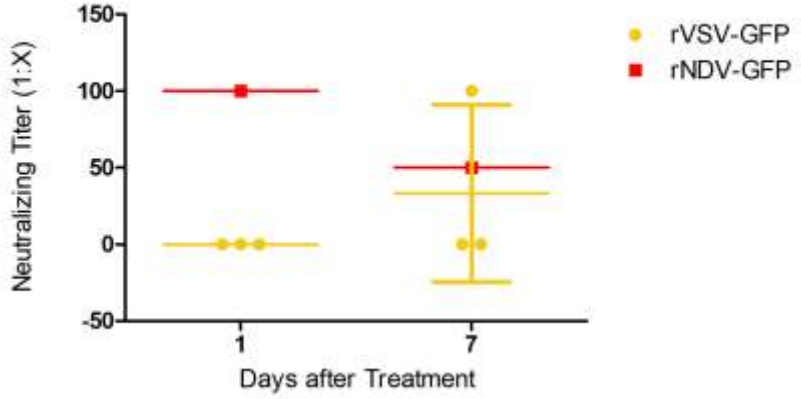

Figure 30: Neutralizing antibody titer from serum of virus-treated, HCC-bearing Buffalo rats

Buffalo rats were implanted with single, intrahepatic HCC nodules and treated eleven days after implantation via intra-tumoral injection of either rVSV-GFP, rNDV-GFP, rVSV-NDV or PBS as control. On day 1 or 7 after treatment the rats were euthanized and samples of blood were collected. Blood samples were separated into plasma and PBMCs using a Ficoll- gradient. Depicted are the results of a neutralizing antibody assay from plasma samples of rVSV-GFP and rNDV-GFP treated rats. Means + standard deviation are shown.

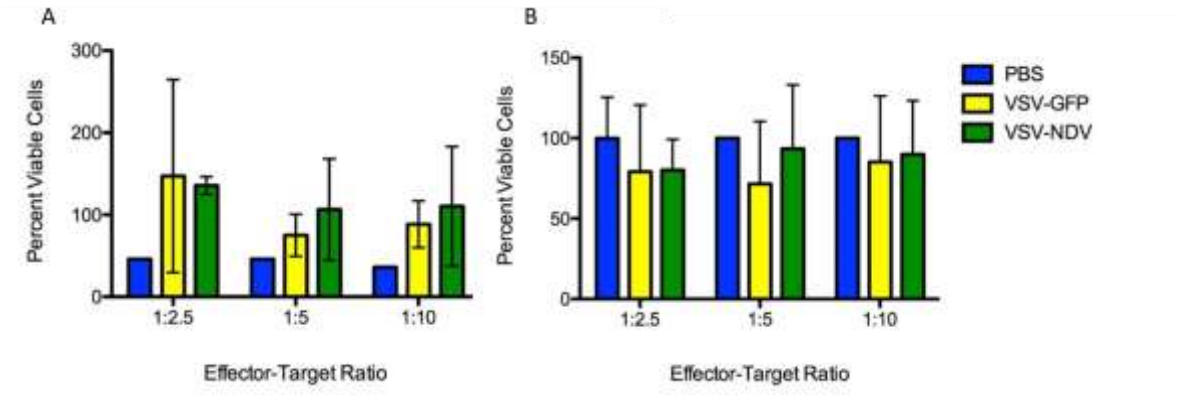

Figure 31: Co-culture of McA-RH7777 cells with PBMCs from HCC-bearing Buffalo rats

Buffalo rats were implanted with single, intrahepatic HCC nodules and treated eleven days after implantation via intra-tumoral injection of either rVSV-GFP, rNDV-GFP, rVSV-NDV or PBS as control. On **A** day 1 or **B** day 7 after treatment the rats were euthanized, and blood samples were separated into plasma and PBMCs using a Ficoll-gradient. Depicted are the results of a Morris cell-PBMC co-culture in three different effector-target ratios (1:2.5, 1:5 and 1:10). Means + standard deviation are shown.

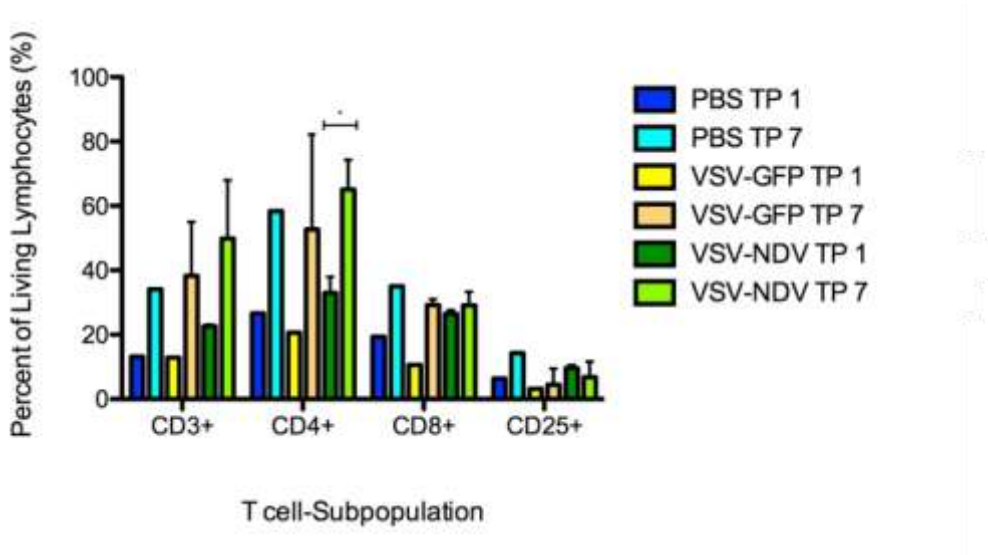

Figure 32: Flow cytometric analysis from blood of PBS and virus-treated, HCC-bearing Buffalo rats on day 1 and 7 after treatment

Buffalo rats were implanted with single, intrahepatic HCC nodules and treated eleven days after implantation via intra-tumoral injection of either rVSV-GFP, rVSV-NDV or PBS as control. On day one or seven after treatment the rats were euthanized and blood was collected. PBMCs were separated from blood samples and analysed by flow cytometric analysis on stimulation of CD3+, CD4+, D8+ and CD25+ T cells. Means + standard deviation are shown.

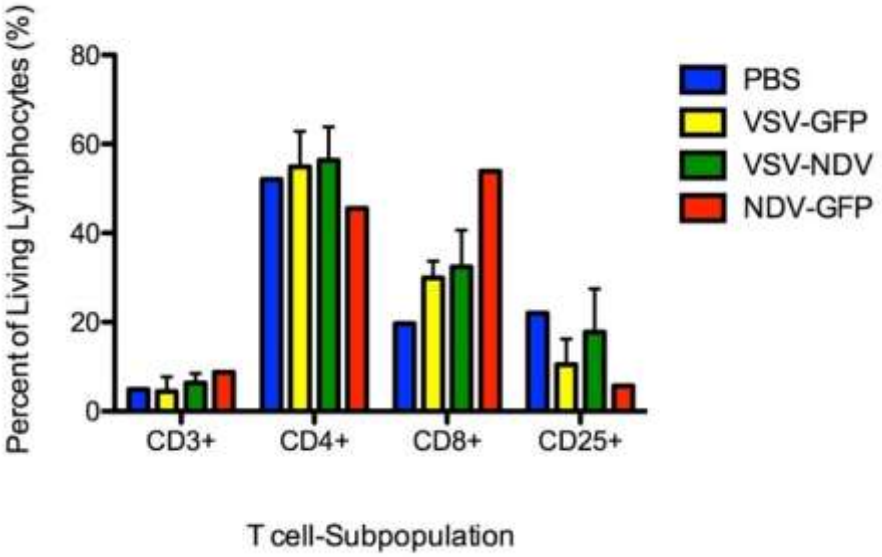

Figure 33: Flow cytometric analysis from tumor cells of PBS and virus-treated rats on day 7 after treatment

Buffalo rats were implanted with single, intrahepatic HCC nodules and treated eleven days after implantation via intra-tumoral injection of either rVSV-GFP, rVSV-NDV or PBS as control. On day one or seven after treatment the rats were euthanized and blood was collected. PBMCs were separated from blood samples and analysed by flow cytometric analysis on stimulation of CD3+, CD4+, D8+ and CD25+ T cells. Means + standard deviation are shown.

7. Statistical Analysis

All data was depicted and analyzed with GraphPad Prism version 7 (GraphPad software, La Jolla California, USA). A confidence interval of 95% was applied in all tests, therefore p-values less than 0.05 were considered to be statistically significant. In all tests a two-sided level of significance was used. Statistical significance is shown in one to three asterisks, one asterisk (*) means p-values are less than 0.05, two asterisks (**) mean p-values are less than 0.01 or three asterisks (***) mean p-values are less than 0.001.

Survival data are in general depicted in Kaplan-Meier survival curves and were analyzed using the log-rank test.

Survival data of rats treated with the OV via intra-arterial injection were additionally plotted as Whisker-plot. As there are more than three unpaired groups and Gaussian distribution can be expected, the applied test method to determine if variances differ significantly between the groups is one-way ANOVA.

Levels of viral titer in any given tissue were depicted in scatter plots and analyzed using Mann-Whitney-U test. Compared were two independent groups with assumed arbitrary distribution.

The differences in body weight of NOD-SCID mice on their day of death for the viral safety study were depicted as line graph. The compared values are independent values with parametric distribution, therefore t-test for independent samples was chosen as statistical test.

To analyze statistical significance of the difference in start of tumor growth after Ad.Cre-induction in slow growing and fast growing tumors, depicted as bar charts, Mann-Whitney-U test was used as 2 independent groups with assumed arbitrary distribution of the test results were analyzed.

The t-test for independent samples was used to analyze statistical significance of the difference of tumor seize at treatment start in the inducible HCC model, viral titer of organs between treatment groups and immune stimulation between the treatment groups. This test method was chosen as comparison was drawn between two independent and unpaired treatment groups and parametric distribution of the results was assumed. The results are depicted as bar charts.

Figure #	**Experiment**	**Comparison**	**Significance**	**P-Value**	**Test Method**
21	survival in safety study	rVSV-GFP vs. rVSV-NDV	*	0.0246	logrank test
23	viral titer in organs in	Brain: rVSV-GFP vs. rVSV-NDV	ns	0.0636	Mann-Whitney U test
23	viral titer in organs in	Liver: rVSV-GFP vs rVSV-NDV	ns	1000	Mann-Whitney U test
24	serum titer in safety study	Day 1: rVSV-GFP vs. rVSV-NDV	ns	0.1967	Mann-Whitney U test

24	serum titer in safety study	Day 7: rVSV-GFP vs. rVSV-NDV	ns	0.1967	Mann-Whitney U test
24	serum titer in safety study	Day 13: rVSV-GFP vs. rVSV-NDV	ns	0.5050	Mann-Whitney U test
25	weight development in safety study	Date of death: rVSV-GFP vs. rVSV-NDV	*	0.0146	unpaired t-test
26	HCC-model	slow growing vs. fast growing in male and female mice	***	0.0005	Fisher's exact test
26	HCC-model # of tumors at treatment start	slow growing vs. fast growing tumors	ns	0.2718	Mann-Whitney U test
26	HCC-model seize of tumors at treatment start	slow growing tumors vs. fast growing tumors	ns	0.1298	t-test for independent samples
27	survival in AST mice	PBS vs. rVSV-NDV	**	0.0034	logrank test
27	survival in AST mice	rVSV-GFP vs. rVSV-NDV	ns	0.0625	logrank test
28	survival in rats i.a. injection	PBS vs. rNDV vs. rVSV-GFP vs. rVSV-NDV	ns	0.8413	logrank test
28	survived days i.a injection	PBS vs. rNDV vs. rVSV-GFP vs. rVSV-NDV	ns	0.8717 0.3615	one-way ANOVA: means one-way ANOVA: variances
28	survival in rats i.t. injection	PBS vs. rVSV-NDV	*	0.0246	logrank test
28	survival in rats i.t. injection	rVSV-GFP vs. rVSV-NDV	ns	0.2689	logrank test
29	$TCID_{50}$ of organs in kinetics study	day 1 tumor: rVSV-GFP vs. rVSV-NDV	ns	0.2721	t-test for independent samples
29	$TCID_{50}$ of organs in kinetics study	rVSV-GFP brain: day 1 vs. day 7	ns	0.5415	t-test for independent samples
29	$TCID_{50}$ of organs in kinetics study	rVSV-GFP tumor: day 1 vs. day 7	ns	0.5415	t-test for independent samples
32	flowcytometric analysis from blood in kinetics study	rVSV-NDV $CD4^+$: day 1 vs.- day 7	*	0.0112	t-test for independent samples

32	flowcytometric analysis from blood in kinetics study	rVSV-NDV $CD3^+$: day 1 vs.- day7	ns	0.115	t-test for independent samples
33	FACS analysis from tumor on day 7	$CD25^+$: rVSV-GFP vs. rVSV-NDV	ns	0.2445	t-test for independent samples

Table 6: Statistical Analysis

8. Discussion

Experiments conducted on viral safety of rVSV-NDV compared to rVSV-GFP show an enhanced safety profile in immune deficient NOD-SCID mice treated with a dose of $1x10^6$ $TCID_{50}$. rVSV-NDV treated mice survived without any compromise to their general condition, weight development or parameters of renal function, which is even more impressive as immune deficient mice were used in this experiment. The parameters for liver function appear to be unsteady and fluctuate in a wide range around reference values, although several measurements of the serum sample were required until a result within measurable range was achieved. The measurement of GPT might be inaccurate because of the high dilution of the serum samples required due to limitation in plasma sample volume and the detection limit of the photometer used to evaluate the samples. The safety aspect of rVSV-NDV treatment is underlined by the comparatively high viral titers of rVSV-GFP found in brain tissue of infected NOD-SCID mice and their illness with neurological symptoms on their day of euthanization. Those findings go along with the viral titers found in blood of rVSV-GFP treated mice on day one and seven after injection. In comparison, there was no titer of rVSV-NDV found in brain tissue or blood at the time of euthanasia of NOD-SCID mice. Both treatment groups showed low titers of virus in the liver on their day of sacrifice, which might partly be responsible for the parameter on liver function to be out of range, although none of the treated mice showed any liver specific symptoms. Also, the body weight of rVSV-GFP treated mice decreased along with their neurological illness, which were presented in wandering in circles and paralysis, probably due to their inability to reach the food source.

Another interesting parameter for the study of viral safety would have been the maximum tolerated dose. Those experiments were not performed, as it was not possible to achieve titers of rVSV-NDV high enough to treat mice with the maximum allowed volume of 100µl per day. It might have been possible to get an exception to the maximum applicable volume approved, but due to the production process of the virus, where virus-containing supernatant is run over a sucrose gradient and forms a band between the 30% and 60% sucrose layer, it is to be expected that the virus is solved in approximately 45% Sucrose. As it is unpredictable to foresee side effects of the injection of an even increased volume of such a high concentrated sucrose-virus mixture, we decided to stay within the recommended volume for intravenous injections. Experiments in mice were conducted with $1x10^7$ $TCID_{50}$ as this is the safe dose for rVSV-GFP in immunocompetent mice. Problems in the production of rVSV-NDV might occur due to the ability of the virus to form syncytia. This property allows rVSV-NDV to spread inside a given tissue or cell layer, thus being protected from the innate immunity, and bypassing the need to produce high yields of progeny virus. This could also contribute to the safety aspect of the virus. Furthermore, as an infected cell will fuse to its neighbouring cells, a single virion can theoretically infect and kill hundreds of cells, thereby greatly limiting the concentration of virus that can be produced from monolayer cell cultures. This problem could be addressed by using a non-adhesive cell line for virus production. The lack of cell-to-cell contact and therefore the reduced syncytia formation could lead to higher virus yields.

Regarding virus shedding, no measurable titer was detected in excretions of AST-LTAg mice in the first three days after injection. Concerning the handling of laboratory animals this means that although animals can be downgraded to biological security level "S1" after treatment, the body remains "S2" after death by German "Act on Genetic Engineering". It can be concluded that an involuntary contamination of the environment by execretions and secretions of treated patients becomes unlikely. Nevertheless, viral shedding needs to be verified specifically in the species under investigation and for each virus vector.

Although we determined that no virus is shed by AST-LTAg mice after 24 hours, it needed to be clarified if rVSV-NDV, that might be shed by human patients, or accidentally released into the environment, poses an environmental risk for bird populations. The conducted virulence test in 10-day old, embryonated chicken eggs led to the conclusion, that rVSV-NDV can be classified as apathogenic. None of the tested viral doses killed all the embryos in its group. rVSV-NDV was compared to the parental virus NDV. The virulence test for NDV resulted in a minimum lethal dose of 100PFU and a mean death time of 84h, therefore it can be classified as mesogenic.

For the survival study of rVSV-NDV compared to its parental viruses in AST-LTAg mice, the inducible HCC model via Ad.Cre injection was used. HCC developed in a gender-specific manner, closely mirroring the clinical situation in human patients, whereby males are more susceptible to HCC [7], underlying the translational aspect of the model. In our model female mice developed HCC, not only significantly(***) later than male mice, but also presented with fewer tumor nodules, which required more time to take over the whole liver. Therefore, this survival study was conducted in male mice only, to diminish the impact of different tumor growth rates, which would increase the standard deviations within treatment groups and require larger group sizes in order to reach statistically significant differences. The survival results of male AST-LTAg mice treated with two injections, one when tumors reached inclusion criteria and the second after one week, showed a significantly (**) prolonged survival in the rVSV-NDV-treated group compared to PBS-treated mice. The mice treated with rVSV-GFP did not show a significant prolongation of survival. It is already well-known that systemic delivery is not the optimal delivery route for oncolytic viruses due to immunological barriers between the injection site and the tumor[107]. As the proportions in mice did not allow for hepatic artery injection, the delivery route via tail vein injection represents the limitation of this model. Consequently, an impaired oncolytic effect in this model was suspected. The fact that the survival of rVSV-NDV-treated mice is already prolonged in contrast to the rVSV-GFP-treated mice, could indicate that the mechanisms were predominantly immune-mediated rather than a direct oncolytic effect, as we can assume that the tumor transduction efficacy was probably minimal. It could indicate an efficient spread inside the tumor tissue, thus needing only minimal doses of virus to reach the tumor. An additional kinetics experiment in this model will be necessary to get information about the mechanism for the prolonged survival of rVSV-NDV-treated mice.

The experiments on survival in Buffalo rats did not reveal any significant prolongation of survival in any of the virus treated groups compared to the PBS control group. Although the implantation of Morris Hepatoma cells is a well-established method in our lab, the tumors implanted in the liver of the Buffalo rats, used for this study, led to contact metastases predominantly in the intestines, causing starvation of the implanted rats

before they could develop liver-specific symptoms. The survival curve in this case is dependent on the localization of the implanted tumor. Tumors implanted far caudal on the left lateral hepatic lobe with only a short distance to the intestines tended to metastasize earlier than tumors implanted higher on the liver lobe. Because the route of administration of our therapies was semi-selective to the hepatic tumors, via infusion into the hepatic artery, it was not expected that the therapy would reach peritoneal metastases. Therefore, we speculate that the survival data was greatly skewed by the rapid growth of metastatic lesions, and we believe that the data obtained from the respective survival experiment conducted in AST mice and in Buffalo rats, treated via intratumoral injection, is more reliable.

Survival experiments conducted in Buffalo rats with implanted, unifocal HCC lesions and treated via inratumoral injection resulted in significantly (*) prolonged survival of rVSV-NDV treated rats compared to the PBS control. Again, rVSV-GFP prolonged survival in a not statistically significant scale. That survival prolongation could be reached in this model and not via intraarterial injection could be due to the higher doses of the oncolytic virus that reach the tumor site when administered intratumorally. After all, AST-mice in which significant survival prolongation was achieved, were treated with the same dose ($1x10^7$ $TCID_{50}$) as Buffalo-rats. Considering the smaller blood volume of a mouse (mouse approximately 1.7ml, rat approximately 22.5ml) the same virus dose was not only exposed to a lower amount of immune-components in the mouse model, which probably decreased interference, it also was applied in a higher ratio of OV to tumor mass. In addition, the dose of $1x10^7$ $TCID_{50}$ that was used, as has been proven previously, was the maximum tolerated dose for rVSV-GFP in AST-mice. Buffalo rats could, as mentioned above, probably tolerate higher virus titers, that were not possible to yield up to know. The fact that the intratumorally treated rats showed a prolonged survival compared to the intraarterially injected rats, indicates that a higher virus titer administered intraarterially could possibly not only prolong survival of treated rats, but also reach and affect metastases.

Considering statistical significance in the survival studies in combination with the flaws and advantages of each model it becomes clear that repeated injections as performed in the mouse model can be an efficient approach. Of course, the use of the highest possible safe-dose is beneficial for the outcome and needs to be investigated urgently in the rat and mouse model, as the maximum tolerated dose for rVSV-GFP was used to perform the experiments. Another factor that could have supported the success in the mouse model is the heterogeneity of this highly translational tumor model. It can be assumed that tumor cells of different susceptibility to the OV are present in a heterogenic tumor environment, so that the virus can enter the tumor tissue via highly susceptible cells and afterwards spread the tumor tissue from the inside. In the homogenic tumor model the effectiveness of the treatment depends on the susceptibility of the one cell line used for tumor implantation. The contrast between the rat survival studies reveals the necessity to circumvent the immune system in the early phase of treatment. This can of course be achieved by intratumoral injection as performed in this study or in a hopefully even more effective manner by shielding the virus from recognition by the immune system.

HCC-bearing Buffalo rats were used for experiments on viral kinetics as well. However, these experiments were not completed. Therefore, no statistical analyses should be performed and, although we can speculate on trends in the data, no conclusions can be drawn. In this experiment, viral vectors were injected intratumorally. Neutralizing antibody assays were performed with plasma of either rNDV-GFP, rVSV-GFP or rVSV-NDV treated rats, that were euthanized one or seven days after treatment. The assay showed low neutralizing antibody titers for rNDV-GFP as early as on day one after treatment with a titer of 1:100 and a similarly low titer on day seven with 1:50. As there was only one rNDV-GFP treated rat, we cannot say whether these data are representative. rVSV-GFP treated rats showed an average titer of 1:25 on day seven after treatment. This is significantly lower than what was previously reported by the group. Possible reasons for the different outcome could be the inter-investigator variation, as well as the different source from which the Buffalo rats were obtained. It appears that the rats may have been altered in their immune response, as they tended to higher susceptibility to infections after surgery than rats from previous experiments. There was no neutralizing antibody titer detected in rVSV-NDV-treated rats at either time-point, but again, group size is too small to draw a conclusion. To reveal the point in time when antibodies against rVSV-NDV are produced, days 14 and 21 after treatment need to be tested. A potentially delayed production of neutralizing antibodies against rVSV-NDV gives opportunity to treat a tumor with a booster injection at day seven after treatment, when viral titers decreased in the tumor tissue. This property could also indicate that rVSV-NDV could be an optimal vaccine vector, as the immune response could be more directed against the targeted tumor antigen, rather than against the virus. Although there were titers of rVSV-GFP and rVSV-NDV on day one after treatment, there was no titer detected in rVSV-NDV-treated tumors on the seven-day time-point. To get more information on the kinetics of viral replication in tumor tissue, additional time-points need to be investigated. On day seven after treatment, there were rather high titers of rVSV-GFP in the brains of treated rats, although they were injected with a save dose previously determined to be safe in this model ($1x10^7$ $TCID_{50}$/rat), and no signs of neurological symptoms could be detected. In contrast, there was no titer of rVSV-NDV or rNDV-GFP in the brains of treated rats. This also stresses the importance of the development of a viral vector that is non-replicative in neurons. Although there were higher titers of rVSV-GFP found in tumor tissue, the titers of rVSV-GFP in healthy liver tissue on the seven-day time-point and the titer found in brain tissue make rVSV-GFP appear less tumor-specific than rVSV-NDV. Furthermore, it remains to be seen whether the increased intratumoral titer translates to enhanced efficacy compared to rVSV-NDV.

The co-culture experiment of McA-RH7777 cells with PBMCs derived from blood of rVSV-NDV, rVSV-GFP or PBS treated rats turned out to be inaccurate and not suitable to detect delicate variances as would be necessary in the test results. The amount of cell-counting steps involved in this experiment, might have led to a subsequent aberration, explaining variation in detected cell viability within experimental groups. A better way to test antitumor immune responses could be an ELISA assay from serum samples for T cells directed against TAEs. To better determine any effect of tumor-specific T cells in response to the respective therapies, later time-points will need to be investigated.

T cells were also used for flow cytometric analysis. The results indicate an increased T cell activation in rVSV-NDV treated rats in comparison to rVSV-GFP treated rats on day one after treatment, although this data is only based on one or two treated rats per group. These findings go along with other studies that revealed a strong immunogenic effect of the F and HN protein of NDV[64], which in VSV-NDV seems to activate T cells as well. However, it is unlikely that this effect would be evident already after only 24hours post treatment. Seven days after intra-tumoral injection, there are higher percentages of living T cells to be found in blood samples. The increased stimulation of T cells on day seven after treatment, even in the PBS treated rat, indicates that the surgery performed to inject substances into the tumor might be partly responsible for the immune stimulation. To overcome the impact of immune stimulation through surgical intervention, ongoing experiments could be performed via ultrasound guided intra-tumoral injection through the skin. Findings from flow cytometric analysis of tumor invading T cells on day seven after treatment resulted in enhanced CD8+ T cell activation in the rNDV-GFP group.

Ongoing experiments on the effectiveness of rVSV-NDV will be performed by the addition of days 3, 14 and 21 after treatment to the experiments on viral kinetics and addition of AST-LTAg mice to the survival experiment. Histological and immunohistochemical data from tumor tissue will also provide important information regarding necrosis, apoptosis, and inflammatory cell infiltration. Moreover, insight into replication, kinetics and biodistribution of rVSV-NDV can be gained by PET/CT- or PET/MR-imaging of animals through the use of reporter genes, such as the herpes simplex thymidine kinase gene, into the rVSV-NDV vector. Other plans to enhance the efficacy of the hybrid-virus include the introduction of molecules to modulate immune checkpoints, such a soluble PD1 into rVSV-NDV vector, to circumvent T cell inactivation by tumoral PD-L1. Furthermore, a combination with adoptive T cell therapy will be investigated.

In conclusion, rVSV-NDV proved to be a safe oncolytic agent in the investigated doses. There was no neurotoxicity or other organ failure detectable in treated immunosuppressive mice. In addition, concerns in terms of viral shedding are diminished by the fact that there is no virus measurable in excretions of treated AST-LTAg mice. The pathogenicity of rVSV-NDV in avian species was tested by inoculation of embryonated chicken eggs to confirm its degree of pathogenicity. rVSV-NDV is proven to be apathogenic.

In terms of rVSV-NDV's effectiveness, it showed tendencies of promising survival prolongation in AST-LTAg mice and Buffalo rats, treated via intratumoral injection, and a stronger antitumor immune stimulation than its viral backbone VSV. The fact that rVSV-NDV-specific antibodies are not produced within the first seven days after application gives the opportunity to use a booster application one week after treatment start to enhance the oncolytic effects of rVSV-NDV.

rVSV-NDV can be a safer replacement of the already effective parental viruses. Ongoing experiments with the hybrid virus will be conducted to prove its enhanced effectiveness and to establish a safe delivery route that shields the virus from early, unspecific immune responses. The viral vector VSV-GP[95] is in many aspects comparable to our developed VSV-pseudotype. A direct comparison of the key aspects important for

preclinical investigations will pronounce weaknesses and strengths of both vector types and set them apart as both valuable contributions to the OV- therapy landscape.

Both recombinant virus vectors follow the strategy to replace the tropism-mediating glycoproteins on the VSV envelope with glycoproteins of a different oncolytic agent to circumvent VSVs efficient infection of neurons[108] and also to gain new functions such as syncytia development[4] and advantages like loss of neutralizing antibody development by a well-matched pairing. To prove the success in achieving a safer oncolytic agent, vector administration in rodents was tested and led to the conclusion that both viruses can be applied safely in these model organisms. Both vectors have been tested in immunodeficient mice to further underline the safety aspect. As it was possible to achieve higher virus titers for the rVSV-GP pseudotype, it was injected in a dose of 10^8 PFU, whereas rVSV-NDV was injected in a dose of 10^6 PFU. Nevertheless, application of both vectors did aside from a minor loss in body weight at the beginning not lead to any health concerns in the immunodeficient mice. All mice in those studies have been euthanized at the end of the observation period without any signs of illness. For rVSV-GP systemic safety was tested by injection of 10^9PFU in immunodeficient CD-1 mice. There were no death events in the rVSV-GP treatment group to be observed. Although rVSV-NDV has not been tested to specifically prove systemic safety, it was used for treatment of immune competent AST mice that had to be euthanized in the end, but due to tumor burden and not as a result of toxic events induced by the virus.

VSV-NDV and VSV-GP were tested to rule out off-target toxicity. Here the results do as well show a similarity. There were no elevated titers of creatinine to be measured, neither in the rVSV-GP[95] nor in the rVSV-NDV treated mice. Serum level for GPT on the other hand were slightly increased in the rVSV-GP treated animals and off-range for the rVSV-NDV treated animals, although measurements in the rVSV-NDV treated group had to be repeated several to times to achieve a result within the detection range of the instrument. Despite these findings that indicate a marginal damage of liver cells RT-PCR of rVSV-GP treated animals to determinate viral existence in non-tumoral liver cells revealed a rapid clearance from the tissue after injection and histologic examination of non-tumoral liver cells in rVSV-NDV treated animals did not display cell damage.

The most interesting aspect of course is the recombinants efficacy in treatment of tumor cells and spheroids *in vitro* and massive tumors *in vivo* by different application routes (intratumoral or systemic).

Both vectors have been tested in a variety of tumor cells and rodent tumor models. As susceptibility of the tumor cells is highly dependent on their impaired IFN response, an IFN assay can reveal first clues about the likeliness of a successful infection of the tumor in question. Even cell lines with an intact innate immune response can be made susceptible to the OV treatment by a pre-treatment with ruxolitinib. This inhibitor of Janus kinase (JAK)1 and 2 can successfully overcome the cells IFN protection as shown in *in vitro* assays as well as *in vivo* studies on treatment efficacy of VSV-GP in tumors with reduced susceptibility[29]. Nevertheless, a co-application of both, ruxolitinib and the oncolytic vector should be considered carefully and the effects on off-target toxicity should be re-evaluated.

The viruses under investigation were tested for susceptibility and efficacy in different types of cancer, the following section will give a short overview over their outstanding features. More details of the tested model systems (cell lines implanted, model organism, implantation site, administration route etc.) are attached in a table. It has to be mentioned that a direct comparison of treatment doses between the viruses VSV-GP and VSV-NDV is complicated, because VSV-GP has generally been measured in PFU, whereas VSV-NDV (as a syncytia forming virus) cannot be measured in the same way and is quantified in $TCID_{50}$.

In general, VSV-NDV has been tested for the use in HCC. Here we have data showing successful infection of human HCC cell lines derived from patients and we are able to show not only successful infection, but also a delayed tumor growths in immune competent rodent HCC models after intratumoral injection and in the mouse model as well after systemic injection of the OV as described in [6. Results]. Other tests that have been conducted on VSV-NDV revealed a good susceptibility to a lung carcinoma cell line in an *in vitro* Interferon response assay [3.2 Preliminary data]. The virus VSV-GP has been tested in several cancer models with different outcome. The infection and treatment success seems to be pronounced especially in models of glioma *in vitro* and *in vivo*. Susceptibility was variable in different models of ovarian cancer, malignant melanoma (human, mouse and dog cell lines) and prostate cancer. All models revealed cell types with different infection rates. It was possible to circumvent reduced susceptibility with great treatment success via a combination treatment scheme of VSV-GP and ruxolitinib.

As mentioned above VSV-GP proved as a competent oncolytic vector in the treatment of malignant glioma. Although it showed lower infection and replication rates compared to wild type VSV, infection of monolayers or spheroids of malignant glioma *in vitro* led to rapid replication and complete cell cytotoxicity within a few days. Tests concerning the oncolytic abilities of VSV-GP were conducted in immunodeficient mice in a heterotopic tumor model and an orthotopic tumor model as well as in immune competent mice. Intratumoral injection of VSV-GP in subcutaneously implanted tumors in SCID mice cured all of the treated mice. SCID mice implanted with intracerebral tumors showed prolonged survival after the intratumoral treatment with VSV-GP (71 days post transplantation or event-free long time survival over more than 125 days) when compared to the PBS control group (median survival 33 days post transplantation). Immune competent mice with intracerebral tumors treated via i.t. injection also enhanced survival after transplantation. Median survival in the treatment group was 81 days post transplantation (treatment 10 days after transplantation) compared to the PBS control with 29 days post transplantation. Additionally five out of ten animals showed event free long-term survival[95]. VSV-GP has been tested as well in ovarian cancer. *In vitro* susceptibility of the tested cells showed different outcomes among the tested cells. As it turned out human ovarian surface epithelial cells (HOSE) do only show limited susceptibility and do not lyse the cells even at an MOI of 1. Nevertheless, HOSE cells were implanted subcutaneously in NOD-SCID mice and different treatment schemes from OV monotherapy to a combination therapy of OV and ruxolitinib have been tested. The VSV-GP monotherapy treatment scheme led to seven cured animals out of ten, but tumors recurred approximately between 25 and 50 days after treatment start. The combinational therapy with VSV-GP and ruxolitinib led to a reduced recurrence of cured tumors in only three out of nine cured mice. Via i.p. injection orthotopically implanted

ovarian cancer cells in immunodeficient mice could partly be cured with VSV-GP treatment. Tumor remission was observed in three out of eight mice. Again the combination treatment scheme of VSV-GP and ruxolitinib increased the treatment success and led to tumor remission in seven out of eight mice, which were considered cured after a 100 day observation period[29]. Tests on the therapeutic efficacy for the treatment of malignant melanoma again revealed different infection rates when used *in vitro* in human, murine and dog cell lines. Five out of ten cell lines derived from primary human melanoma were susceptible for infection with VSV-GP. The one tested mouse and dog cell line showed good susceptibility. Heterotopic implantation of the mouse melanoma cell line in immune competent mice and treatment via intratumoral injection of VSV-GP showed dose-dependent effects. Mice in the PBS control group had a median survival of 18 days, whereas treatment with VSV-GP in the highest administered dose ($2.36x10^7$ PFU) led to a median survival of 25.5 days with complete remission in three out of twelve treated mice. In this tumor model a treatment via the systemic administration route ($2.36x10^7$ PFU) was applied as well and led to a median survival of 22 days (maximum 32 days) in the virus treated group compared to the PBS control with 17.5. days median survival[109]. VSV-GP has also been tested in prostate cancer. In contrast to the melanoma and ovarian cancer cell lines were reduced susceptibility was observed, all cultures of prostate cancer seemed to be sensitive for infection *in vitro*, yet heterogeneous killing rates ranging between 60% and 20% have been observed. The treatment efficacy was investigated *in vivo* by intratumoral or systemic injection into immunodeficient mice with heterotopic tumors and by systemic injection into immune competent mice. Tumors were generated by implantation of either of two susceptible cell lines with reduced IFN competence. A treatment scheme of 2 intratumoral injections of 10^7 PFU in subcutaneous tumors led to full tumor remission without relapse in a 100 day observation period. Systemic treatment of heterotopic tumors had dose dependent outcome with six out of six animals cured without relapse in a 86 day observation period, when treated with the highest dose (10^8 PFU). Systemic treatment of heterotopic tumors in immune competent mice led to growth delay and significant prolongation of median survival[110].

Comparing the treatment success of VSV-NDV and VSV-GP, it is noteworthy that none of the animals under investigation in survival studies had to be euthanized due to neurological illness or other sickness caused by organ failure. VSV-GP has been tested in a broad variety of different tumor models, administration schemes and combination treatment with the ruxolitinib. It became apparent that VSV-GP does not efficiently kill all the tumor cell lines under investigation, but was often successful when used in combination treatment with ruxolitinib to circumvent IFN responses. When compared to the oncolytic activity of VSV-NDV it becomes apparent that both viruses seem to improve upon sequential application. The most successful application route still seems to be the intratumoral injection for both viruses tested, although treatment success for VSV-GP in the prostate cancer and melanoma models and for VSV-NDV in the treatment of HCC in the mouse model showed promising results via systemic application as well. Intratumoral injection of VSV-GP in different tumor models in immunodeficient mice often led to complete remission, which is a great treatment success, but still the more artificial system than immune competent rodents. For models tested with VSV-GP or VSV-NDV under the same attributions (immune competent host, orthotopic cancer model, virus monotherapy, administration by intratumoral injection) which applies

for treatment of malignant glioma treated with VSV-GP and HCC treated with VSV-NDV the outcome is comparably well in both virus vector systems. All things considered, treatment with the oncolytic vector VSV-GP was able to cure immunodeficient mice with different tumor models, both viral vectors led to prolonged survival in immune competent mice (and rats) after intratumoral injection and partly after systemic injection.

Another important aspect as already described before is the circumvention of humoral immune responses as this might give the viral vector the advantage of time to lyse the tumor cells before being cleared. For VSV-GP, treatment does not induce neutralizing antibodies against VSV or VSV-GP, at least within a time frame of 26 days. This gives the opportunity for booster injections of the vector to induce a second stage of cell lysis and enhance inflammation within the tumor bed by CTLs[32]. For VSV-NDV, no production of neutralizing antibodies could be observed within 7 days after treatment. This period was successfully used for a booster application of the oncolytic vector and we were able to show an improvement of the survival data in the mouse survival studies upon repeated administration.

Another approach that will be tested with VSV-NDV in future studies is the effect on using the virus as a vaccine against tumoral antigens. VSV-GP has been tested in that matter by introducing an OVA antigen into the vector and treatment of naïve C57BL/6 mice with the serum of VSV-GP-OVA or VSV-OVA treated mice. The study resulted in T cell responses after challenge with VSV-GP-OVA directed against OVA in the VSV-GP-OVA group, but not in the VSV-OVA group. To further prove the effectiveness of the vaccination scheme VSV-GP-OVA pre-immunized mice were challenged with a *Listeria monocytogenes* (Lm) expressing OVA. After scarification of the mice the bacterial load measured in the spleen was below detection limit, whereas in the control group high levels of Lm-OVA could be found[32] .

The comparison of both vectors underlines what is already well known, that oncolytic virus face similar obstacles especially concerning the accessibility of the tumor and rapid clearing by immune responses. On the other hand, a broad landscape of OV vectors with different profiles in susceptibility and immunologic impact can contribute to an individualized treatment scheme for different cancerous diseases.

The use of the oncolytic virus vector investigated in our studies could not only provide a benefit for survival of HCC patients on the transplant list until a suitable transplant is available, with some additional effort in terms of shielding the virus or improved delivery routes it could even be curative and not only for the solid primary tumor lesion but as well for metastases in all kinds of organs. Until now the most successfully treated tumors have been melanomas, as they are mostly available for intratumoral treatment because of their comparingly superficial location.

A barrier in veterinary medicine poses the treatment of equines, cattle, pig and poultry. The virus's origin from animal viruses affects its usability for animal patients. It can be assumed that the use in the parental virus's natural hosts cannot be considered safe. In addition, the effectiveness of the treatment will probably suffer from preexisting immunity, due to a much higher epidemic infestation than can be assumed in humans. Nevertheless small animal patients could profit from the development of this treatment approach.

For future patients of carcinogenic diseases of all kinds it will be vital for the treatment success to have a broad variety of treatment strategies to choose from. Not only to address the individuality of each tumor, but as well to attack cancer with ever changing approaches and eventually exhaust its ability to circumvent destruction. Oncolytic viro-immunotherapy in general and specifically rVSV-NDV as oncolytic agent could provide an alternative platform to target tumor cells, break immune tolerance towards tumor antigens, stimulate the immune response and even vaccinate against tumor antigens to protect from recurring tumor growth.

9. Summary

This study investigated the recombinant virus, rVSV-NDV, for its safety and effectiveness *in vivo*. To gain insight into the safety of the application of the hybrid-virus, experiments on toxicity in liver, kidney and brain of treated NOD-SCID mice were performed in comparison to NOD-SCID mice treated with the parental virus VSV. The results revealed that a safe use of the oncolytic viral vector is possible and no harm to basic organ function is expected. To rule out an environmental risk to exposed birds a study on the pathogenicity of rVSV-NDV in embryonated chicken eggs was performed. Based on this experiment, the hybrid-virus, rVSV-NDV, can be classified as apathogenic. Conducted Survival experiments in AST mice, treated via tail vein injection, and Buffalo rats, treated via intratumoral injection, resulted in enhanced prolongation of survival in the rVSV-NDV-treated group compared to the rVSV-GFP treated group and significantly enhanced prolongation compared to the PBS control. A survival experiment, conducted in Buffalo rats, treated via intraarterial injection, was performed in order to safe the virus from unspecific immune responses by a more translational delivery route via the hepatic artery. The results from the mouse survival experiment were not reproducible in this rat survival experiment. Although the tumor model, used in this experiment is well-established in our group, there were peritoneal metastases in tumor implanted rats that were interfering with the survival results. The contrast to the results of the intratumorally injected rats suggests that a smaller virus dose reached the tumor bed compared to the direct injection, which stresses the need to investigate improved virus production protocols that lead to higher virus yield and allow to treat using the maximum tolerated dose. Experiments on viral kinetics were conducted in groups too small to draw a real conclusion, but give a hint referring to the virus's replication in different tissues and development of neutralizing antibodies. The results indicated a potentially delayed development of neutralizing antibodies, which gives the opportunity for a booster injection of the oncolytic virus. In addition, the hybrid-virus does not seem to replicate in the brain of treated NOD-SCID mice or rats. In tumor tissue it replicates to titers lower than the titers of the parental virus VSV.

To get rVSV-NDV into clinical translation the most important step will be to further improve virus production and examine the maximum tolerated dose as a safe and effective treatment dose. Additionally a multi-injection regimen as already used in OV-therapy in the clinic should be applied.

10. Zusammenfassung

In dieser Arbeit wurde das rekombinante Virus VSV-NDV auf seine Sicherheit und Effektivität *in vivo* untersucht. Um die Sicherheit der Anwendung des neuen Hybridvirus zu untersuchen, wurden Experimente bezüglich der Toxizität in Leber, Niere und Gehirn in NOD-SCID Mäusen durchgeführt. Die Ergebnisse zeigen, dass eine sichere Anwendung von rVSV-NDV möglich ist und nicht zu einer Einschränkung der Funktion grundlegender Organe führt. Des Weiteren wurde die Virulenz des Virus in Vögeln an embryonierten Hühnereiern untersucht, um ein eventuell vorhandenes Risiko für exponierte Tiere abschätzen zu können. Die Ergebnisse der Untersuchung lassen eine Einstufung von rVSV-NDV als in Vögeln apathogenes Virus zu. Durchgeführte Überlebensexperimente bezüglich des Therapieeffekts in AST-Mäusen, behandelt über Injektion des OV in die Schwanzvene, und in Buffalo-Ratten, behandelt über intratumorale Injektion des OV, resultierten in verlängerter Überlebenszeit rVSV-NDV behandelter Mäuse im Vergleich zu rVSV-GFP behandelter Mäuse und signifikant verlängerter Überlebenszeit gegenüber der PBS-Kontrollgruppe. Es wurde ebenfalls ein Überlebensexperiment in Buffalo-Ratten durchgeführt, bei dem das Virus über eine Injektion in die tumorversorgende A. hepatica propria appliziert wurde, um das Virus auf seinem Weg ins Tumorbett vor unspezifischen Immunreaktionen zu schützen. In diesem Experiment konnten die Ergebnisse aus dem Experiment an AST-Mäusen nicht reproduziert werden. Obwohl das in diesem Versuch angewendete Tumormodell in unserer Arbeitsgruppe bereits lange etabliert ist, neigten die tumorimplantierten Tiere zur Ausbildung von peritonealen Metastasen, die maßgeblich die Überlebenszeit der Tiere beeinflussten. Die stark unterschiedlichen Ergebnisse der Überlebensstudien in Ratten lassen den Rückschluss zu, dass bei der intraarteriellen Injektion des OV eine wesentlich kleinere Virusmenge das Tumorbett erreicht, im Vergleich zur direkten Applikation über die intratumorale Injektion. Dieser Schluss unterstreicht die Notwendigkeit ein effizienteres Protokoll zur Virusproduktion zu untersuchen, das zu höheren Virustitern führt und die Applikation der maximal tolerierten Dosis zur Behandlung erlaubt. Experimente zur Untersuchung der Viruskinetik wurden in sehr kleinen Gruppen durchgeführt, die eventuell einen Hinweis geben auf die Replikation von rVSV-NDV in verschiedenen Geweben und die Bildung neutralisierender Antikörper. Die Ergebnisse weisen auf eine, im Vergleich zu den Kontrollviren VSV und NDV, verzögerte Bildung neutralisierender Antikörper hin. Zu den untersuchten Zeitpunkten an Tag eins und sieben nach Therapiebeginn liegen keine Hinweise auf neutralisierende Antikörper gegen rVSV-NDV vor. Dadurch könnte die Möglichkeit einer Auffrischungsinjektion an Tag sieben nach Therapiestart bestehen. Weitere Untersuchungen zur Replikation des Hybridvirus in Gehirn, Leber und Tumorgewebe weisen darauf hin, dass rVSV-ND nicht im Gehirn behandelter NOD-SCID-Mäuse oder Ratten repliziert. Im Tumorgewebe behandelter Ratten wurden niedrigere Virustiter für rVSV-NDV nachgewiesen als für den Kontrollvirus VSV.

Die wichtigsten Schritte um rVSV-NDV auf einen Start im klinischen Alltag vorzubereiten, werden die Optimierung der Produktion und die Untersuchung der maximal tolerierten Dosis als sichere und effektive Behandlungsdosis sein. Außerdem sollte ein Behandlungsregime mit wiederholter OV-Applikation, wie bereits üblich in der Krebstherapie mit onkolytischen Viren, angewendet werden.

11. References

1. Kelly, E. & Russell, S. J. History of Oncolytic Viruses: Genesis to Genetic Engineering. *Mol. Ther.* **15**, 651–659
2. Bell, J. & McFadden, G. Viruses for Tumor Therapy. *Cell Host Microbe* **15**, 260–265 (2014).
3. Altomonte, J. & Ebert, O. Sorting Out Pandora's Box: Discerning the Dynamic Roles of Liver Microenvironment in Oncolytic Virus Therapy for Hepatocellular Carcinoma. *Front. Oncol.* **4**, 85 (2014).
4. Abdullahi, S. *et al.* A Novel Chimeric Oncolytic Virus Vector for Improved Safety and Efficacy as a Platform for the Treatment of Hepatocellular Carcinoma. *J. Virol.* **92**, e01386-18 (2018).
5. Hastie, E. & Grdzelishvili, V. Z. Vesicular stomatitis virus as a flexible platform for oncolytic virotherapy against cancer. *J. Gen. Virol.* **93**, 2529–2545 (2012).
6. Ferlay, J. *et al.* Cancer incidence and mortality worldwide: Sources, methods and major patterns in GLOBOCAN 2012. *Int. J. Cancer* **136**, E359–E386 (2014).
7. European Association for the Study of the Liver & European Organisation for Research and Treatment of Cancer. EASL–EORTC Clinical Practice Guidelines: Management of hepatocellular carcinoma. *J. Hepatol.* **56**, 908–943
8. Ringehan, M., McKeating, J. A. & Protzer, U. Viral hepatitis and liver cancer. *Philos. Trans. R. Soc. B Biol. Sci.* **372**, 20160274 (2017).
9. Kai, K. *et al.* Correlation between smoking habit and surgical outcomes on viral-associated hepatocellular carcinomas. *World J. Gastroenterol.* **24**, 58–68 (2018).
10. But, D. Y.-K., Lai, C.-L. & Yuen, M.-F. Natural history of hepatitis-related hepatocellular carcinoma. *World J. Gastroenterol. WJG* **14**, 1652–1656 (2008).
11. Kinsey, J. R., Gilson, S. D., Hauptman, J., Mehler, S. J. & May, L. R. Factors associated with long-term survival in dogs undergoing liver lobectomy as treatment for liver tumors. *Can. Vet. J. Rev. Veterinaire Can.* **56**, 598–604 (2015).
12. Gheorghe, L., Popescu, I., Iacob, R., Iacob, S. & Gheorghe, C. Predictors of death on the waiting list for liver transplantation characterized by a long waiting time. *Transpl. Int.* **18**, 572–576 (2005).
13. Nomaguchi, M., Fujita, M., Miyazaki, Y. & Adachi, A. Viral Tropism. *Front. Microbiol.* **3**, 281 (2012).
14. Laing, K. Immune response to viruses.

15. Critchley-Thorne, R. J. *et al.* Impaired interferon signaling is a common immune defect in human cancer. *Proc. Natl. Acad. Sci.* **106**, 9010 (2009).

16. Chauhan, V. S. *et al.* Vesicular stomatitis virus infects resident cells of the central nervous system and induces replication-dependent inflammatory responses. *Virology* **400**, 187–196 (2010).

17. Hastie, E., Cataldi, M., Marriott, I. & Grdzelishvili, V. Z. Understanding and altering cell tropism of vesicular stomatitis virus. *Virus Res.* **176**, 10.1016/j.virusres.2013.06.003 (2013).

18. Yamauchi, Y. & Helenius, A. Virus entry at a glance. *J. Cell Sci.* **126**, 1289 (2013).

19. Green, D. R., Ferguson, T., Zitvogel, L. & Kroemer, G. IMMUNOGENIC AND TOLEROGENIC CELL DEATH. *Nat. Rev. Immunol.* **9**, 353 (2009).

20. Lu, W. *et al.* Intra-tumor injection of H101, a recombinant adenovirus, in combination with chemotherapy in patients with advanced cancers: A pilot phase II clinical trial. *World J. Gastroenterol. WJG* **10**, 3634–3638 (2004).

21. Garber, K. China Approves World's First Oncolytic Virus Therapy For Cancer Treatment. *JNCI J. Natl. Cancer Inst.* **98**, 298–300 (2006).

22. Parato, K. A. *et al.* The Oncolytic Poxvirus JX-594 Selectively Replicates in and Destroys Cancer Cells Driven by Genetic Pathways Commonly Activated in Cancers. *Mol. Ther.* **20**, 749–758 (2012).

23. Heo, J. *et al.* Randomized dose-finding clinical trial of oncolytic immunotherapeutic vaccinia JX-594 in liver cancer. *Nat. Med.* **19**, 329–336 (2013).

24. Pol, J., Kroemer, G. & Galluzzi, L. First oncolytic virus approved for melanoma immunotherapy. *Oncoimmunology* **5**, e1115641 (2016).

25. Andtbacka, R. H. I. *et al.* Talimogene Laherparepvec Improves Durable Response Rate in Patients With Advanced Melanoma. *J. Clin. Oncol.* **33**, 2780–2788 (2015).

26. Csatary, L. K. *et al.* Attenuated veterinary virus vaccine for the treatment of cancer. *Cancer Detect. Prev.* **17**, 619–627 (1993).

27. Hotte, S. J. *et al.* An Optimized Clinical Regimen for the Oncolytic Virus PV701. *Clin. Cancer Res.* **13**, 977 (2007).

28. Muik, A. *et al.* Re-engineering Vesicular Stomatitis Virus to Abrogate Neurotoxicity, Circumvent Humoral Immunity, and Enhance Oncolytic Potency. *Cancer Res.* **74**, 3567 (2014).

29. Dold, C. *et al.* Application of interferon modulators to overcome partial resistance of human ovarian cancers to VSV-GP oncolytic viral therapy. *Mol. Ther. Oncolytics* **3**, 16021–16021 (2016).

30. Miletic, H. *et al.* Selective Transduction of Malignant Glioma by Lentiviral Vectors Pseudotyped with Lymphocytic Choriomeningitis Virus Glycoproteins. *Hum. Gene Ther.* **15**, (2004).

31. Urbiola, C. *et al.* Oncolytic activity of the rhabdovirus VSV-GP against prostate cancer. *Int. J. Cancer* **143**, 1786–1796 (2018).

32. Tober, R. *et al.* VSV-GP: a potent viral vaccine vector that boosts the immune response upon repeated applications. *J. Virol.* **88**, 4897–4907 (2014).

33. Koske, I. *et al.* Oncolytic virotherapy enhances the efficacy of a cancer vaccine by modulating the tumor microenvironment. *Int. J. Cancer* **0**, (2019).

34. Sen, G. C. Viruses and Interferons. *Annu. Rev. Microbiol.* **55**, 255–281 (2001).

35. Delneste, Y., Beauvillain, C. & Jeannin, P. [Innate immunity: structure and function of TLRs]. *Med Sci Paris* **23**, 67–74 (2007).

36. Zaru, R. Pattern recognition receptors.

37. Stewart, C. E., Randall, R. E. & Adamson, C. S. Inhibitors of the Interferon Response Enhance Virus Replication In Vitro. *PLOS ONE* **9**, e112014 (2014).

38. Ivashkiv, L. B. & Donlin, L. T. Regulation of type I interferon responses. *Nat. Rev. Immunol.* **14**, 36–49 (2014).

39. Gershwin, M. E., Vierling, J. & Manns, M. *Liver Immunology*. (Hanley and Belfus Inc., 2003).

40. B Cells and Antibodies. in *Molecular Biology of the Cell* (Garland Science, 2002).

41. Borghesi, L. & Milcarek, C. *From B Cell to Plasma Cell: Regulation of V(D)J Recombination and Antibody Secretion*. **36**, (2006).

42. Sioud, M. Overcoming Self-Tolerance to Tumour Cells. *Methods Mol. Biol.* **629**, 495–505 (2010).

43. Blair, G. E. & Cook, G. P. Cancer and the immune system: an overview. *Oncogene* **27**, 5868 (2008).

44. Vinay, D. S. *et al.* Immune evasion in cancer: Mechanistic basis and therapeutic strategies. *Broad-Spectr. Integr. Des. Cancer Prev. Ther.* **35**, S185–S198 (2015).

45. Liu, Z. *et al.* RIG-I suppresses the migration and invasion of hepatocellular carcinoma cells by regulating MMP9. *Int. J. Oncol.* **46**, 1710–1720 (2015).

46. Noser, J. A. *et al.* The RAS/Raf1/MEK/ERK Signaling Pathway Facilitates VSV-mediated Oncolysis: Implication for the Defective Interferon Response in Cancer Cells. *Mol. Ther.* **15**, 1531–1536

47. Chirmule, N., Jawa, V. & Meibohm, B. Immunogenicity to Therapeutic Proteins: Impact on PK/PD and Efficacy. *AAPS J.* **14**, 296–302 (2012).

48. Slingluff, C. L. The Present and Future of Peptide Vaccines for Cancer: Single or Multiple, Long or Short, Alone or in Combination? *Cancer J. Sudbury Mass* **17**, 343–350 (2011).

49. Aitken, A. S., Roy, D. G. & Bourgeois-Daigneault, M.-C. Taking a Stab at Cancer; Oncolytic Virus-Mediated Anti-Cancer Vaccination Strategies. *Biomedicines* **5**, 3 (2017).

50. Cornax, I. *et al.* Newcastle disease virus fusion and haemagglutinin-neuraminidase proteins contribute to its macrophage host range. *J. Gen. Virol.* **94**, 1189–1194 (2013).

51. Goff, P. H., Gao, Q. & Palese, P. A Majority of Infectious Newcastle Disease Virus Particles Contain a Single Genome, while a Minority Contain Multiple Genomes. *J. Virol.* **86**, 10852–10856 (2012).

52. Macpherson, L. W. Some Observations On The Epizootiology Of NewCastle Disease. *Can. J. Comp. Med. Vet. Sci.* **20**, 155–168 (1956).

53. Mayr, A. & Rolle, M. *Medizinische Mikrobiologie, Infektions- und Seuchenlehre (8., überarbeitete Auflage)*. **149**, (Enke, Verlag, 2007).

54. Awan, M. A., Otte, M. J. & James, A. D. The epidemiology of Newcastle disease in rural poultry: A review. *12.11.2007* **23**, 405–423

55. Zamarin, D. & Palese, P. Oncolytic Newcastle Disease Virus for cancer therapy: old challenges and new directions. *Future Microbiol.* **7**, 347–367 (2012).

56. Aldous, E. W. & Alexander, D. J. Detection and differentiation of Newcastle disease virus (avian paramyxovirus type 1). *Avian Pathol.* **30**, 117–128 (2001).

57. Newcastle Disease. (2016).

58. Huang, Z., Krishnamurthy, S., Panda, A. & Samal, S. K. Newcastle Disease Virus V Protein Is Associated with Viral Pathogenesis and Functions as an Alpha Interferon Antagonist. *J. Virol.* **77**, 8676–8685 (2003).

59. Sánchez-Felipe, L., Villar, E. & Muñoz-Barroso, I. Entry of Newcastle Disease Virus into the host cell: Role of acidic pH and endocytosis. *Biochim. Biophys. Acta BBA - Biomembr.* **1838**, 300–309 (2014).

60. Samal, S. K. *The Biology of Paramyxoviruses*. (Caister Academic Press, 2011).

61. Yu, X. *et al.* The glutamic residue at position 402 in the C-terminus of Newcastle disease virus nucleoprotein is critical for the virus. *Sientific Rep.* **7**, (2017).

62. Elankumaran, S., Rockemann, D. & Samal, S. K. Newcastle Disease Virus Exerts Oncolysis by both Intrinsic and Extrinsic Caspase-Dependent Pathways of Cell Death. *J. Virol.* **80**, 7522–7534 (2006).

63. Washburn, B. *et al.* TNF-Related Apoptosis-Inducing Ligand Mediates Tumoricidal Activity of Human Monocytes Stimulated by Newcastle Disease Virus. *J. Immunol.* **170**, 1814 (2003).

64. WANG, K., SUI, H., LI, L., LI, X. & WANG, L. Anti-tumor Immunity of Newcastle Disease Virus HN Protein is Influenced by Differential Subcellular Targeting. *Chin. J. Lung Cancer Vol 13 No 8 2010 Chin. J. Lung Cancer* (2010).

65. Altomonte, J., Marozin, S., Schmid, R. M. & Ebert, O. Engineered Newcastle Disease Virus as an Improved Oncolytic Agent Against Hepatocellular Carcinoma. *Mol. Ther.* **18**, 275–284 (2010).

66. Park, M.-S., García-Sastre, A., Cros, J. F., Basler, C. F. & Palese, P. Newcastle Disease Virus V Protein Is a Determinant of Host Range Restriction. *J. Virol.* **77**, 9522–9532 (2003).

67. Zamarin, D. *et al.* Enhancement of Oncolytic Properties of Recombinant Newcastle Disease Virus Through Antagonism of Cellular Innate Immune Responses. *Mol. Ther. J. Am. Soc. Gene Ther.* **17**, 697–706 (2009).

68. Wu, Y. *et al.* Apoptin Enhances the Oncolytic Properties of Newcastle Disease Virus. *Intervirology* **55**, 276–286 (2012).

69. Vigil, A. *et al.* Use of Reverse Genetics to Enhance the Oncolytic Properties of Newcastle Disease Virus. *Cancer Res.* **67**, 8285 (2007).

70. Pühler, F. *et al.* Generation of a recombinant oncolytic Newcastle disease virus and expression of a full IgG antibody from two transgenes. *Gene Ther.* **15**, 371 (2008).

71. Vigil, A., Martinez, O., Chua, M. A. & García-Sastre, A. Recombinant Newcastle disease virus as a vaccine vector for cancer therapy. *Mol. Ther. J. Am. Soc. Gene Ther.* **16**, 1883–1890 (2008).

72. Buijs, P. R. A. *et al.* Intravenously injected Newcastle disease virus in non-human primates is safe to use for oncolytic virotherapy. *Cancer Gene Ther.* **21**, 463 (2014).

73. Fields, B. N., Knipe, D. M. & Howley, P. M. *Fields virology*. (Wolters Kluwer Health/Lippincott Williams & Wilkins, 2007).

74. Cureton, D. K., Massol, R. H., Whelan, S. P. J. & Kirchhausen, T. The Length of Vesicular Stomatitis Virus Particles Dictates a Need for Actin Assembly during Clathrin-Dependent Endocytosis. *PLoS Pathog.* **6**, e1001127 (2010).

75. Sun, X., Roth, S. L., Bialecki, M. A. & Whittaker, G. R. Internalization and fusion mechanism of vesicular stomatitis virus and related rhabdoviruses. *Future Virol.* **5**, 85–96 (2010).

76. Underwood, W. J. *et al.* Chapter 15 - Biology and Diseases of Ruminants (Sheep, Goats, and Cattle) A2 - Fox, James G. in *Laboratory Animal Medicine (Third Edition)* (eds. Anderson, L. C., Otto, G. M., Pritchett-Corning, K. R. & Whary, M. T.) 623–694 (Academic Press, 2015). doi:10.1016/B978-0-12-409527-4.00015-8

77. Bauerfeind, R. *Zoonosen: von Tier zu Mensch übertragbare Infektionskrankheiten*. (Dt. Ärzte-Verlag, 2013).

78. Lvov, D. K., Shchelkanov, M. Y., Alkhovsky, S. V. & Deryabin, P. G. Chapter 5 - Order Mononegavirales. in *Zoonotic Viruses in Northern Eurasia* 77–106 (Academic Press, 2015). doi:10.1016/B978-0-12-801742-5.00005-2

79. Finkelshtein, D., Werman, A., Novick, D., Barak, S. & Rubinstein, M. LDL receptor and its family members serve as the cellular receptors for vesicular stomatitis virus. *Proc. Natl. Acad. Sci. U. S. A.* **110**, 7306–7311 (2013).

80. Sun, X., Yau, V. K., Briggs, B. J. & Whittaker, G. R. Role of clathrin-mediated endocytosis during vesicular stomatitis virus entry into host cells. *Virology* **338**, 53–60 (2005).

81. Carter, J. & Saunders, V. *Virology: Priciples and Applications, 2nd Edition*. (2013).

82. Chapter 18 - Rhabdoviridae A2 - MacLachlan, N. James. in *Fenner's Veterinary Virology (Fifth Edition)* (ed. Dubovi, E. J.) 357–372 (Academic Press, 2017). doi:10.1016/B978-0-12-800946-8.00018-0

83. Yacovone, S. K. *et al.* Migration of Nucleocapsids in Vesicular Stomatitis Virus-Infected Cells Is Dependent on both Microtubules and Actin Filaments. *J. Virol.* **90**, 6159–6170 (2016).

84. Ebert, O. *et al.* Syncytia Induction Enhances the Oncolytic Potential of Vesicular Stomatitis Virus in Virotherapy for Cancer. *Cancer Res.* **64**, 3265 (2004).

85. Chakraborty, P. *et al.* Vesicular stomatitis virus inhibits mitotic progression and triggers cell death. *EMBO Rep.* **10**, 1154–1160 (2009).

86. Blower, M. D., Nachury, M., Heald, R. & Weis, K. A Rae1-Containing Ribonucleoprotein Complex Is Required for Mitotic Spindle Assembly. *Cell* **121**, 223–234

87. Ciciarello, M. *et al.* Importin β is transported to spindle poles during mitosis and regulates Ran-dependent spindle assembly factors in mammalian cells. *J. Cell Sci.* **117**, 6511 (2004).

88. Balachandran, S. *et al.* Alpha/Beta Interferons Potentiate Virus-Induced Apoptosis through Activation of the FADD/Caspase-8 Death Signaling Pathway. *J. Virol.* **74**, 1513–1523 (2000).

89. Laterra, J., Keep, R. & Betz, L. *Blood—Brain Barrier*. (Lippincott-Raven, 1999).

90. Ganten, D. & Ruckpaul, K. *Erkrankungen des Zentralnervensystems. Handbuch der molekularen Medizin*. (Springer-Verlag, 1999).

91. Shinozaki, K., Ebert, O., Suriawinata, A., Thung, S. N. & Woo, S. L. C. Prophylactic Alpha Interferon Treatment Increases the Therapeutic Index of Oncolytic Vesicular Stomatitis Virus Virotherapy for Advanced Hepatocellular Carcinoma in Immune-Competent Rats. *J. Virol.* **79**, 13705–13713 (2005).

92. Hoffmann, M. *et al.* Fusion-active glycoprotein G mediates the cytotoxicity of vesicular stomatitis virus M mutants lacking host shut-off activity. *J. Gen. Virol.* **91**, (2010).

93. Heiber, J. & Barber, G. N. Vesicular Stomatitis Virus Expressing Tumor Suppressor p53 Is a Highly Attenuated, Potent Oncolytic Agent. *J. Virol.* **85**, 10440–10450 (2011).

94. Ozduman, K., Wollmann, G., Ahmadi, S. A. & van den Pol, A. N. Peripheral Immunization Blocks Lethal Actions of Vesicular Stomatitis Virus within the Brain. *J. Virol.* **83**, 11540–11549 (2009).

95. Muik, A. *et al.* Re-engineering Vesicular Stomatitis Virus to Abrogate Neurotoxicity, Circumvent Humoral Immunity, and Enhance Oncolytic Potency. *Cancer Res.* **74**, 3567 (2014).

96. Fernandez, M., Porosnicu, M., Markovic, D. & Barber, G. N. Genetically Engineered Vesicular Stomatitis Virus in Gene Therapy: Application for Treatment of Malignant Disease. *J. Virol.* **76**, 895–904 (2002).

97. Obuchi, M., Fernandez, M. & Barber, G. N. Development of Recombinant Vesicular Stomatitis Viruses That Exploit Defects in Host Defense To Augment Specific Oncolytic Activity. *J. Virol.* **77**, 8843–8856 (2003).

98. Jenks, N. *et al.* Safety Studies on Intrahepatic or Intratumoral Injection of Oncolytic Vesicular Stomatitis Virus Expressing Interferon-β in Rodents and Nonhuman Primates. *Hum. Gene Ther.* **21**, 451–462 (2010).

99. Shin, E. J. *et al.* Interleukin-12 Expression Enhances Vesicular Stomatitis Virus Oncolytic Therapy in Murine Squamous Cell Carcinoma. *The Laryngoscope* **117**, 210–214 (2007).

100. Miller, J. M., Bidula, S. M., Jensen, T. M. & Reiss, C. S. Vesicular stomatitis virus modified with single chain IL-23 exhibits oncolytic activity against tumor cells in vitro and in vivo. *Int. J. Interferon Cytokine Mediat. Res.* **2010**, 63–72 (2010).

101. Altomonte, J. *et al.* Exponential Enhancement of Oncolytic VSV Potency by Vector-Mediated Suppression of Inflammatory Responses In Vivo. *Mol. Ther. J. Am. Soc. Gene Ther.* **16**, 146–153 (2008).

102. Kelly, E., Nace, R., Barber, G. N. & Russell, S. J. Attenuation of Vesicular Stomatitis Virus Encephalitis through MicroRNA Targeting ▿. *J. Virol.* **84**, 1550–1562 (2009).

103. Wakamatsu, N., King, D. J., Seal, B. S., Samal, S. K. & Brown, C. C. The pathogenesis of Newcastle disease: A comparison of selected Newcastle disease virus wild-type strains and their infectious clones. *Virology* **353**, 333–343 (2006).

104. Spisek, R. & Dhodapkar, M. Towards a Better Way to Die with Chemotherapy: Role of Heat Shock Protein Exposure on Dying Tumor Cells. *Cell Cycle* **6**, 1962–1965 (2007).

105. Breedis, C. & Young, G. The Blood Supply of Neoplasms in the Liver. *Am. J. Pathol.* **30**, 969–985 (1954).

106. Runge, A. *et al.* An Inducible Hepatocellular Carcinoma Model for Preclinical Evaluation of Antiangiogenic Therapy in Adult Mice. *Cancer Res.* **74**, 4157 (2014).

107. Willmon, C. *et al.* Cell Carriers for Oncolytic Viruses: Fed Ex for Cancer Therapy. *Mol. Ther. J. Am. Soc. Gene Ther.* **17**, 1667–1676 (2009).

108. Huszthy, P. C. *et al.* Remission of invasive, cancer stem-like glioblastoma xenografts using lentiviral vector-mediated suicide gene therapy. *PloS One* **4**, e6314–e6314 (2009).

109. Kimpel, J. *et al.* The Oncolytic Virus VSV-GP Is Effective against Malignant Melanoma. *Viruses* **10**, 108 (2018).

110. 12_2018_oncolytic activity of the rhabdovirus VSV-GP against prostate cancer.pdf.

12. List of Figures

13. List of Tables

14. Abbreviations

Ad.Cre	Cre-recombinase expressing Adenovirus
AST-LTAg	Albumin-floxstop-large T-antigen
APC	Antigen presenting cell
BUN	Blood urea nitrogen
Caspase	Cysteine-Aspartatic-Proteases
CD	Cluster of differentiation
CNS	Central nervous system
CPE	Cytopathic effect
CREA	Creatinine
CSF	colony-stimulating factor
DC	Dendritic cell
DNA	Deoxyribonucleic acid
EDTA	Ethylenediaminetetraacetic acid
EMA	European Medicines Agency
ER	Endoplasmic reticulum
ERK	Extracellular signal-regulated kinases
FACS	Fluorescence-activated cell sorting
Fas	First apoptosis signal receptor
FDA	U.S. Food and Drug Administration
F Protein	Fusion protein
GFP	Green fluorescent protein
GM-CSF	Granulocyte-macrophage colony-stimulating factor
G Protein	Glycoprotein
GPT	Glutamate-Pyruvate-Transalaminase
HBV	Hepatitis B virus
HCC	Hepatocellular carcinoma
HCV	Hepatitis C virus

HepG2	Human HCC cell line
hIFNβ	Human interferon β
HN Protein	Hemagglutinin-Neuraminidase
Huh7	Human HCC cell line
ICP	Infected cell protein
IFN	Interferon
IL	Interleukin
ISG	Interferon stimulated genes
IVC	Individually ventilated cage
LDH	Lactate dehydrogenase
LDH(R)	High density lipoprotein (Receptor)
LDL(R)	Low density lipoprotein (Receptor)
L Protein	Large protein
MHC	Major histocompatibility complex
MOI	Multiplicity of infection
M Protein	Matrix protein
mRNA	Messenger RNA
MTS	3-(4,5-dimethylthiazol-2-yl)-2,5-diphenyltetrazolium bromide
NDV	Newcastle Disease Virus
NK	Natural killer cell
NOD-SCID	Non Obese Diabetic-Severe Combined Immunodeficiency
N protein	Nucleocapsid protein
NS1	NS1 influenza protein, non-structural protein
OIE	World Organization for Animal Health
OV	Oncolytic virus
P53	Tumor suppressor gene
PAMP	Pathogen associated molecular patterns
PBMC	Peripheral blood mononuclear cells
PBS	Phosphate buffered saline

PD-1	Programmed cell death protein
PD-L1	Programmed cell death 1 ligand 1
PFU	Plaque forming unit
P Protein	Phosphoprotein
PRR	Pattern recognition receptor
Raf 1	Proto-oncogene
Ran	Ras-related nuclear protein
Ras	Proto-oncogene
Rcf	Relative centrifugal force
RdRp	RNA-dependent RNA polymerase
RIG-I	retinoic acid inducible gene I
RNA	Ribonucleic acid
STAT	Signal transducer and activator of transcription
TAA	Tumor associated antigen
TACE	Transarterial chemoembolization
$TCID_{50}$	50% Tissue culture infective dose
TCR	T-cell receptor
TGF	transforming growth factor
TK	Thymidine kinase
TLR	Toll-like receptor
TNF	Tumor necrosis factor
TRAIL	TNF-related apoptosis-inducing ligand
T-VEC	Talimogene laherparepvec
USDA	United States Department of Agriculture
VSV	Vesicular stomatitis virus
VSV-IN	VSV, serotype Indiana
VSV-NJ	VSV, serotype New Jersey
VSV-NDV	Pseudotyped vesicular stomatitis virus with glycoproteins of Newcastle Disease Virus

15. Attachments

Supplementary Table 1: Experimental conditions and results in the development of rVSV-(LCMV)GP

Cancer type	**Model specifications**			**Response to Treatment**
Malignant glioma	In vitro			Good performance in monolayers and spheroids
	In vivo	Hetero-topic	Immuno-deficient	Mouse model: NOD.CB17-*Prkdc*^{scid}/J Tumor model: G62 human glioblastoma Treatment dose: 2x10^5 PFU Heterotopic (s.c.) tumors from G62 cells treated by i.t. injection were cured
		Ortho-topic	Immuno-deficient	Mouse model: NOD.CB17-*Prkdc*^{scid}/J Tumor model: U87-RFP human glioblastoma Treatment dose: 1x10^8 PFU Orthotpic (intracerebral) tumors from U87 cells treated by i.v. injection led to median survival of either 71 days post transplantation or event free survival of more than 125 days compared to 33 days in PBS control group
			Immune competent	Mouse model: C57BL/6NCrl Tumor model: CT2A glioma (CT26-lacZ) Treatment dose: 2.5x10^7 PFU Treatment with and rVSV-GP administered intracranially led to median survival 81days post transplantation (dpt) vs. PBS 29 dpt. 5 of 10 animals showed event-free long-term survival. Test of effectiveness for brain metastases with colon carcinoma injected intracranially led to 9 animals durable cured without off-target effects out of 11.
Melanoma	In vitro			• 6 human melanoma cell lines showed good susceptibility for VSV. VSV-GP had different susceptibility between the cell lines. • 1 mouse melanoma cell line (B16-OVA) → good susceptibility of both viruses. • 1 dog melanoma cell line (UCDK9-M1) → high susceptibility of both viruses (VSV, VSV-GP). Efficient killing of melanoma cell lines in mouse and dog cell line and 4 out of 6 human cell lines. Susceptibility and killing efficacy in primary human melanoma derived from 10 patients: Successful infection with VSV-GP-GFP in 5 out of 10 cell lines

	In vivo	immunodeficient	Mouse model: NOD.CB17-*Prkdc*^{scid}/J Tumor model: A375 (xenograft) Treatment dose: 10^7PFU Treatment via i.t. injection led to median survival of 45 days (PBS 22 days).
		immune competent	Mouse model: C57BL/6J Tumor model: murine B16-OVA cells Treatment doses: $2.36x10^4$PFU, $4.72x10^5$, $2.36x10^7$ Treatment via i.t. injection was most efficient with the highest dose $2.36x10^7$ tested. Median survival was prolonged to 25.5. days compared to PBS control (18days). Complete remission was observed in 3 out of 12 animals. Treatment via i.v. injection was tested with $2.36x10^7$PFU. Median survival was prolonged to 22 days (longest survived 32) in contrast to PBS 17.5 days.
Ovarian cancer	In vitro		• Both viruses (VSV*ΔG-G and VSV*ΔG-GP) infected all cell lines, most cell lines are more susceptible to VSV*ΔG-G • Reduced susceptibility of both viruses in benign cell line HOSE • Experiments on replication show a slightly attenuated behavior of the chimeric VSV*ΔG-GP (titer one log lower than wt-VSV at 24h post infection) compared to wt-VSV (replication peak 24h after infection) • MOI of 0.1 leads to complete loss of cell viability 72h after infection • HOSE cell line could not be lysed by either virus at MOI 1 • Addition of ruxolitinib enhanced virus titers significantly → comparable levels to control cells
	In vivo	Heterotopic immunodeficient	Mouse model: NOD.CB17-*Prkdc*^{scid}/J Tumor model: A2780 human ovarian caner Treatment dose: $5x10^6$ PFU 7 day interval Combination therapy of s.c. tumors treated with VSV-GP and ruxolitinib or monotherapy with VSVS-GP significantly reduced the tumor size. Combination therapy led to smaller tumors and reduced recurrency (3/9 mice) in contrast to monotherapy (7/10).
		Orthotopic immunodeficient	Mouse model: athymic nude-Foxn1^{nu} Tumor model: A2780 human ovarian cancer expressing luciferase Treatment dose: 10^7PFU

			Tumors were implanted by i.p. injection of A2780 cells. Four treatment groups have been tested (non-treated, ruxolitinib, virus, virus + ruxolitinib). Treatment was performed with ruxolitinib and virus via i.p. injection (10^7PFU at days 0, 3 and 7). The group treated with the virus only showed tumor remission in 6 out of 8 animals. The group treated with virus + ruxolitinib led to tumor remission in 1 out of 8 animals. Doses of 10^8 or 10^9 did not lead to toxicity in ruxolitinib treated animals (toxicity is not enhanced).
Prostate cancer	In vitro		• 6 human and 1 murine cell line (PCa) → VSV-GP efficiently killed 4 cell lines • 2 cell lines in bone marrow (mimic metastases) → effectively killed by VSV-GP • Inefficient cell killing in VCaP and LNCaP (maybe due to lack of a-destroglycan expression on the surface) → increasing virus dose 100fold induced killing rates comparable to sensitive cell lines • Primary cultures from patient samples have been tested for sensitivity and killing rates → all cultures were sensitive, yet killing rates heterogeneous ranging between 60%-20% survival • PCa cell lines have heterogeneous capability of producing an IFN-response
	In vivo	Immunodeficient	Mouse model: Balb/c Rag2$^{-/-}\gamma c^{-/-}$ Tumor model: Du145 cells, 22Rv1 cells Treatment dose: 10^7 PFU VSV-GP-Luc or VSV-GP-GFP Treatment via i.t. injection: Intratumoral injection in xenograft models (s.c. Du145) tumors were treated with 2 injections of 10^7 PFU VSV-GP via i.t. injection. The treatment induced full tumor remission and no relapse during a 100-day observation period. 22Rv1 tumors implanted s.c. were treated with a single dose $2.3x10^8$PFU VSV-GP. 6 out of 7 mice responded well to the treatment (5/7 tumor remission, 1/7 stable disease). Mice treated with a single dose of $3.3x10^5$ led to tumor growth delay in 3 out of 7 mice , stable disease in 1 out of 7 mice. 2 out of 7 mice showed tumor remission. VSV-GP-Luc was detectable in tumors as early as day 1-9 after treatment. Treatment via i.v. injection: Subcutaneously implanted 22Rv1 tumors treated with 10^8 PFU showed complete response in 6 out of 6 animals. Those survived the 86 days observation period.

		Immune competent	Mouse model: C57BL/6JRj Tumor model: TRAM-C1 cells Treatment dose: 10^8 PFU 3 doses of VSV-GP administered i.t. led to tumor growth delay and significant increase of median survival (presence of VSV-GP-Luc in the syngeneic model was shorter than in xenograft model).